Bilateral Control – Operational Enhancements

By

AHMET ALTINIŞIK

Submitted to the Graduate School of Engineering and Natural Sciences
in partial fulfillment of
the requirements for the degree of
Master of Science

SABANCI UNIVERSITY

Spring 2006

Bilateral Control – Operational Enhancements

APPROVED BY:

ASIF ŠABANOVİĆ _____

(Thesis Supervisor)

ERKAY SAVAŞ _____

GÜLLÜ KIZILTAŞ ŞENDUR _____

KEMALETTİN ERBATUR _____

MUSTAFA ÜNEL _____

DATE OF APPROVAL: _____

BILATERAL CONTROL – OPERATIONAL ENHANCEMENTS

Ahmet Altınışık

EECS, M.Sc. Thesis, 2006

Thesis Supervisor: Prof. Dr. ASIF ŠABANOVİĆ

Keywords: Bilateral Control, Acceleration controller, Disturbance Observer, Digital Tachometer, Multi-rate control, Four channel controller

ABSTRACT

A succinct definition of the word *bilateral* is having two sides [1]. In robotics the term bilateral control is used to define the specific interaction of two systems by means of position and/or force. Bilateral systems are composed of two sides named master and slave side. The aim of such an arrangement is such that position command dictated by master side is followed by a slave side, and at the same time the force sensation of the remote environment experienced by slave is transferred to the mater - human operator. This way bilateral system may be perceived as an "impendanceless" extension of the human operator providing the touch information of the remote (or inaccessible) environment. In a sense bilateral systems are a mechatronics extension of the teleoperated systems. There are many applications of this structure which requires critical manipulations like nuclear material handling, robotic surgery, and micro material handling and assembly. In all these applications a human operator is required to have as close to real as possible contact with object that should be manipulated or in other word the telepresence of the operator is required.

In this thesis work various important aspects of bilateral control systems are discussed. These aspects include problems of (i) acquisition of information on master and slave side, (ii) analysis and selection of the proper structure of the control systems

to ensure fidelity of the system behavior. The work has been done to enhance the performance of the bilateral control system by:

(i) Enhancing position and velocity measurements obtained from incremental encoder having limited number of pulses per revolution. A few algorithms are investigated and their improvements are proposed;

(ii) Increasing system robustness by using acceleration controller based on disturbance observer. The robust system design based on disturbance observer is known but its application requires very fast sampling and high bandwidth of the observer. In this work the discrete time realization of the observer is presented in details and selection of the necessary filters and the sampling so to achieve a good trade-off for observer realization is discussed and experimentally confirmed;

(iii) Increasing the bandwidth of force sensation by using reaction force observer. For transparent operation of a bilateral system the bandwidth of force sensation is of the major interest. All force sensors do have relatively slow dynamics and observer based structures seems providing better behavior of the overall system. In this work the observer of the interaction force is examined and design procedure is established.

In order to verify all of the proposed ideas a versatile bilateral system is designed and built and experimental verification is carried out on this system.

ÇİFT TARAFLI KONTROL – UYGULAMAYA YÖNELİK İYİLEŞTİRMELER

Ahmet Altınışık

EECS, Yüksek Lisans Tezi, 2006

Tez Danışmanı: Prof. Dr. ASIF ŠABANOVİĆ

Anahtar Kelimeler: Çift taraflı kontrol, İvme denetleyicisi, Dijital takometre, Farklı-hızlı denetleme, Dört Kanallı Kontrol

ÖZET

Robotikte karşılıklı iki sistemin pozisyon ve/veya kuvvet ilişkisiyle birbirlerini etkilediği sistemlerin kontrolüne çift-taraflı (bilateral) kontrol denir. Çift-taraflı sistemler kullanıcı tarafı (master side) ve iş tarafı (slave side) olarak adlandırılan iki alt sistemden oluşmaktadır. Bu sistemin genel geçer kullanımında kullanıcı tarafından gönderilen konum referanslarını iş tarafı, iş tarafından gönderilen kuvvet referanslarını da kullanıcı tarafı takip etmektedir. Bu sayede kullanıcı iş tarafında kumanda ettiği robota etki eden dış kuvvetleri hisseder. Orada bulunmadığı halde iş tarafındaki etkileşim kuvvetlerini hissedebilmesiyle dokunma hissi gerektirecek hassas ve özel görevleri becerebilmektedir. Çift taraflı kontrol insanın çalışmasının tehlikeli veya imkansız olduğu nükleer santral, okyanus dibi ya da uzay gibi bölgelerdeki işlerde kullanılabileceği gibi insan ölçeğinden çok altında hassasiyet gerektirecek endoskopik mikro cerrahi, mikro montaj gibi alanlarda da kullanılmaktadır.

Bu tez içinde çift taraflı kontrol sistemlerinin performansının arttırılması için uygulamaya yönelik çeşitli iyileştirmeler tartışılmış, bunlardan uygun bulunanları hazırlanan deney düzeneğiyle test edilerek sağlaması yapılmıştır. Sisteme yapılan iyileştirmeler: (i) kısıtlı çözünürlükteki artımsal enkoderden gelen pozisyon bilgisinden

geniş hız aralığında hassas ölçüm sağlaması, (ii) sistem gürbüzlüğünün (robustness) bozucu gözlemleyici (disturbance observer) tabanlı çalışan ivme kontrolcüsü kullanılarak arttırılması. (iii) ivme kontrolcüsünün farklı hızlarda (multirate) çalışan dijital kontrolcü ve yüksek hassasiyetli hız ölçümleri sayesinde bant genişliğinin arttırılması. (iv) Etkileşim kuvvetlerinin algılanması için kuvvet sensörünün çok daha yüksek bant genişliğine sahip tepki kuvveti gözlemleyicisi (reaction force observer) kullanılarak sistemlerin dokunma stabilitesi arttırılması olarak sayılabilir.

Bunlara ek olarak, literatürdeki çift taraflı kontrol sistemleri incelenmiş, çift taraflı kontrol sistemlerindeki genel tasarım ve performans kriterleri açıklanmıştır. Dört kanallı bir çift taraflı kontrol sistemi benimsenerek bu kontrol mimarisi kullanılarak oluşturulan çift taraflı sistemde bazı deneyler yapılmış ve sonuçları sunulmuştur.

“To the people that care about me”

ACKNOWLEDGEMENTS

First of all I would like to thank to Professor Asif Şabanoviç for his cheerful existence, he taught me much more than numbers and wires with his helpful attitude and endless patience to everybody.

I wish to thank the members of my thesis defence jury for spending their valuable time and valuable comments. Thanks to Çağdaş Önal for his support and time helping me to run the experimental setups which he started to build in his thesis work.

I would also thank to my close friends Başak Alper, Emrah Deniz Kunt, Atakan Ertuğrul, Özge Memiş, Ahmet Teoman Naskali, Eray Doğan, and Onur Gökçe for their fellowship.

I would also like to thank to mechatronic graduate students, Ertuğrul Çetinsoy, Emrah Deniz, Özer Uluçay, Selim Yannier, Emrah Parlakay, Erhan Demirok, Shahzad Khan, Meltem Elitaş, Merve Acer, Şakir Kabadayı, Elif Hocaoğlu, Nusrettin Güleç, Ahmet Fatih Tabak and İlker Sevgen for their support.

TABLE OF CONTENTS

LIST OF FIGURES

Chapter 1

Introduction

1.1 Definition and History

A succinct definition of the word *bilateral* is having two sides [1]. In robotics the term bilateral control is used to define two systems behaving interactively with each other by means of position and/or force. In general bilateral systems aim to provide force sensation of the remote environment to the human operator for delicate teleoperation. Bilateral systems are composed of two sides named master and slave side. The human operator manipulates the master side and feels the forces acting on the slave side. Initially, such systems are required for the critical manipulation tasks where visual feedback is insufficient as in radioactive lab works or minimal invasive surgery.

Figure 1-1 First mechanical master slave manipulator by Ray Goertz [11]

First mechanical master-slave manipulator is invented by R. Goertz for the radioactive lab work in 1949 [10]. The term master slave is taken from mechanical and electrical fields where it is used for defining similar systems [11]. Goertz's master-slave mechanism is implemented with electric-servo manipulators with force feedback in 1950s [10]. Force sensation in the master side is a direct outcome of the mechanically coupled systems. Since then a great amount of work has been done in the area by various researchers. Sheridan published a useful survey in 1989 [73]. A recent historical survey by Hokayem and Spong is also available [74]. Researches in bilateral control lead to the advancements in many other research fields like psychophysical force perception force control, contact stability, communication delay, distributed systems and virtual reality.

Since a bilateral system is used for very delicate tasks, the single most crucial quality of the system is its stability. Followed after stability, transparency of a bilateral system is also a key property [4]. Transparency of a bilateral system is defined as equality of force and position responses of master and slave sides apart from dynamics of the environments [2]. Yokokohji and Yoshikawa define the same concept as kinesthetic coupling. The ideal kinesthetic coupling allows the operator to manipulate the system as if he were manipulating the object directly [2], or to transfer accurately the task impedances to the master side [3]. Katsura showed that perfect transparency in a bilateral system is not possible [12]. Since perfect transparency of the system is not possible, system designers should try to have the highest transparency possible. A question arises from the transparency discussions: How much transparency is enough or acceptable for a human to operate with a bilateral system? [15] In section 4.4 a relative answer is given based experiments on human operators.

1.2 Applications for Bilateral Control

Since 50's bilateral control systems found a wide area for application, Level of telepresence and usability in these systems are still way behind the demands. As importance (price) of the human increases in modern society requirements of usable bilateral systems increases. Below various different applications areas of bilateral systems are discussed very briefly.

1.2.1 Hazardous Material Handling

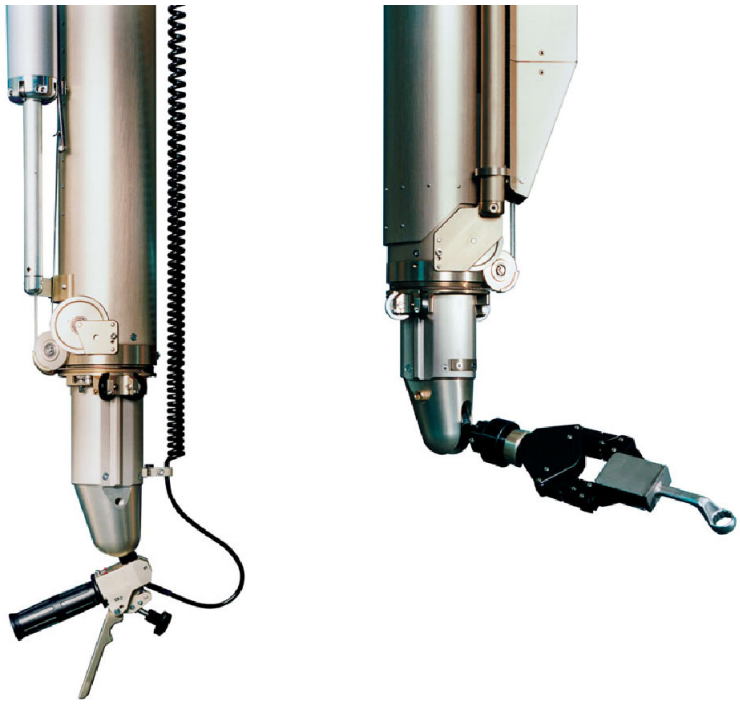

Figure 1-2 Master slave manipulator (www.hmw.com)

As discussed previously hazardous material handling is the reason for the invention of the master-slave manipulators. Mechanical and servo controlled master slave manipulators are widely used in research and industry. Figure 1-2 shows a master-slave manipulator.

1.2.2 Medical Robotics - Minimal Invasive Surgery

Bilateral systems found its place in biomedical applications also. First mechanical tools used in minimal invasive surgery started to be replaced by the small robotics tools and cameras and after gaining confidence further advanced towards teleoperated surgery workplace are now visible. Intuitive surgical systems inc. produces da-Vinci surgical system. Which compose of a stereo vision system and 4 highly dexterous robotic tools controlled from a station next to the patient. Surgeon can monitor the environment with 3D stereo vision system. However system lacks the force feedback to the surgeon.

Figure 1-3 da Vinci minimal invasive surgical robot from intuitivesurgical.com

Figure 1-4 highly dexterous 7 DOF end effector of da Vinci robotic system

1.2.3 Underwater Robotics

Figure 1-5 ROV with manipulators courtesy of www.seaice.com

As deep sea is one of the most dangerous environments for human beings, teleoperation and telepresence is required for construction, research and military applications. Underwater vehicles are one of the main applications of teleoperation. Underwater remotely operated vehicles (ROV) are mostly controlled with supervisory control algorithms for operation in environments with hard limitations on communication. A remotely operated vehicle also has manipulators for manipulation and similar tasks, bilateral control systems are mostly used in these tools.

1.2.4 Space Robotics

Figure 1-6 Robot at International Space Station courtesy of www.space.gc.ca

Like underwater applications space operation is also very dangerous and costly. Space robots operated from the ground stations is subject to long communication delays due to the distance. Currently there are many researchers working on control of manipulators or observer vehicles at space. Figure 1-6 shows an image of a manipulator currently in use in international space station for assisting astronauts.

1.2.5 Mobile Robotics

Recently there are also applications of bilateral control with group of mobile robots in research level. Bilateral control can be applied in many tasks requiring more than one robot at master and slave sides. Cooperated mobile robots can be used in construction and other areas requiring controlled large forces from different sides of an object. Figure 1-7 depicts a bilateral system which single master operating a large object with 3 mobile robots.

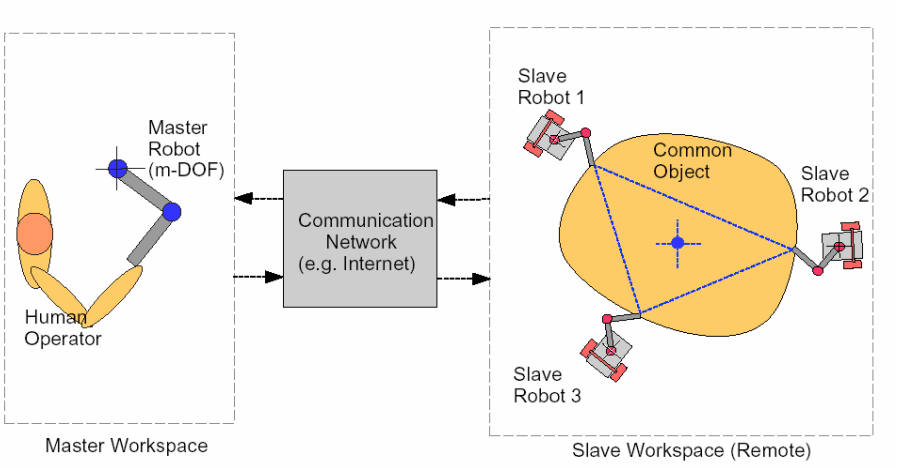

Figure 1-7 single master operator operating multiple robots with a bilateral control system [74]

1.2.6 Micro Manipulation and Assembly

Micro manipulation and micro assembly is one of the hardest task for a human being as the forces at the micro world are very different from the human environment. Bilateral control system working with force and position scaling and impedance shaping methods provides a similar environment to the human operator working with the micro objects.

1.2.7 Other Possible Applications

There are many other possible applications for bilateral control. Exoskeleton human power amplifying robots has been developed in 1970's. Such exoskeletons can also be used to help disabled people for assistance in walking.[74]

Military applications of bilateral control are also considered very attractive for military. Mine inspection and deactivation, remote observation of enemy operations, remotely operated vehicles, aircrafts and tanks etc are few of many possible applications for military.[73]

1.3 Aim of This Work

The goal of this thesis is to discuss various aspects for enhancing the operational performance of the bilateral control system and experimentally confirm selected techniques. As a part of the effort issues of:

1. Robust system design based on disturbance observer and improvements in disturbance observer design with improved velocity measurement and high bandwidth control scheme. Discrete time multirate realization of the observer is presented in details and selection of the necessary filters and the sampling so to achieve a good trade-off for observer realization is discussed and experimentally confirmed in chapter 2.

2. Selection of proper velocity measurement method providing fast and smooth velocity measurement based on incremental encoder for use in acceleration controller is done with comparing few methods experimentally in chapter 3.

3. Increasing the bandwidth of force sensation by using reaction force observer for better contact stability and increased transparency. An observer for the interaction force is examined and design procedure is established. Same Reaction force observer is built and used in bilateral control experiments in proceeding parts.

4. A brief survey of bilateral control, and control architectures available in the literature is done. Different design aspects for bilateral control such as, transparency, stability, scaling, and required limits for human operator is discussed. Additionally experiment results using a four channel controller demonstrated at different environments in chapter 4.

Chapter 2

Acceleration Controller with Disturbance Observer

Ohnishi et al. defines the robustness of a motion controller as “high fidelity” to the input reference. A robust motion control system achieves the tracking of the input reference despite the presence of the variable parameters like frictions and loading conditions of the motion system. The acceleration controller for mechanical systems is designed in such a way that acceleration command is treated as a input to the system and mechanical single DOF system is treated as a double integrator system. In such approach system internal dynamics, system parameters change, variable load and friction are handled within the acceleration controller itself, so that the higher level control (motion coordination of many DOF) does not deal with those changes. [25]

If achieved properly, the robust acceleration controller can be used as the core controller of any mechanical motion control system since the controller deals with nearly most of the lower level control problems. Due to the fact that acceleration has a dimension of force the acceleration controller can easily be extended to handle motion, force and impedance control as a basic task in any interconnected mechanical systems. In order to avoid discussion on the impact forces in this work the acceleration reference to the acceleration controller is assumed a continuous – but there is n a theoretical problem in assuming it discontinuous except the possible problem in generating discontinuous force.

Disturbance observer methods are proposed in [26] to achieve a robust motion control. Disturbance is defined as the behavioral changes in the system due to the parameter variations in the plant, friction, and varying load. The disturbance observer estimates the difference of actual plant behaviors and the predefined (nominal) plant model. Many studies have been made on disturbance observer and it is a well

recognized technique for robust motion control. Functional abilities of disturbance rejection systems as presented in [26] are depicted in Figure 2-1.

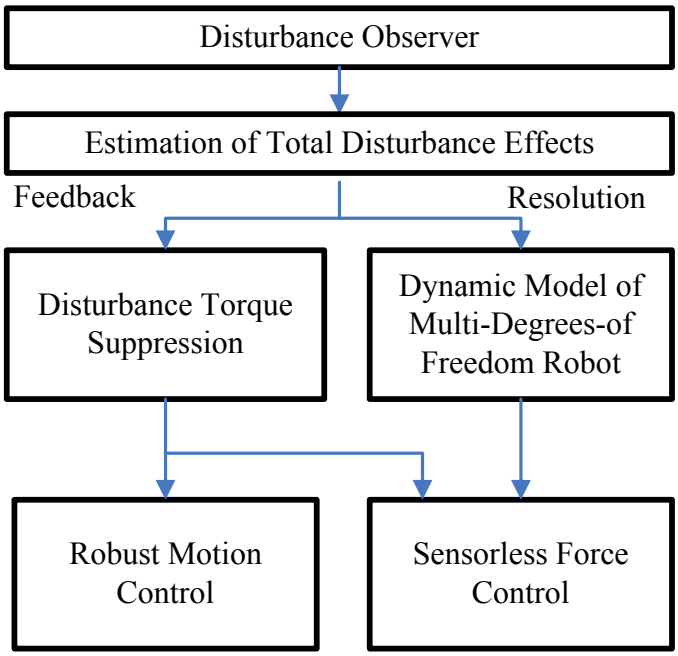

Figure 2-1 Functional abilities of disturbance observer [26]

2.1 Disturbance Observer

A disturbance observer is the structure that estimates the disturbance acting on the system. In a motion control system, disturbance can be thought as the total load acting on the motion system plus the effect of changes in the system parameters. Formulation of the disturbance observer for a mechanical system with one rotational degree of freedom is defined as follows [28].

Let us write the equation of motion for a system with one rotational degree of freedom (or a simple electrical motor)

$$\frac{d\theta}{dt} = \omega \tag{2.1}$$

$$J\frac{d\omega}{dt} = \tau_m - \tau_L \tag{2.2}$$

J is the moment of inertia of the rotating system. τ_m is the torque generated by the motor and τ_L is the load torque acting on the system. For simplicity we will assume that control of the electromagnetic processes in the electrical machine is such that motor torque τ_m is product of motor torque coefficient K_t and the motor armature current i_a. Such dependence can be achieved for all controlled electrical machines, with K_t being considered as a gain in the torque channel which is close to a constant value for most operating conditions. Under the assumption that an ideal current controller is realized then a controller reference current i_a^{ref} can be used in calculations instead of the motor current i_a. Then torque developed by an electrical machine can be expressed as:

$$\tau_m = K_t i_a = K_t i_a^{ref} \tag{2.3}$$

Load torque τ_L consists of centrifugal term, Coriolis term, and gravity all dependent on the state of the machine, denoted here as τ_{int}, and external torque acting on the system τ_{ext}. Friction terms F and $B\omega$ stands for coulomb and viscous friction in (2.4) where total load torque is depicted

$$\tau_L = \tau_{\text{int}} + \tau_{ext} + F + B\dot{\theta} \tag{2.4}$$

Combining (2.2),(2.3), and (2.4) we get (2.5)

$$J\frac{d\omega}{dt} = K_t i_a^{ref} - (\tau_{\text{int}} + \tau_{ext} + F + B\omega) \tag{2.5}$$

In (2.5) J stands for inertia and K_t stands for torque coefficient. These parameters can be expressed as a sum of so-called nominal value and the term representing variations of these parameters as defined in (2.6).

$$J = J_n + \Delta J$$
$$K_t = K_{tn} + \Delta K_t \tag{2.6}$$

By putting (2.6) into the (2.5) and rearranging the equation by lumping all the terms that we will assume as disturbance (the parameter variations (in torque dimension) plus load torque) one can write.

$$J_n \frac{d\omega}{dt} = K_t i_a^{ref} - \underbrace{\left\{ \tau_{\text{int}} + \tau_{ext} + F + B\omega + \Delta J \frac{d\omega}{dt} - \Delta K_t i^{ref} \right\}}_{Disturbance} \tag{2.7}$$

Disturbance torque is defined as in (2.8)

$$\tau_{dis} = \tau_{\text{int}} + \tau_{ext} + F + B\omega + \Delta J \frac{d\omega}{dt} - \Delta K_t i_a^{ref} \tag{2.8}$$

For calculation of the disturbance torque τ_{dis} (2.7) can be rearranged to obtain (2.9) as the formulation for the disturbance observer. Figure 2-2 shows the calculation of disturbance observer.

$$\tau_{dis} = K_t i_a^{ref} - J_n \frac{d\omega}{dt} \tag{2.9}$$

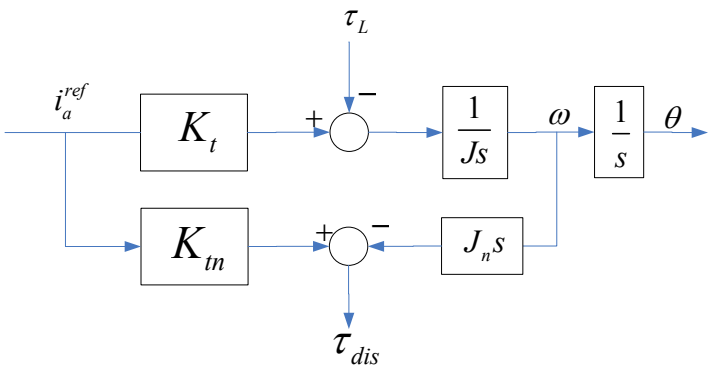

Figure 2-2 Disturbance torque observer based on velocity measurement [28]

As the disturbance observer in Figure 2-2 includes differentiation, a low pass filter is applied to the output of the disturbance observer. With a first order LPF having a cutoff frequency of g_{dis} output of the disturbance observer $\hat{\tau}_{dis}$ becomes (2.10)

$$\hat{\tau}_{dis} = \frac{g_{dis}}{s + g_{dis}} \tau_{dis} \tag{2.10}$$

The structure of the disturbance observer is depicted in Figure 2-3 and Figure 2-4. The only difference is the reconfiguration of the blocks in order to realize the derivation. In the literature there are many different structures of the disturbance observer but structures depicted by (2.10) will be used in this work.

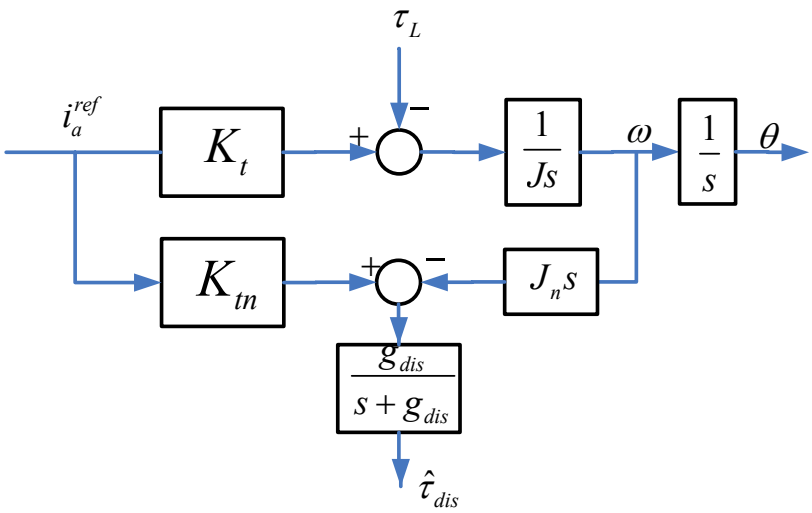

Figure 2-3 Disturbance observer with Low Pass Filter [28]

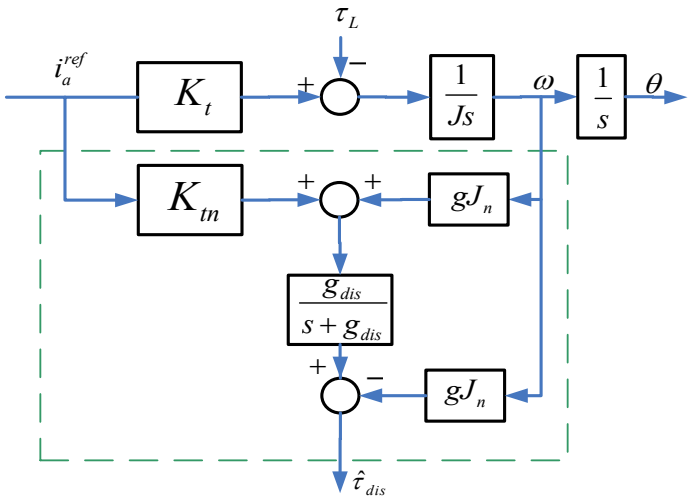

Figure 2-4 Disturbance observer without direct differentiation [28]

2.2 Disturbance Rejection

Disturbance rejection is the method that adds the estimated disturbance acting on the system as an additional input in opposite direction to the real disturbance. To reject the effects of the disturbances in the system, estimated disturbance in acceleration dimension should be converted to the current by using motor's nominal torque coefficient and added to the system input as in Figure 2-5.

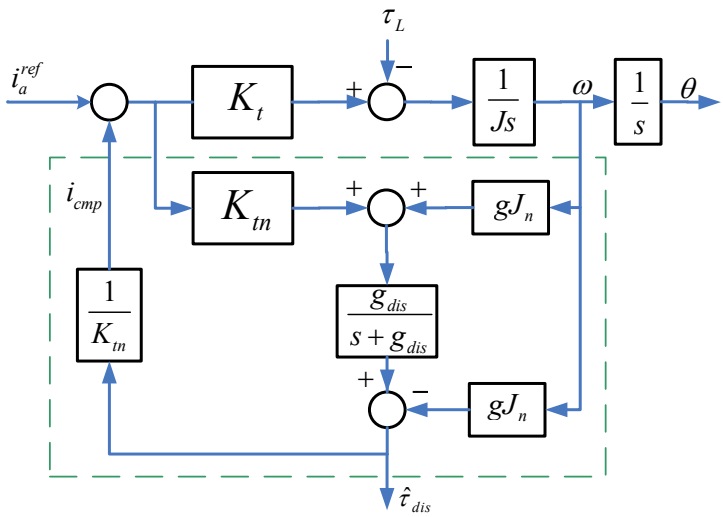

Figure 2-5 Disturbance feedback [28]

However, due to the structure of the low pass filter used in Figure 2-4, the disturbance observer can estimate only the disturbances at frequencies lower than the cutoff frequency of the low pass filter (2.10). The acceleration controller takes acceleration reference as input, to turn current reference i_a^{ref} into acceleration J_n/K_{tn} to be introduced and added to the input of the controller. Figure 2-7 shows the equivalent diagram for acceleration control system with disturbance feedback.

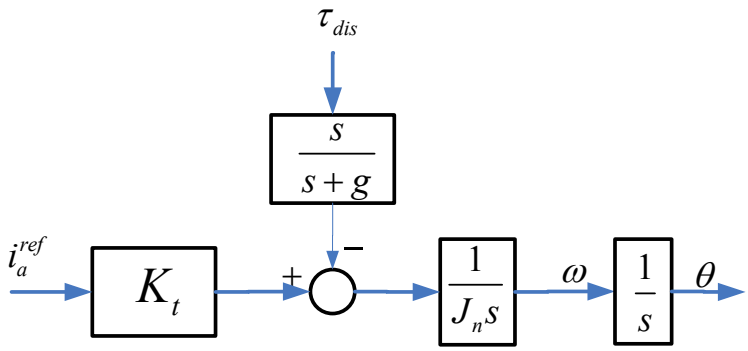

Figure 2-6 acceleration controller equivalent diagram [28]

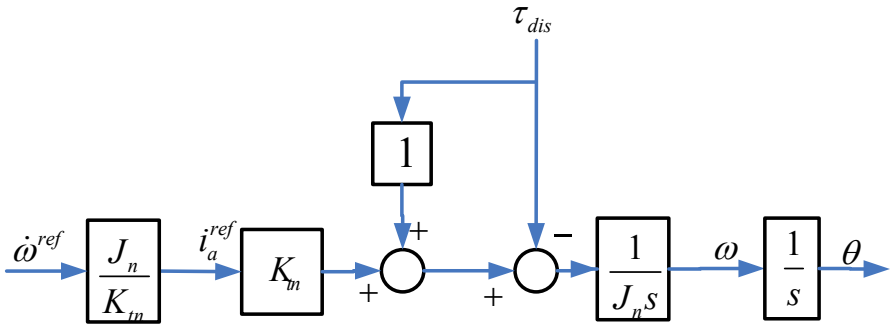

Figure 2-7 ideal disturbance rejection [28]

If we assume that the disturbance observer is working perfectly, the system in Figure 2-5 would be identical with the Figure 2-7. Since all disturbances are rejected, the motion control system is reduced to a simple second order system.

2.3 Realization of disturbance observer

In section 2.1, the disturbance observer was implemented by using continuous time analysis. Since almost all of the control systems in our era are working on digital computers, discrete time implementation of the disturbance observer is required for implementation. In this section discrete time realization of the disturbance observer will be given. Additionally, the stability issues in discrete time and variations of observer's bandwidth due to the variations in the system parameters will be presented.

2.3.1 Effects of the parameter variation on bandwidth of the disturbance observer

In Figure 2-5 disturbance is calculated and fed back to the system. Variations in the ratio of $\frac{K_t}{K_{tn}}$ and $\frac{J_n}{J}$ change the observer's bandwidth g_{dis} as in equation (2.11). Since variation of the motor torque coefficient is small, the bandwidth is affected mostly from the variation of the inertial load.

$$g_{dis}^{*} = \frac{K_t}{K_{tn}} \frac{J_n}{J} g_{dis} \tag{2.11}$$

2.3.2 Discrete time implementation of disturbance observer

Godler *et al* [32] realized the disturbance observer (2.10) by deriving the invariant impulse response on Z-transform (2.12) instead of utilizing a low pass filter. Figure 2-8 shows the block diagram of the discrete time disturbance observer with velocity control.

$$\hat{\tau}_{dis} = \frac{1 - e^{-g_{dis}T}}{z - e^{-g_{dis}T}} \tau_{dis} \tag{2.12}$$

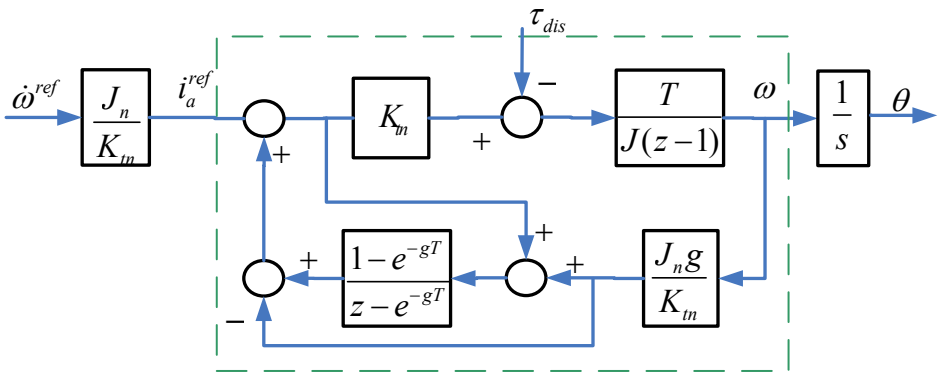

Figure 2-8 Discrete realization of disturbance observer [32]

It is also shows that even though the disturbance observer is stable for any bandwidth in continuous time, the observer can cause instability of the system in discrete time. System's stability depends on the sampling time T_s of the observer, cutoff frequency of the low pass filters g_{dis} and ratio u, which is the ratio of $K_t J_n / K_{tn} J$. For a stable operation relation equation (2.13) should be satisfied. As a result, the stability of the disturbance observer necessitates limiting the disturbance observer's bandwidth as in [32].

$$u = K_t J_n / K_{tn} J$$
$$u g_{dis} T_s < 2 \tag{2.13}$$

The current controller is part of the disturbance observer loop. Bertoluzzo *et al.*[29,32], analyzed the stability conditions for disturbance observers by taking the bandwidth of the current loop into consideration.

$$m = \frac{K_t J_n}{K_{tn} J} \cong \frac{J_n}{J} \tag{2.14}$$

m in equation (2.14) is the disturbance observer's parameter mismatch ratio. By denoting the ratio of observer's bandwidth g to the current controller bandwidth c *by* r and using a parameter a as in (2.15) the stability criteria for the high bandwidth disturbance observer can be expressed as in (2.16) and (2.17) [29,32].

$$r = g / c$$
$$a = \frac{r}{\frac{1}{cT} + r} \tag{2.15}$$

$$rg_{dis}T_s \le 1 \tag{2.16}$$

$$ma < \frac{-1(1+e^{-cT}) + \sqrt{(1-e^{-cT})^2 + 4}}{2(1-e^{-cT})} \tag{2.17}$$

Stability criteria (2.16) and (2.17) are useful for designing stable discrete disturbance observer in motion control systems.

2.3.3 Multi rate control in acceleration control

Achieving a higher bandwidth for acceleration controller while maintaining stability requires shorter control cycle as discussed in section 2.3.2. However, increasing the control sampling frequency requires compatible hardware for input, control, and output stages. Sampling frequency cannot be greater than any of these three components. In order to overcome this frequency bottleneck multirate sampling control has been proposed in [34] by using different sampling periods for input, output and control inputs. Such an organization improves control system performance as shown in [35] In a motion system equipped with incremental encoder, it is important to update the control and the estimated values as soon as new position data arrives for low velocity regions where position updates becomes sparse.[37] Multirate control is a candidate to achieve this kind of solution. When running with a system composing of a relatively high resolution encoder (40000 ppr), a high speed real-time computer (>400 MHZ), and power stage with 1 kHz bandwidth, current controller limits the overall system frequency.

Formulation in this subsection follows closely Mizuochi *et al.* [38]

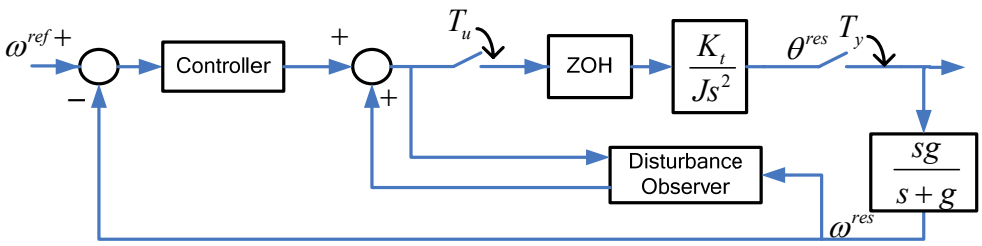

Figure 2-9 Multirate sampling control system T_u>T_y [38]

Multirate sampling method generally applied to the systems with a fast input u(t) and slow output y(t) signals, however in system described above input is slower than the output. A different multirate sampling method proposed in [38] has input sampling time T_u and a shorter measurement sampling time T_y. Figure 2-9 shows the block diagram of the proposed method.

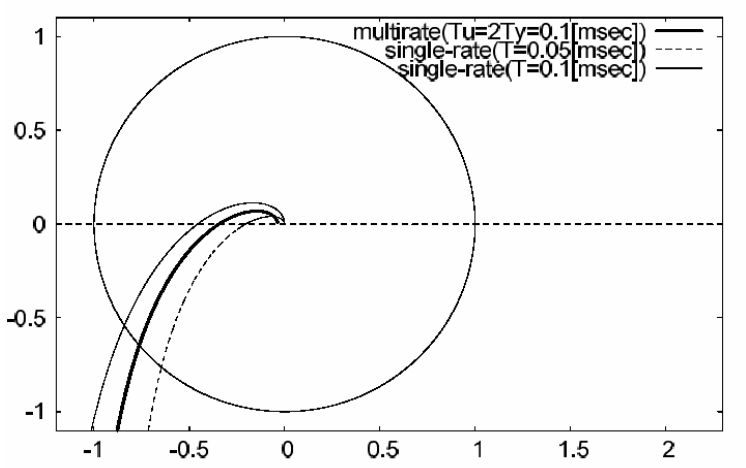

Figure 2-10 Nyquist Diagram[38]

In Figure 2-10 the Nyquist plot for a system with two different single rate $T_{u,y}$=0.1 msec ,and $T_{u,y}$=0.05 msec and multirate with input T_u=0.1 msec and output T_y=0.05 msec sampling rates are depicted. Figure 2-10 shows that multirate achieved better result than system with $T_{u,y}$=0.1msec. Similar result is depicted in Figure 2-11.

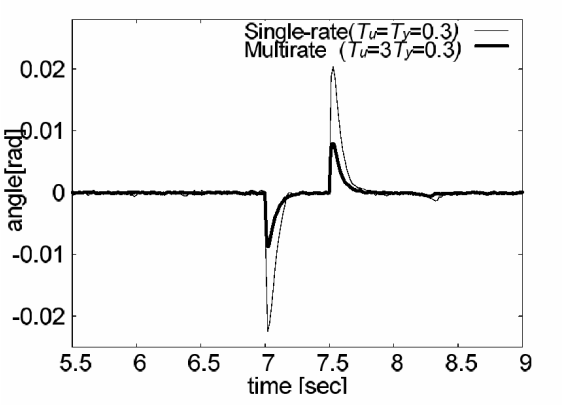

Figure 2-11 Control Error comparison for multirate method [38]

2.3.4 Experimental verification of Disturbance observer

Although robust control with disturbance rejection is a widely accepted motion control technique, an experiment has been done to certify the functionality of the disturbance observer. The detailed description of experimental setup is provided in appendix 1. Briefly a 400 watts 3-phase Maxon brushless DC motor is driven by controller in current regulation mode with a bandwidth of 1 kHz. Current driver is fed from the dSPACE® 1103 real-time outer loop controller with a 1 msec sampling time.

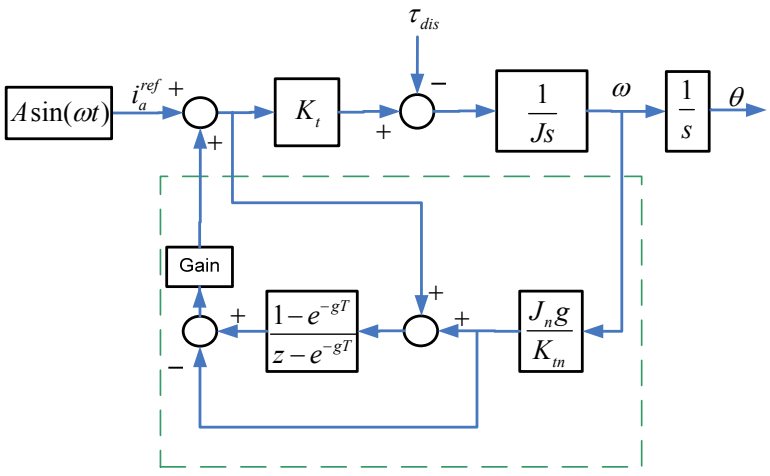

Figure 2-12 Block diagram for disturbance observer experiment

The input current to the system (Figure 2-12) is composed of a sinusoidal current reference and an input from a disturbance observer. In order to demonstrate the work of the disturbance observer the same experiments are repeated for system without and with disturbance observer output fed to the current input. Initially a sinusoidal current reference is sent to the system with the disturbance observer's gain off. Amplitude of the signal is increased until the motor could overcome the friction forces in the system. Figure 2-13 shows the motor input current and the output velocity.

Disturbance observer cutoff frequency	250 rad/s
Velocity filter cutoff frequency	250 rad/s
Sampling Time (s)	1 msec
Current reference (A)	0.1sin(t)

Table 2-1Experiment Parameters

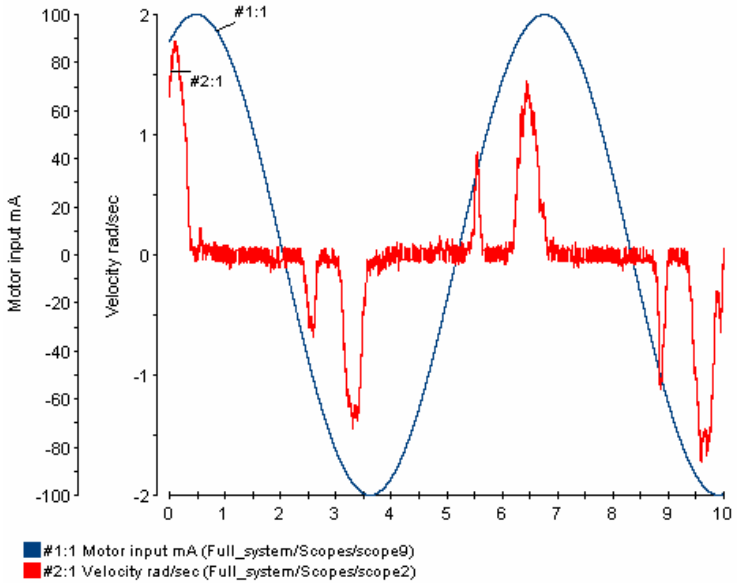

Figure 2-13 Motor input current & Motor velocity with no DOB

Due to the frictions acting on the system, motor can hardly move with a 0.1 sin(t) Amps current reference. In the second phase of the experiment, the feedback gain of the disturbance observer is increased to ½. Consequently, the motor starts to turn with a distorted sinusoidal pattern, as in figure 2.14.

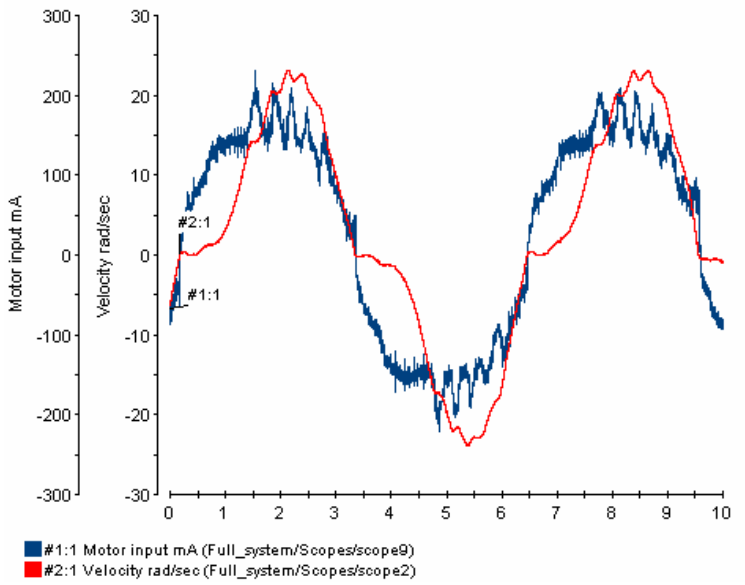

Figure 2-14 Motor input current & shaft velocity with 1/2 DOB gain

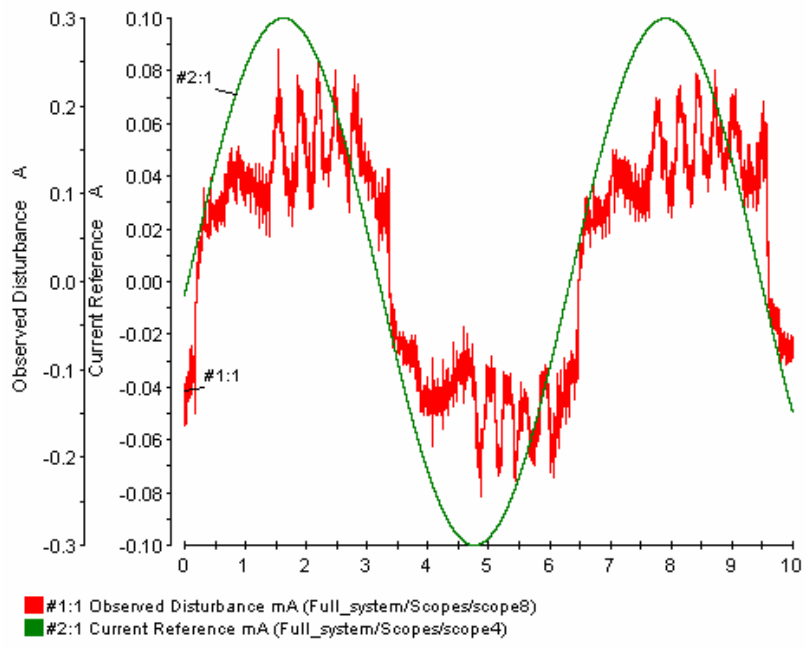

Figure 2-15 Disturbance observer output and current reference with

Figure 2-15 shows the inputs of the system coming from the observer for rejection and the current reference. Sum of these two signals is sent as the input to the motor driver. When motor rotates at low speed with no load, friction becomes the largest disturbance acting on the system. It can be noticed that disturbance observers

output is changing with the absolute angle position of the motor shaft. Misalignment of the motor and the encoder shaft causes this adverse effect and it is very undesirable for precise motion control. Even though the added nonlinear friction is undesirable in motion control, it happens to be an opportunity for the disturbance observer to showoff.

To see the full effect of the disturbance observer, output gain of the observer is set to 1. As it is seen in Figure 2-17, a smooth nice sinusoidal velocity output is accomplished with the disturbance rejection. It might be noticed that with full disturbance rejection, the amplitude of the output velocity is increased and becomes sinusoidal.

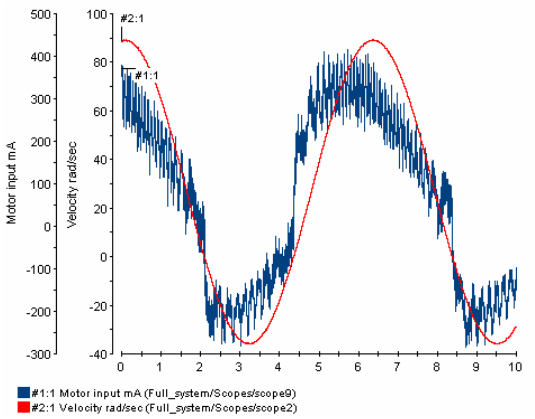

(a) Motor input current and output velocity

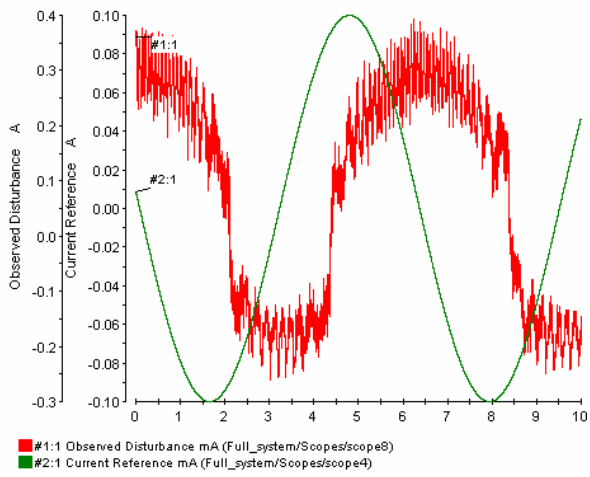

(b) Observed disturbance and Current reference

Figure 2-16 100 mA sinusoidal current reference with full disturbance rejection

As a result of disturbance rejection, friction effect is suppressed within the bandwidth of the disturbance observer. To illustrate this result, amplitude of the current

reference is reduced by 10 times of the previous value to 0.01sin(t), yet the system still gives a nice sinusoidal velocity response (see Figure 2-17 below). In addition, when an initial velocity is given to the motor manually, the motor continues to turn for a very long time with initial velocity under heavy friction.

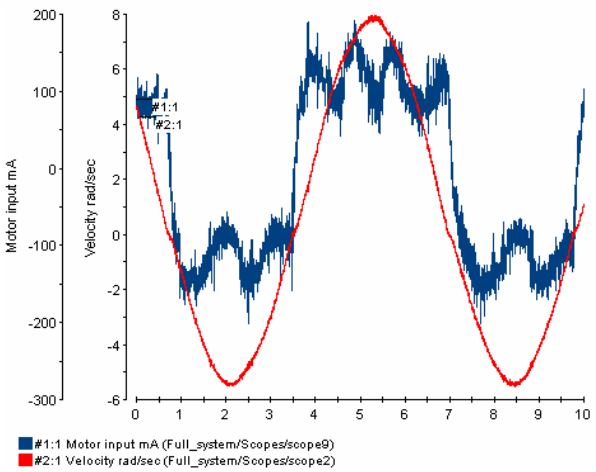

(a) Motor input current and output velocity

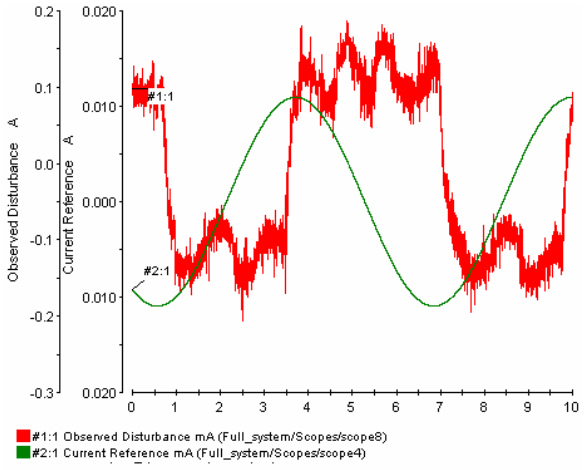

(b) Observed disturbance and Current reference

Figure 2-17 10 mA sinusoidal current reference with full disturbance rejection

As discussed before disturbance seems to be a function of the rotor angle. To verify this, an experiment depicted in Figure 2-18 is performed. Figure shows the three

sections on top disturbance observer's output, in the middle absolute shaft angle from 0 to 2π radians and at the bottom motor velocity.

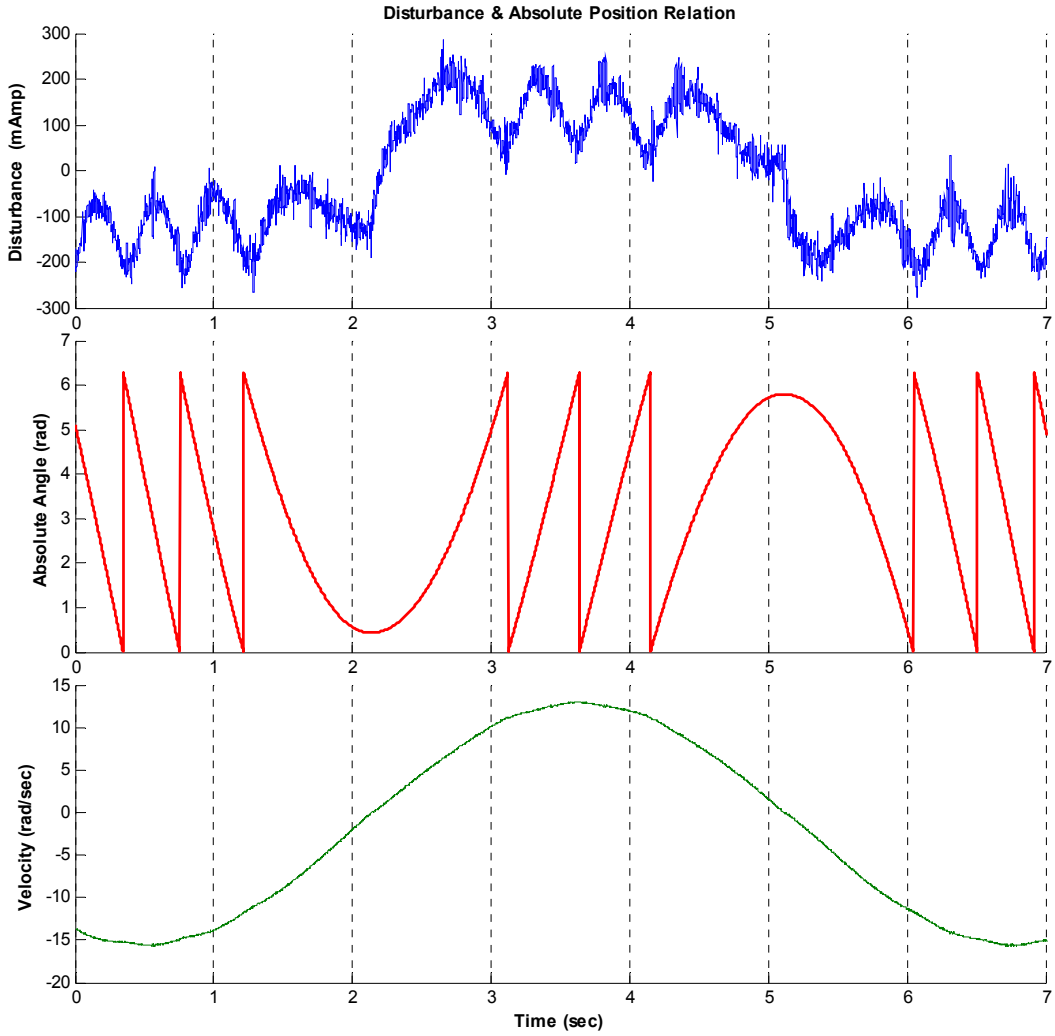

Figure 2-18 Friction generated by misaligned shafts

From this it is obvious that friction is varying with the angle of the motor shaft.

2.4 Improvements for Disturbance Observer

A single degree of freedom mechanical system with disturbance observer feedback behaves like an ideal second order system (double integrator). However this is true only if bandwidths of all disturbances acting on the system are considerably lower than the cutoff frequency of disturbance observer. In other words, disturbance observer estimates disturbances slower than its cutoff frequency; therefore a high bandwidth of

the disturbance observer is desirable. However, too much increase in disturbance observer's cutoff frequency causes instability in the system. Relation (2.17) gives a basic stability criterion by considering parameter mismatch ratio r, sampling time T_s and disturbance observer's cutoff frequency g. In (2.17) bandwidth of the internal current control loop is also taken into account for the criteria. In addition to these results, as the main purpose of the filter in disturbance observer is to reduce noise, inputs of the observer also affect the selection of the bandwidth of the disturbance observer. In following paragraphs variables in a system affecting the disturbance observer bandwidth and some suggestions to overcome these affects are discussed.

Parameter mismatch ratio is defined as the ratio between real system parameters K_t, J and their nominal values used in disturbance calculation (K_{tn}, J_n). Equation (2.11) shows the variation of the observer bandwidth with the change of the mismatch ratio. Relation (2.16) shows the relation between the mismatch ratio and stability criteria. Combining these two equations show that the parameter mismatch ratio higher than 1 does not increase the bandwidth, additionally it corrupts the disturbance observer output. For that reason the mismatch ratio should be close to 1.

Sampling time, the sampling time for the disturbance observer should be as small as possible. Computational power, speed of the control system's inputs and outputs are also factors constraining the sampling time. With the current developments in computers and technologies like FPGA, system output and input bandwidths have become the main limiting factors for sampling time. Multirate sampling method is a workaround for this problem.

Bandwidth of the current controller is also a stability constraint for disturbance observer as depicted in (2.17). Current controller should be fast enough to cope with the disturbance observer's high frequency feedback. A slower current control loop would not allow a high bandwidth in terms of stability and system performance. Therefore current controller should be fast for high bandwidth disturbance rejection. Multirate method can be used for slower current controller loop.

Velocity measurement is a key measure for disturbance observer's performance. Since disturbance observer's filter is mostly for eliminating noise coming from the

double differentiation process, any improvements in the velocity measurement process ensures observer performance.

Bandwidth of the velocity measurement has also an important role, since it also affects the bandwidth of the disturbance observer. Section 3.2 discusses velocity measurement techniques for increasing disturbance observer's performance. High resolution velocity measurement makes it possible to have a velocity data for very small sampling times and provides faster velocity measurement.

Chapter 3

Measurement

When designing a motion control system measurements techniques need to taken into account. As control routines run in digital computers measurement methods, quantization of measurement and other variables require great attention since it affects the system performance very much.

In bilateral control high system stability margin and vivid force sensation is required. In this chapter position and velocity measurement techniques will be overviewed and some experiment results will be introduced for making comparisons between these techniques. Besides velocity and position measurements measurement of analog signals will be also discussed.

3.1 Position Measurement Sensors

There are mainly three different kinds of rotational angle sensors in the market: Resolver, quadrature encoder and sinusoidal encoder [7].

A resolver is an ac machine that can be modeled as a transformer with two secondary windings [7]. Secondary windings are usually placed with a 90 degrees shift on stator and two sinusoidal signals with the 90 degrees shift are created if rotor angle is changing. Using the two sinusoidal signals, instantaneous angle of the rotor can be calculated by inspecting momentary difference between the two sine waves [7] without using any other sensor information or memory. Turning direction can be identified with the phase difference between the two sine waves. Motor velocity can be calculated by counting the sine waves for a period of time. Resolver generates a whole sine wave for one turn, and the resolution of the measurement is limited with the resolution of the

ADC used and noise level of the signal hence for high resolution applications resolver is not suitable.

The most widely used sensor for rotor angle measurement is digital quadrature incremental encoders. Quadrature encoders are usually composed of a disc with some marks that the sensor can count, in quadrature encoders two sensors are mounted with an offset to have their outputs shifted for 90 degrees. By observing the leading signal direction of the rotation can be observed. With the rotation of the encoder shaft, a counter is increased or decreased by inspecting the phase shift of the two signals. Encoder resolution is determined by the number of pulses that encoder can generate during one whole turn. For absolute position determination an index signal is also added to the encoder so absolute position can be extracted by counting pulses after the index pulse [7]. As the encoder work as a counter converting the continuous position value to a digital count with the encoder resolution it can be modeled as a quantizer [6]. If nonidealities in manufacturing and transition noises are taken into consideration quadrature encoders can be analyzed as non-ideal analog to digital converter [6].

For low speed applications quadrature encoder needs to have very high counts per revolutions for a good speed measurement. However a high resolution encoder cannot be used at high speeds due to the bandwidth limits of the encoder signals and the counter hardware. Therefore control system designer should select an appropriate encoder for the velocity range that system will run.

Sinusoidal encoders are developed to overcome some drawbacks of quadrature encoder and resolver. Sinusoidal encoder is like an incremental encoder generating sinusoidal signals like resolver instead of square waves. As a result sinusoidal encoder generates two sine waves with a 90 degrees phase lag like the resolver but it can generate thousands of sine waves in a turn as resolver can only generate one.[5] The two output sinusoidal signals can be used with just a quadrature interface like in digital incremental encoder and got resolutions like digital incremental encoders or sinusoidal signals can be interpolated like in analog revolvers and have resolutions limited with signal noise. This interpolation level is around 2^{10} in the market today. By this hybrid structure encoder resolution can be set by the controller suitable with speed range and same sensor can be used with a dynamic resolution [7].

As a final point decision of the measurement system mostly depends on the price tag of the encoder and the interface hardware. For now digital quadrature encoder is the cheapest solution among others and in the market up to 100.000 pulses per revolutions digital quadrature encoders are available. For the interface side digital quadrature encoder is also the cheapest solution among all. For now sinusoidal encoders are just used for very high precision control systems, with their very high dynamic resolution optical sinusoidal encoders promises a lot for the future. In this thesis work a digital quadrature encoders with 10000 ppr resolution has been used at 4x mode.

3.2 Velocity measurement techniques for encoders

Acceleration control requires very high resolution velocity data. In order to have velocity reading at a high speed and high resolution, various speed measurement method has been searched. In this subsection you will see main techniques for velocity measurement for digital quadrature encoders.

3.2.1 M Method (Pulse counting)

M method is the standard method for encoder velocity measurements. Pulses generated by digital quadrature encoder (p_s) counted for a certain period of time (T_s) are used to determine motor speed (ω_m). Equation (3.1) shows the velocity formulation for the M method.[24] As the sampling time is fixed in M method accuracy of the measurement decreases when number of pulses per sampling time decreases. M method is not useful for low speeds where number of pulses per sampling time is small.[21]

$$\omega_m = \frac{2\pi p_s}{PT_s} \tag{3.1}$$

3.2.2 T method (Measuring the elapsed time)

In T method time between two encoder pulse is measured and velocity calculated with this information. Equation (3.2) shows the velocity formulation. Since the sample

T_s is fixed width accuracy of measurement increases with slower encoder signals meaning small velocities. However if time interval between to pulses gets less than sampling interval T_s then T method cannot be applied. As a result T method is not useful for high velocities.

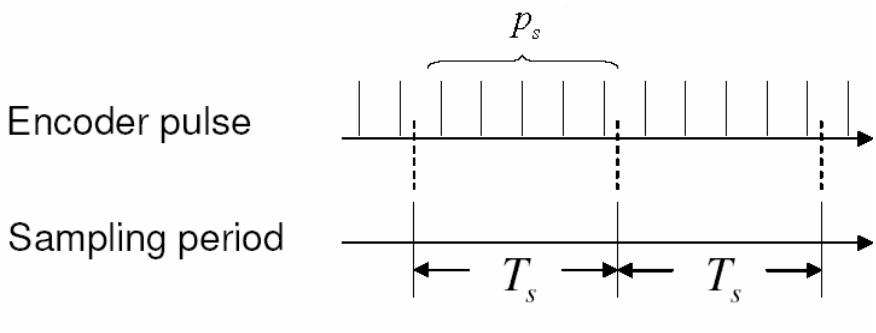

Figure 3-1 M method [24]

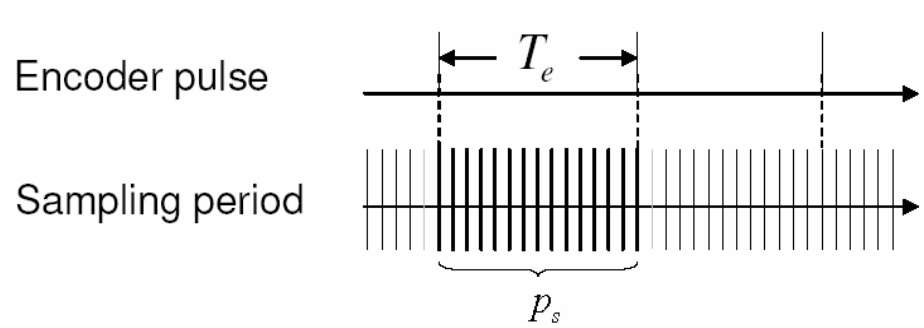

Figure 3-2 T method [24]

$$\omega_T = \frac{2\pi}{p_s P T_s} \tag{3.2}$$

3.2.3 Performance comparison of M & T methods

As discussed earlier M method loses its accuracy with decreasing number of pulses per sampling time. This means as velocity decreases accuracy of the M method decreases too. In equation 2.3 Q_{vm} denotes the absolute velocity resolution for the M

method. On the other side in T method absolute resolution decreases (2.3) as the encoder pulses get closer to each other.[24]

Since resolutions of each method change with the velocity, relative velocity resolution is a useful criterion for comparing the velocity measurement methods.

M method (a)	T Method (b)	
$Qv_m = \frac{2\pi}{PT_s}$	$Qv_T = \frac{2\pi}{p_s(p_s-1)PT_s}$	(3.3)
$\frac{Qv_m}{V} = \frac{2\pi}{PT_sV}$	$\frac{Qv_T}{V} = \frac{2\pi}{p_s(p_s-1)PT_sV}$	(3.4)
$T_m = T_s$	$T_m = p_sT_s$	(3.5)

3.2.4 M/T Method (combined method)

Besides similar works in time-interval measurement, Ohmae *et al.* [75] proposed the M/T digital tachometer for motion control, M/T method is like a combination of M & T methods. M/T method is illustrated in figure (3.3). Two counters are running at the same time: one fast for T_{aux} time measurement and the second is for counting the number of pulses during the interval time T. In Equation (3.6) measurement is formulated by dividing number of pulses occurred during T_s to the T_s and added residual T_{aux} time interval. If no pulse can be detected during the T_s measuring function adapts itself to the equation (3.7) [20] [19][21]

$$\hat{s}(i) = \frac{M(i)}{T} = \frac{M(i)}{T_s + T_{aux}(i-1) - T_{aux}(i)} \tag{3.6}$$

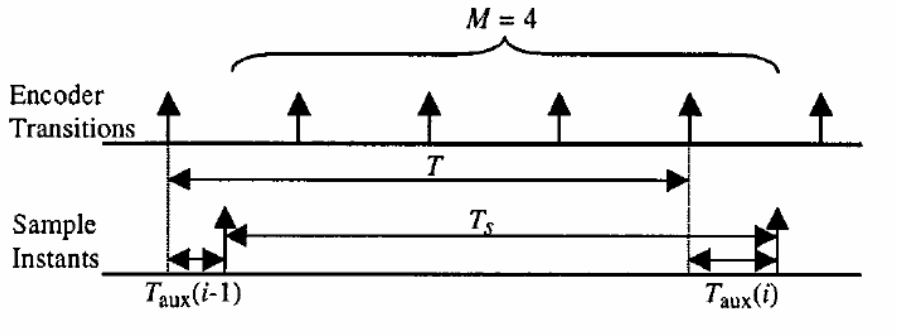

Figure 3-3 M/T digital tachometer operation principle[20]

$$\hat{s}(i) = \frac{M(i)}{m + \frac{T_{aux}(i)}{T_s}} \tag{3.7}$$

M/T method achieves resolution of T method in low speed and achieves accuracy of M methods with LPF. At slow speed if no pulse has counted scheme switches to the (3.7). As this method requires a secondary time measurement system, an interrupt driven mechanism on a secondary processor or specialized hardware is generally needed.

A similar M/T type velocity method constant sample-time digital tachometer (CSDT) [19] is designed to accomplish M/T method with a constant sample-time circuit. CSDT reduces the hardware needs for implementation.

M/T method offers a good velocity resolution both in high and low speeds. This advanced method is a good candidate for velocity measurement in motion control systems.

3.2.5 S Method (Synchronous pulse alteration method)

Tsuji *et al*.[24], proposed the S type digital tachometer. S method works in a way that it applies the principle of T method for the high speed range also, as a result of S method digital tachometer achieves high accuracy in a wide speed range. T method (Figure 3-2) works as counting the time passed in one encoder pulse. Figure 3-4 shows

the velocity and encoder reading output of a accelerating encoder from low to high speeds. Encoder output values in high speed are similar with low speed except a stepped shift in the measurement.

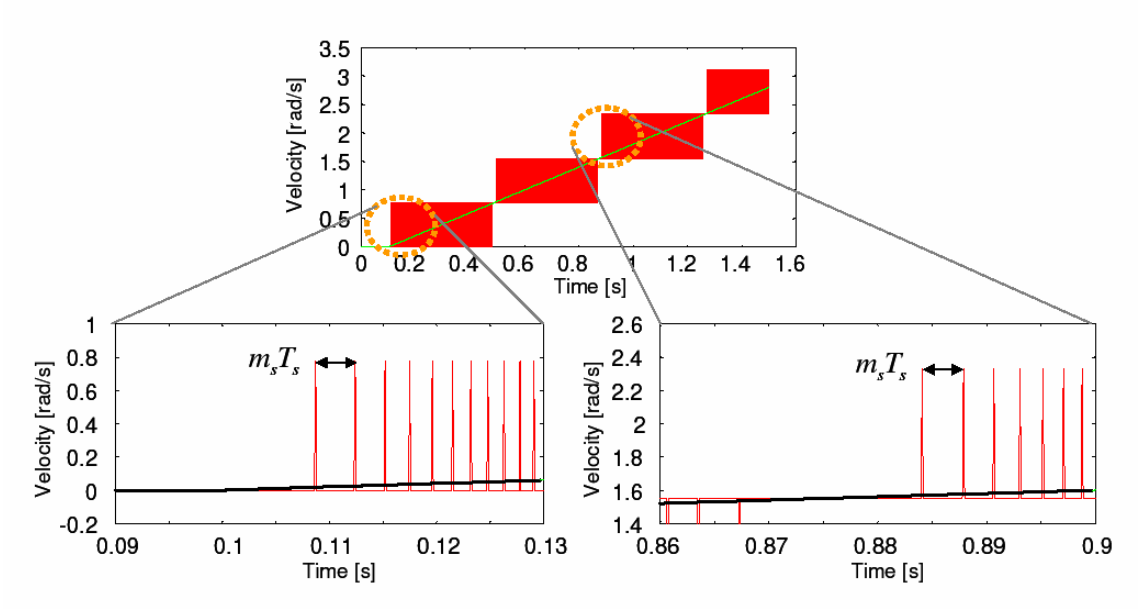

Figure 3-4 Pulse pattern in low and high speed range [18]

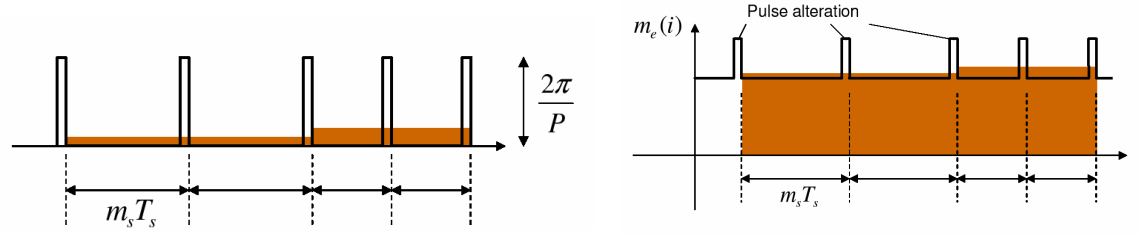

(a) Pulse pattern in low speed

(b) Pulse pattern in high speed

Figure 3-5 Similarity of pulse patterns [18]

Algorithm for the S method is quiet straightforward; encoder reading (m_e) is obtained in every sampling time, if a pulse alteration occur new velocity value ism updated by using (3.8) if no alteration occurred velocity value is not updated.

$$\bar{\omega}_S = \frac{2\pi \sum_{J=1}^{m_s} m_e(i-j)}{m_s P T_s} \tag{3.8}$$

3.2.6 Velocity Observer

Velocity observer can be also used in the system. There are various work for instantaneous speed estimation [23][85][86][56]. A combined structure using Kalman filter [56] with both velocity observer and measurement can supply more robust response.

3.2.7 Selection of the Velocity Measurement Method

Various works have been done in analyzing and comparing digital tachometer methods.[7],[18-[24]. The conclusion is that S & M/T methods are suitable for all speed ranges and S method measurement gives better absolute velocity measurement accuracy than M/T method. In the literature no details on implementation of S method are given.

3.2.8 Experimental investigation of S method

For the experimental work in this thesis S method has implemented and verified. Experiment setup in appendix 1 is used, as brief system has a 2 phase brushless DC motor and a 10K ppr optical quadrature encoder. All calculations are running on dSPACE 1103 real-time platform.

For investigation of S method, velocity is calculated with both M and S methods from the quadrature encoder input and compared. To include effects of high frequency vibrations coming from current controller a PID position controller has been implemented and velocity measurement done.

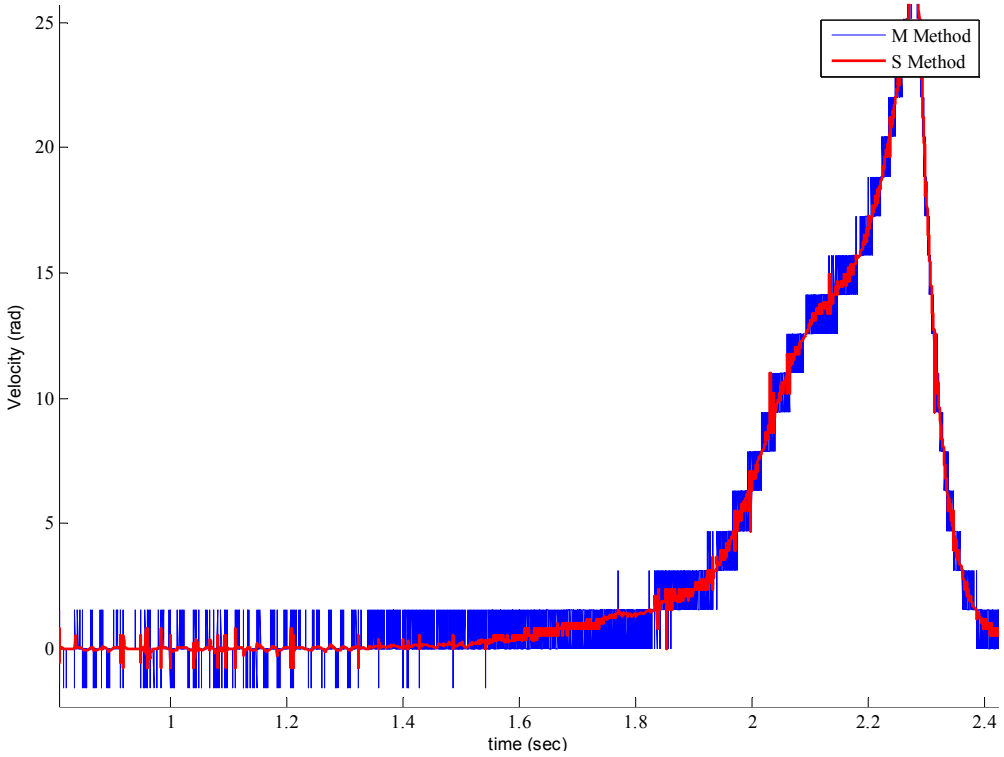

Figure 3-6 Velocity measurements done in M and S methods for 2.5 seconds.

Above you can see in Figure 3-6 above, M method has an oscillatory velocity measurement, On the other hand S method supplies better velocity signal with much less oscillations. In Figure 3-7, it is obvious that for low speed ranges response of the S method is much better. For high speed ranges Figure 3-8 shows that S method also achieves better results. In application Both M and S methods are used with low pass filters. In Figures 3-9 and 3-10 velocity measurements are with low pass filters. The signal of M method has a toothed signal shape and this cause very high noise when taking derivative of the velocity signals. Beside this, S method has noise level in acceleration calculation much less than M method. As a result of this experiment S method is selected for the velocity measurement method for this work. The C language code for M and S methods are given in in appendix 2.

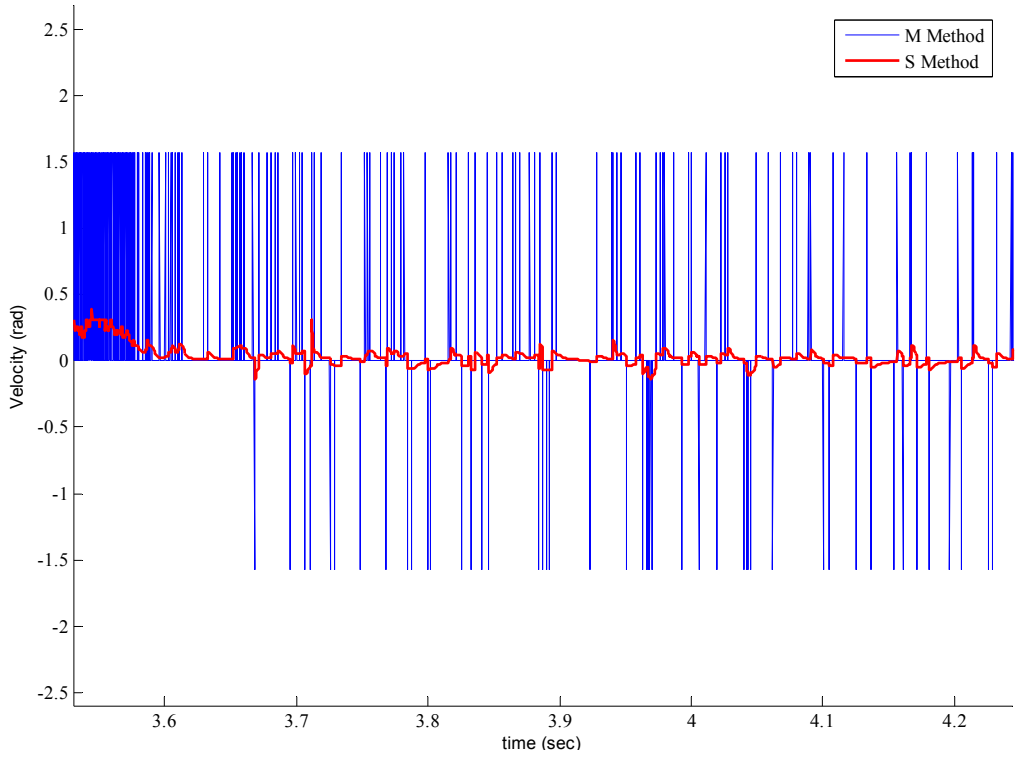

Figure 3-7 Velocity measurements for very low speed range done with M and S method

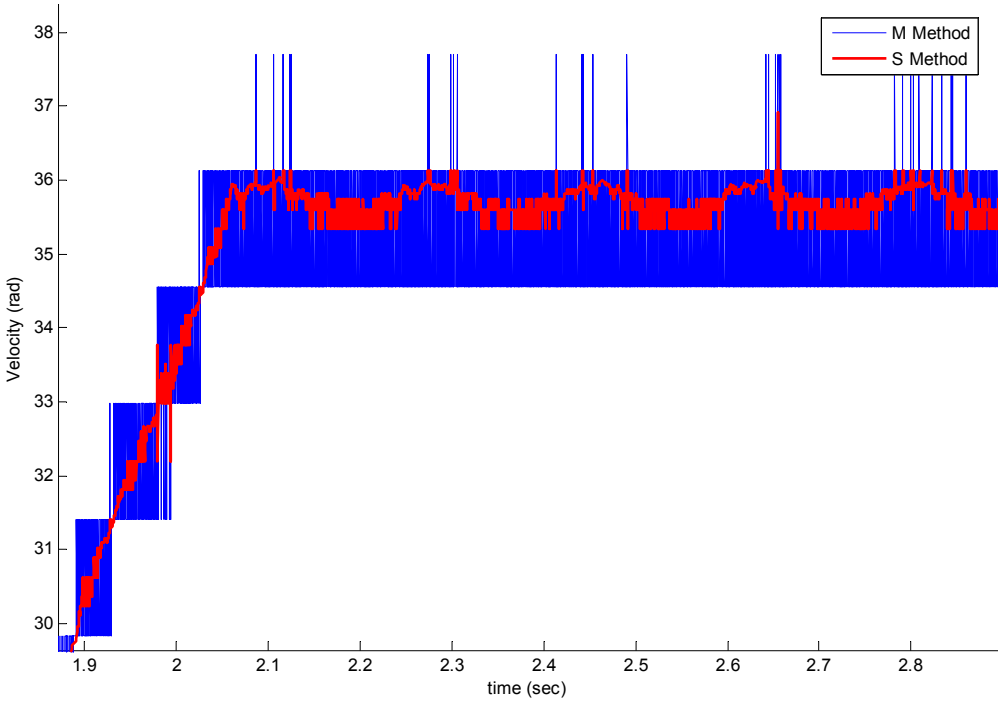

Figure 3-8 Velocity measurements for high speed range done with M and S method

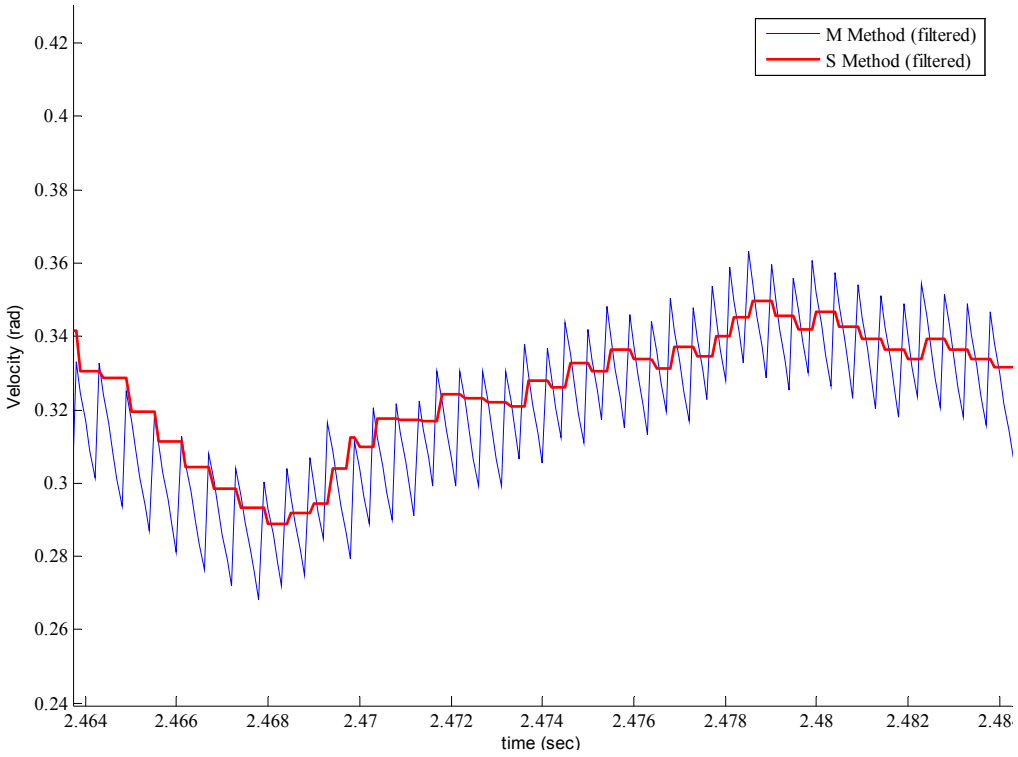

Figure 3-9 Velocity measurements for low speed done with M and S methods

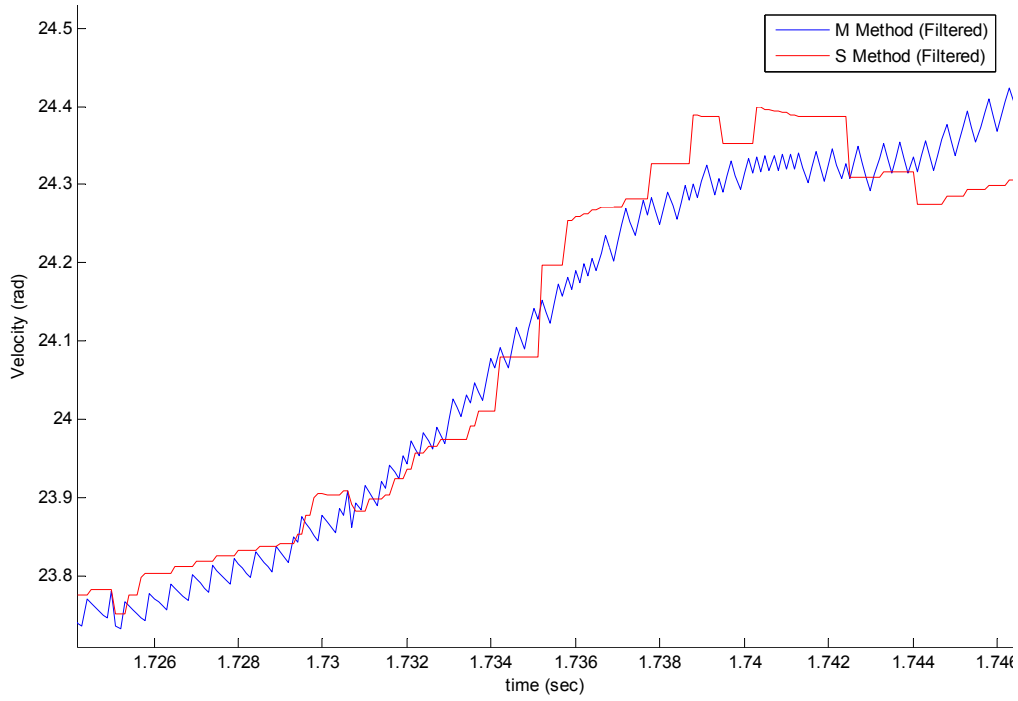

Figure 3-10 Velocity measurements for high speed range done with M and S methods

3.3 Force Measurement

For a better telepresence, sensation of the forces acting on the slave side is crucial. In this section force sensing and estimation methods will be presented. Force sensation by using force sensor and a force observer will be compared.

3.3.1 Force Sensor

Force sensors are used widely for force control to measure the external force acting on the system. There are mainly two different kinds of force sensors available in the market; force sensors based on strain gauges and piezo. Piezo force sensors can detect high frequency forces however low frequency force sensation is hard. Strain gauge force sensor is generally used for force control applications. [76]

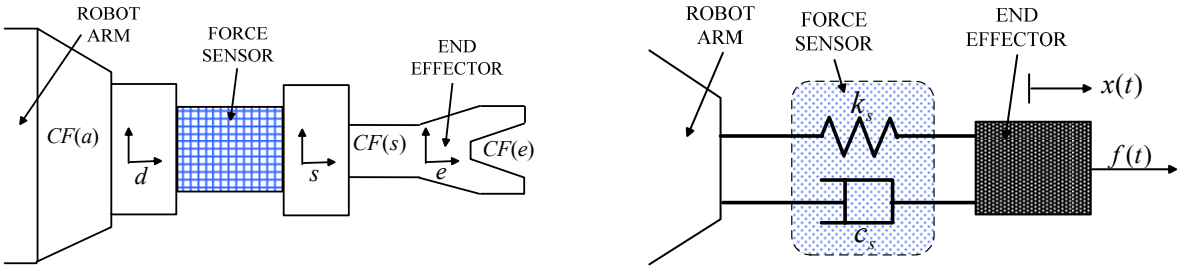

Figure 3-11 Simplified rigid body model of a robot with strain type force sensor and workpiece [39]

Since strain gauge is measuring the strain of the sensor, it has an elastic structure. A strain type force sensor can be simply modeled as a two mass resonant system as in Figure 3-11 [59][39]. Sensor is modeled with a stiffness K_s and a damping C_s. Force sensor forms a part of the control system and its dynamics affects the systems overall performance. However in many cases effects of force sensors are ignored or oversimplified in design of the controllers, [59] this causes instabilities in the control system. The force measurement bandwidth change should also taken into considerations during design otherwise system can enter instability [39][76].

Eppinger *et al.* [60] discusses the bandwidth limitations of the robot force control and emphasize the importance of force sensors dynamic properties in stability for force control. To overcome narrow bandwidth force detection designers tend to increase the viscous damping and slow down the system response to preserver stability [63]. As a result wide bandwidth force measurement for tasks requiring motion in a dynamic environment – being in contact and in free space - is a very challenging task with the current sensor technology.

3.3.2 Reaction Torque Estimator

Since the direct measurement of force in a wide bandwidth is not possible, Ohnishi *et al.* [25] proposed a method of reaction torque estimation based on the disturbance observer. The idea is very simple if one can develop methods to estimate parameters of the system and components of the disturbance torque that are not result of the reaction on system interaction with environment (friction etc.) than by subtracting these from total disturbance one can determine the reaction force. In ((2.8) disturbance torque acting on the system is defined. By subtracting the $\tau_{\text{int}} + B\omega + \Delta J \frac{d\omega}{dt} - \Delta K_t i^{ref}$ from observer input one can determine external (reaction) torque with the same bandwidth as disturbance.

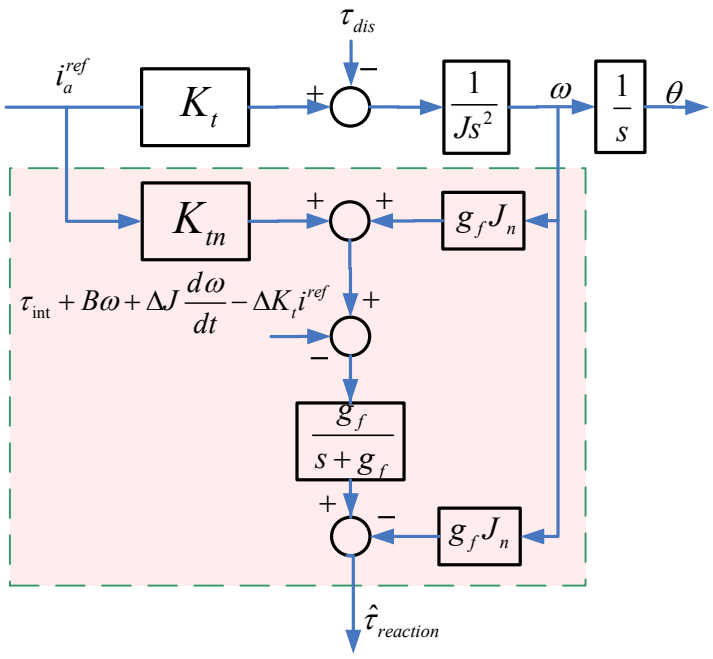

Figure 3-12 Reaction Torque Estimator [12]

3.3.3 Position Error Based Force Estimation

Position error based force estimation is a simple method of force estimation. In this approach robot's reaction to the external forces (impedance) need to be known. It is assumed that slave robot has a linear force-position relation. As an outcome force acting on the slave can be approximated by:

$$F_{ext} \approx Z_{sensor}(x_s - x_m) \tag{3.9}$$

Where Z_{sensor} stands for the slave robot mechanical impedance with respect to the tracking position error (x_s-x_m)

Success of the force sensation depends on the determination process of the friction and other disturbance components. Static friction has a highly nonlinear and discontinuous structure, so in this determination process static friction is very hard to capture and that causes problems. Our experimental setup suffers from friction affect correlated with angular position of the motor shaft due to the mechanical misalignment

between encoder and motor (see Figure 2-18). For accurate force estimation this affect should also identified as in section 2.4.

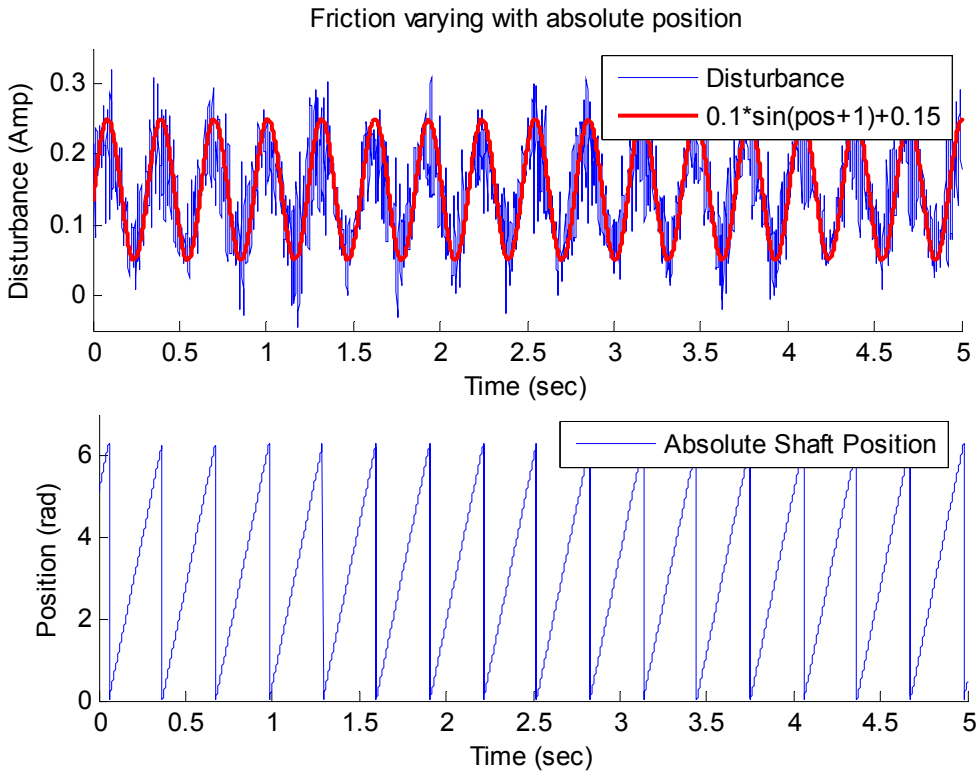

Figure 3-13 identification of friction varying with angle position

3.3.4 Discussion on Force Sensation

In [63] Katsura *et al.* showed that bandwidth force measurement wider than one obtained by force sensor, with reaction torque estimator is viable. They also validated the observer in experiment by achieving stable contact in force control with a 6 DOF robot arm.

As depicted in Figure 3-13 the disturbance observer is capable of detecting the lumped disturbance but detection of the separate components require designing specific experiments in order to single out specific component. For example, by keeping velocity constant the components related to the acceleration (or change of moment of inertia) will be eliminated from the disturbance observer output. The stiction force can be determined by sensing the maximum value of the current fed to the system for which

there is no motion. Similar experiments can be devised for other components of the disturbance torque. When all of these components are determined than just a subtraction as shown in Figure 3-13 will give a external (interaction) force component only.

The limitation on the bandwidth of the observer is discussed in the section 2.4. For tasks that doesn't require precise force measurements position error based force calculation can also be used for force feedback to the operator.

Chapter 4

Bilateral Control

In chapter 1 a general description and historical development of bilateral control has been given. In this chapter bilateral control will be discussed in more details. Scope of the bilateral control and teleoperation will be discussed first. Second, properties of an ideal bilateral control system will be addressed. Thirdly, time delay and its effects on bilateral control will be introduced. Stability, transparency, and scalability for bilateral control will be also argued. At the second subsection model of the human operator and the required limits of the bilateral control for a vivid force sensation will be reasoned. Bilateral control architectures will be examined and bilateral controller that is used in our experiments will be introduced. Experimental results will be discussed.

4.1 Teleoperation vs. Bilateral Control

In literature there are many different definitions for bilateral control, teleoperation, and haptics. The reason for such a complication is usage of the same terms by people from different areas for similar concepts in different contexts. The biggest complication is about the scope and the hierarchy of these terms. Which one of these three covers the others and which one is used for what? In this thesis the following definitions for these terms are used:

Teleoperation is operation of system from remote location, such as controlling an irrigation valve or controlling the Mars observer robots movements from a ground station.

Haptic is used for sense of touch. Master side of bilateral controllers mostly has haptic abilities delivering force sensation to the human operator. Haptic interfaces used

in applications that do not require bilateral control, like simulations, games etc so it can exist without bilateral control.

Bilateral control is control of a system mechanically coupled with environment (slave) by using another mechanically coupled system with human operator (master). Master side has the control over slave side with a force sensation from slave environment. These two sides don't have to be distant from each other so bilateral control can be without teleoperation like in robotic minimal invasive surgery.

As a result none of these three concepts includes others; they are closely related and used together with each other.

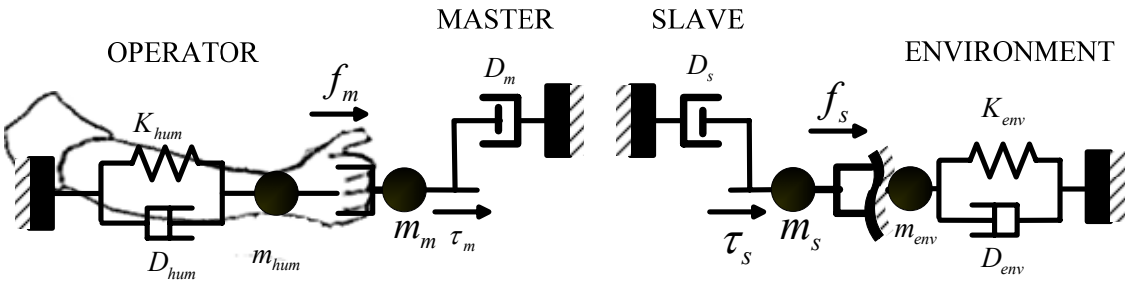

Figure 4-1 Mechanical representation of a bilateral system [2]

4.2 Representation of a Bilateral Control System

The components of a bilateral teleoperation system are: human operator, environment, master and slave robots, and communication channel. Human operator and environment are represented as impedances Z_h and Z_e [77]. Master and slave robot system are generally modeled as a two-port network [41] (Figure 4-2). It is common to analyze bilateral system as a electrical network where Mechanical Impedance is defined as the relation between the force and the velocities acting on a mechanical system. Admittance is also used sometimes representing the reciprocal of the impedance. Norton and Thevenin equivalents of human and environments are used in such analyses.[40]

$$F_e = Z_e V_e$$
$$F_h = Z_h V_h \tag{4.1}$$

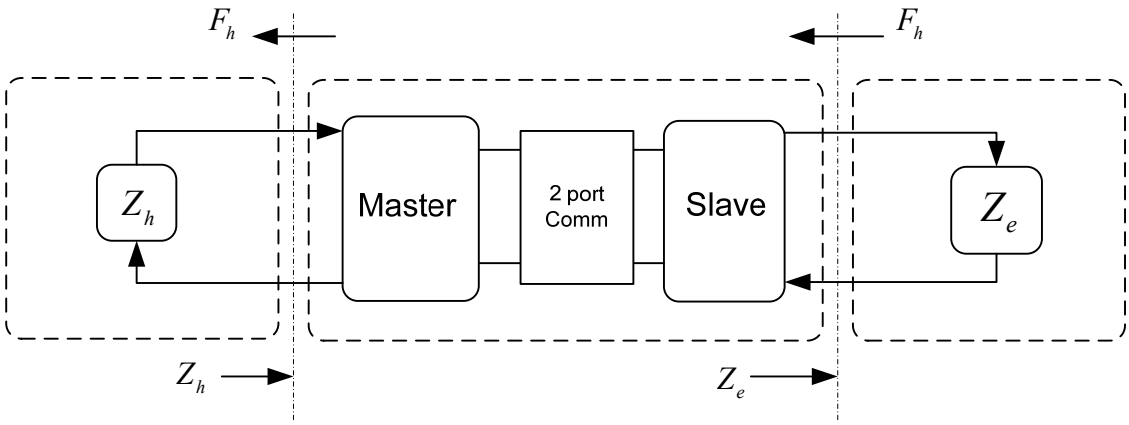

Figure 4-2 Two-port model of a bilateral teleoperation system [78]

When representing the bilateral system as a two-port network the impedance representation of the system can be utilized as in (4.2). *H* matrix representation of the bilateral system is also used for representing and analyzing the transparency of the system [41].

$$\begin{bmatrix} F_m \\ \dot{x}_m \end{bmatrix} = \underbrace{\begin{bmatrix} H_{11} & H_{12} \\ H_{21} & H_{22} \end{bmatrix}}_{H} \begin{bmatrix} \dot{x}_s \\ F_s \end{bmatrix}$$
$$H = \begin{bmatrix} Z_{in} & \text{Reverse Force Scale} \\ \text{Velocity Scale} & \dfrac{1}{Z_{out}} \end{bmatrix} \tag{4.2}$$

Besides *H* matrix, there are also other representations of the system in terms of dynamic relationship between master and the slave or human and the environment with admittance *Y*, impedance *Z* and inverse hybrid *G*.[40]

$$\begin{bmatrix} \dot{x}_h \\ \dot{x}_s \end{bmatrix} = Y \begin{bmatrix} F_h \\ F_s \end{bmatrix} \tag{4.3}$$

$$\begin{bmatrix} F_h \\ F_s \end{bmatrix} = Z \begin{bmatrix} \dot{x}_h \\ \dot{x}_s \end{bmatrix} \tag{4.4}$$

$$\begin{bmatrix} \dot{x}_h \\ F_s \end{bmatrix} = G \begin{bmatrix} F_h \\ \dot{x}_s \end{bmatrix} \tag{4.5}$$

4.3 Ideal Characteristics of Bilateral Control

In chapter 1 it is mentioned that Yokokohji *et al.* [2] defined ideal response of a bilateral system. He proposed three ideal responses for a bilateral system in three phases.

1 - Having the same position response at the master and the slave sides apart from of the object dynamics is the first one,

2 - Having the equal force response is the second one and the same force-position response is the third one.

3 - The third definition of Yokokohji gives the feel to the operator that he is working with the real object.

He defined this as the ideal kinesthetic coupling [2]. Equal impedances at the master and the slave sides is another ideal response definition [3]. By these definitions H (hybrid) matrix representation of an ideal bilateral teleoperator would be

$$H = \begin{bmatrix} 0 & 1 \\ -1 & 0 \end{bmatrix} \tag{4.6}$$

A mechanical analogy of an ideal bilateral system for 1 DOF arm would be two arms connected with a infinitely stiff, zero mass rod as in Figure 4-3.

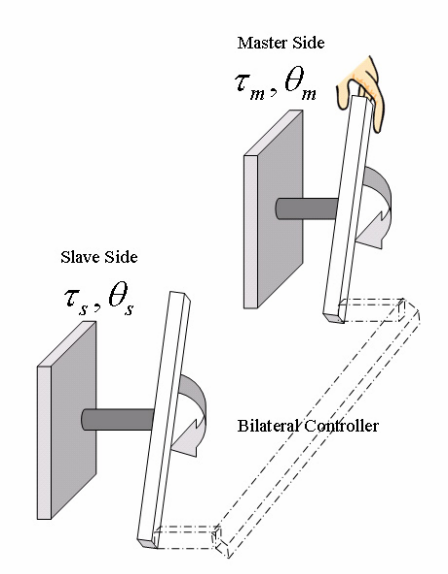

Figure 4-3 Rigid coupled Ideal Bilateral System [78]

4.3.1 Transparency as a Performance Index

Given the ideal response of the bilateral control system above, then the transparency as the evaluation index for a bilateral controller requires the master-slave-transmission line interaction to be invisible to the human operator. Katsura *et al.* showed that ideal transparency of a bilateral system is not possible even without time delay. [78][12].

Even though transparency is the evaluation index for ideality of the bilateral system, there is no an agreed numerical representation for transparency. Raju made experimental evaluation for maneuverability of bilateral systems [42]. Besides that on the design of the system [2] defined "Performance Index of Maneuverability", [43] defined "weighted distance of the hybrid matrix from the ideal hybrid matrix", [44] defined "Z-width factors", in [45] *Z*-width factors is combined with *H* matrix. [46] used a weighted norm of the sensitivity of the transmitted impedance to the changes in the environmental impedance. As a result nearly every group working in this area defined its own criteria. Among others hybrid matrix is the most commonly used to show the transparency of the system. [40]

4.3.2 Stability

Lawrence showed that transparency and stability of the system are two conflicting design goals in bilateral teleoperation systems [3]. On order to design a stable bilateral teleoperation system different methods have been proposed. Hannaford discussed design tradeoff and stability criteria based on transfer function of whole system including dynamic properties of hardware, operator and environment [70]. General teleoperator architecture in section 4.5.1 also provides a general structure to design stable transparent teleoperation considering both of the conflicting design rules.

Passivity based stability method approaches the problem by transforming teleoperation problem to a transmission line problem [66]. Several designs have been made based on this approach. Physically a device is passive if it is unable to increase total energy of the system, and for stability it is necessary and sufficient that system may interact only with passive environments. Human operator is definitely not passive however it is assumed that human operator will not try to destabilize system. [40][66]

Another approach to preserve stability is to add damping (losses) to the system. There are also works on observing the energy level of the system and changing the amount of damping required for the time in a real time basis. As a result transparency of the system only degrades when energy of the system needs to be damped.

Usage of disturbance observer in master and slave also increase the stability of the system, especially when systems are in contact with the environment.

4.3.3 Scaling

Most of the applications requiring bilateral control also require scaling to small scales like in micro assembly or in microsurgery. On the other hand human side should be amplified when the target is in a bigger scale than human by the means of force or position. Force and positional scaling can be applied to the hybrid matrix (4.2) as in (4.7).

$$x_s = \alpha x_m$$
$$F_h = -\beta F_s \tag{4.7}$$

The ideal H matrix becomes

$$H = \begin{bmatrix} 0 & -\beta \\ \alpha & 0 \end{bmatrix} \tag{4.8}$$

It is also suggested that for every bilateral control system human operator should fine-tune the scaling variables for own comfort and demands like resolution gains of mouse in personal computers.

4.3.4 Impedance Shaping

Since the ideal realization of the transparent bilateral system is not possible, another bilateral teleoperation design philosophy proposed. Rather than aiming to have a bilateral system that is fully transparent form user side, system can be constructed in a way that impedance perceived by the human operator is *shaped* in order to give a feeling of a virtual tool in operator's hand. By this method a human operator can execute a task easily designed suitably for a specific task.[40][71].

Impedance shaping gains importance particularly for cases which characteristic impedance of task and the operator are very different from each other like micro manipulation where forces in the micro scale are different from the operator scale. By using a bilateral controller and impedance-shaping the task space impedance can be altered in a way that operator perceives manipulation task as in macro scale.[71][72]. In addition to these Kobayashi *et al.* proposed concept of *time scaling* which can change the frequency response of task space in master side so human can work with the different frequency ranges easily. A micro object with a very high resonant frequency can be scaled to a lower resonant frequency.

4.3.5 Communication Time Delay

Communication channel in a bilateral teleoperation system has delay in its structure for various reasons like distance between two sides, and network structure. Since it is physically impossible to eliminate time delays in a network structure bilateral teleoperation with time delays has been a hot topic since 60's [65]. Supervisory control schemes with local intelligence requiring less real time communication have been developed and used in many teleoperator systems like underwater robots. In [66] passivity based approach is proposed, in [67] wave variables approach for passivity theory is proposed, in [3] a general architecture and made possible to analyze transparency and stability together of teleoperation systems with time delay is discussed. In [4] local force feedback for dealing with delays is introduced. There are many other works in literature for internet based communication and space teleoperation in varying delays and information loss presence.[68][69].

In this thesis work, whole bilateral control system is in one computer, so communication delay is not present and is out of our consideration.

4.4 Human Operator Modeling

Knowledge of the limits of the human operator is important and useful in design of a bilateral control system. Study of human operator should be done in two parts, human motion control and the human force perception. If the environment is assumed as passive, all of the motion is sourced from human operator. In [48][49] frequency response and the modeling of human arm is studied. In [50] is shown that actuation bandwidth ranges from 5 to 10 Hz. Çavuşoğlu *et al.* [46] obtained the range as described in (4.9) for a second order hand model with the Phantom haptic device. These values do change for the different configurations of the hand.

$$Z_h \in (m_h s^2 + b_h s + 1)k_h \text{ with } \begin{cases} 0 \le \mathrm{m_h} \le 0.05 \text{ kg} \\ 21 \le b_h \le \infty \text{ Ns/m} \\ 200 \le k_h \le 2000 \text{ N/m} \end{cases} \tag{4.9}$$

Human kinesthetic perception discussed in a very detailed way in [40]. Kinesthetic perception bandwidth up to 20-30 Hz has been reported and human tactile input up to 400Hz can be sensed. [47]. The motor and perceptive bandwidths of human operator are shown in Figure 4-4.

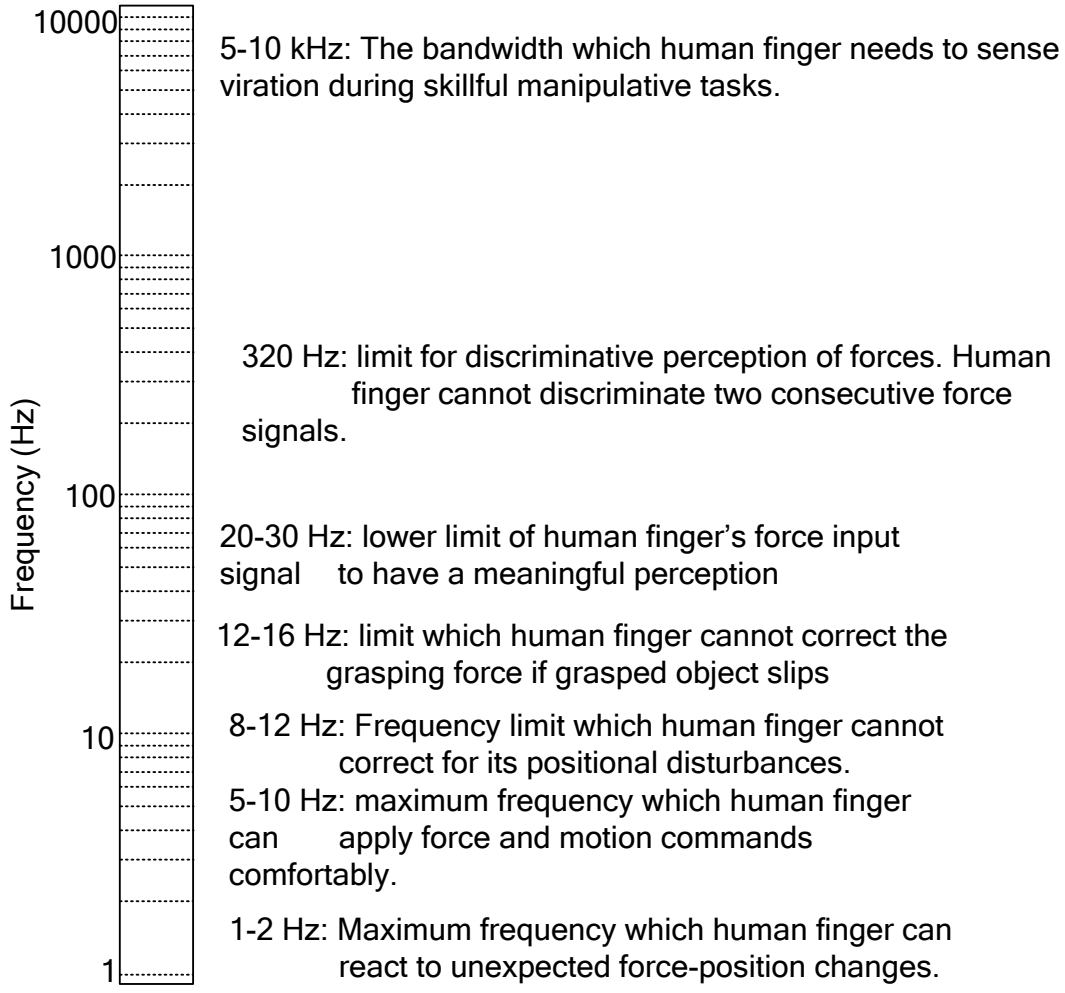

Figure 4-4: Overview of the bandwidths of different functionalities of the human finger [47]

4.5 Bilateral Control Architectures

Since the 40's various bilateral motion control schemes were developed. In this section common bilateral motion control architectures will be examined. Lawrance [3] proposed the general teleoperator architecture which enables to describe all bilateral control applications by suitable specialization of the subsystem dynamics. First this general architecture will be discussed. Following to that, various bilateral schemes will be argued based on the Lawrence's general architecture.

4.5.1 General Teleoperator Architecture

All linear time invariant teleoperation structures can be represented by changing the various subsystems in the general teleoperation architecture of Lawrence. This structure can be used to analyze and quantitatively compare performance indexes like stability and transparency. Figure 4-5 shows the block diagram of the general architecture. Hashtrudi-Zaad *et. al.* [45] has modified the architecture and added C_5,C_6 to the scheme for addition of local force feedback. Since structure is a LTI it is easy to find governing equations [40] . Human operator is modeled by impedance Z_h and a force $F_h^*(s)$, environment is modeled with impedance Z_e and assumed passive.

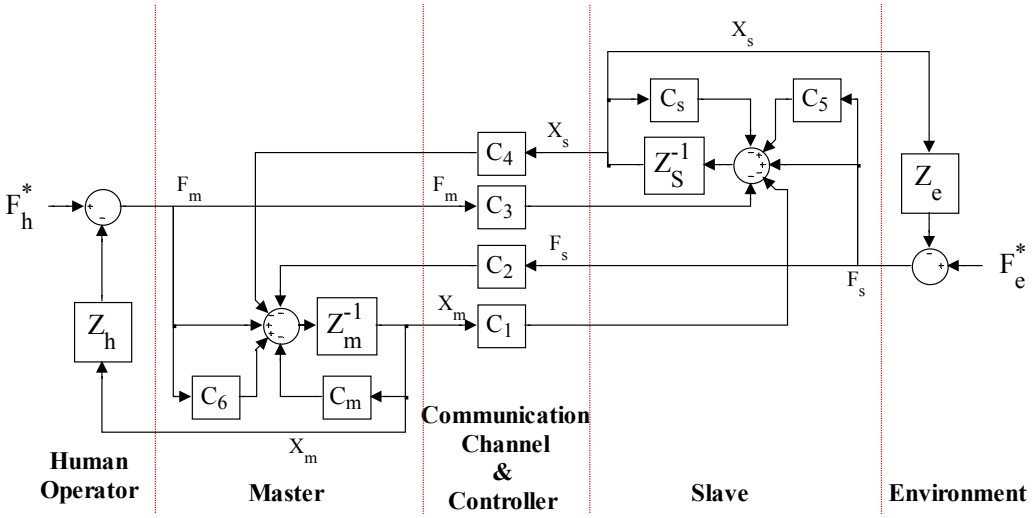

Figure 4-5 General Bilateral Teleoperator system Block Diagram, showing all subsystem dynamic blocks [3], modified as in [45]

Name	Block	Position - Force	Position - Position
Master Impedance	Z_m	$M_m s$	$M_s s$
Master Controller	C_m	B_m	B_m+K_m/s
Slave Impedance	Z_s	$M_s s$	$M_s s$
Slave Controller	C_s	B_s+K_s/s	B_s+K_s/s
Velocity Channel	C_1	B_s+K_s/s	B_s+K_s/s
Force Channel	C_2	K_f	Not used
Velocity Channel	C_3	Not used	$-(B_s+K_s/s)$
Force Channel	C_4	Not used	Not used
Slave Controller Add-on	C_5	Not used	Not used
Master Controllers Add-on	C_6	Not used	Not used
Operator Impedance	Z_h		Not a function of
Environment Impedance	Z_e		Not a function of

Table 4-1 Nomenclature and typical values of subsystems in the general teleoperator architecture of Figure 4-5

Based on such structure the hybrid matrix H can be easily determined as in (4.10)

$$h_{11} = \frac{(Z_m + C_m)(Z_s + C_s) + C_1 C_4}{(1 + C_6)(Z_s + C_s) - C_3 C_4} \tag{4.10}$$

$$h_{12} = \frac{C_2 (Z_s + C_s) - (1 + C_5) C_4}{(1 + C_6)(Z_s + C_s) - C_3 C_4} \tag{4.11}$$

$$h_{21} = \frac{C_3 (Z_m + C_m) + (1 + C_6) C_1}{(1 + C_6)(Z_s + C_s) - C_3 C_4} \tag{4.12}$$

$$h_{22} = \frac{(1 + C_5)(1 + C_6) - (C_2 + C_3)}{(1 + C_6)(Z_s + C_s) - C_3 C_4} \tag{4.13}$$

Total impedance practiced by the human operator (Z_{to}) can be calculated from the relation of force on the master side F_m and the master velocity V_m.

$$Z_{to} = \frac{F_m}{V_m} = h_{11} - \frac{h_{12} h_{21}}{1 + h_{22} Z_e} Z_e \tag{4.14}$$

By using H matrix derived for the general architecture in (4.10)-(4.13) impedance experienced by the human operator for the general architecture becomes.

$$Z_{to} = \frac{(Z_m + C_m)(Z_s + C_s) + (\ ) + Z_e\left((1 + C_5)(Z_m + C_m) + C_1C_2\right)}{(Z_s + C_s)(1 + C_6) - C_3C_4 + Z_e\left((1 + C_5)(1 + C_6) - C_2C_3\right)} \tag{4.15}$$

Having (4.15) it is easy to take a look at influence of different blocks. As mentioned earlier there are many different schemes proposed in literature. Below some common bilateral teleoperation controllers presented in literature will be discussed on the basis of the general architecture.

4.5.2 Two channel Bilateral Control Architectures

4.5.2.1 Position – Force scheme (Direct Force Feedback)

In this scheme master's position is given as reference to the position controller at the slave side, Force acting on the slave manipulator is fed to the force controller at the master side in reverse direction.

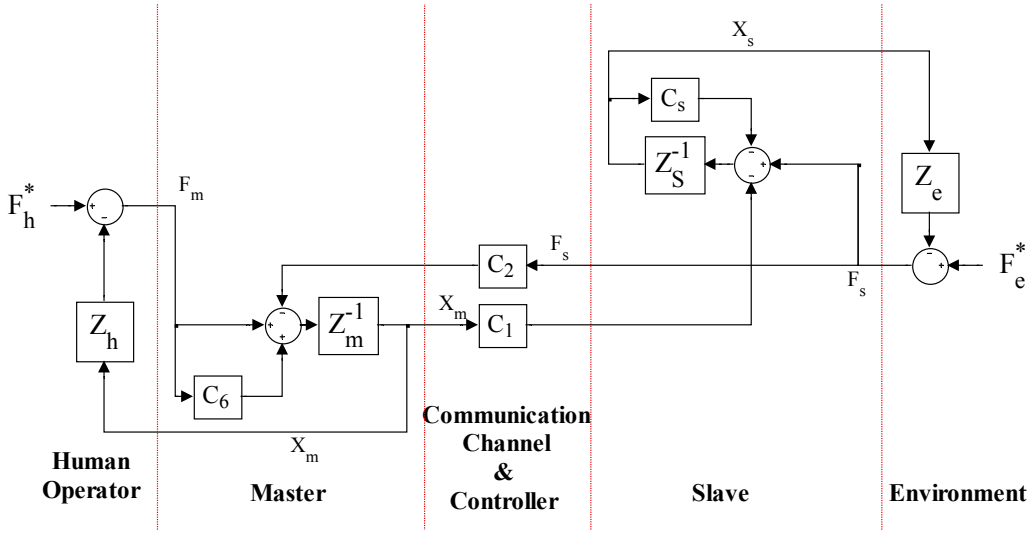

Figure 4-6 Direct Force Feedback scheme in General Architecture

General	C_1	C_2	C_3	C_4	C_5	C_6	C_S	C_m
Position-Force	αC_5	βC_6	0	0	0	C6	Cs	0

Table 4-2 Variable map for Position Force (DFF) scheme

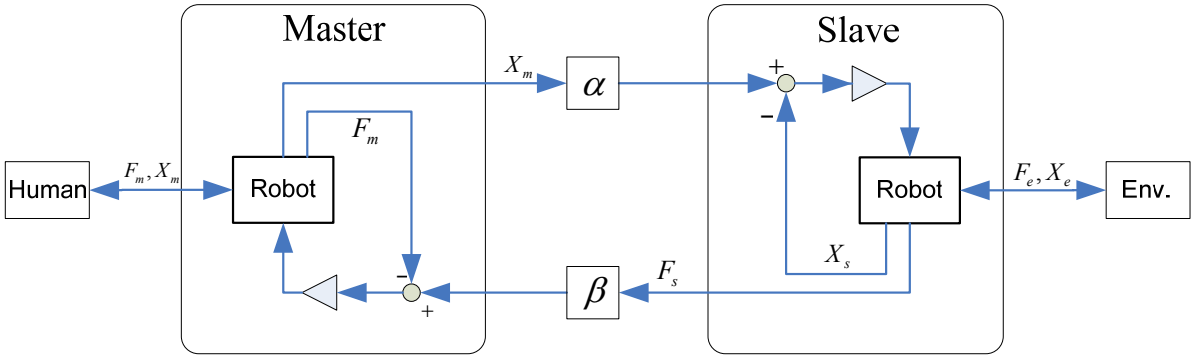

Figure 4-7 Direct Force Feedback Scheme

Hybrid matrix for the position – force scheme H can be calculated by (4.10)-(4.13) and using the variable map in Table 4-2 as

$$H = \begin{bmatrix} \dfrac{Z_m + C_m}{1 + C_6} & -\dfrac{C_2}{1 + C_6} \\ \dfrac{C_1}{Z_s + C_s} & \dfrac{1 + C_5}{Z_s + C_s} \end{bmatrix} \tag{4.16}$$

$$Z_{to} = \frac{Z_m}{1 + C_6} + \frac{C_1 C_2}{(1 + C_6)(Z_s + C_s + Z_e)} \tag{4.17}$$

4.5.2.2 Position-Position scheme

In position-position architecture only positional information is exchanged bi-directional between master and slave sides. Position tracking and force feedback is controlled with only the position data. This architecture can be useful if master and slave sides have good tracking capabilities [40][3].

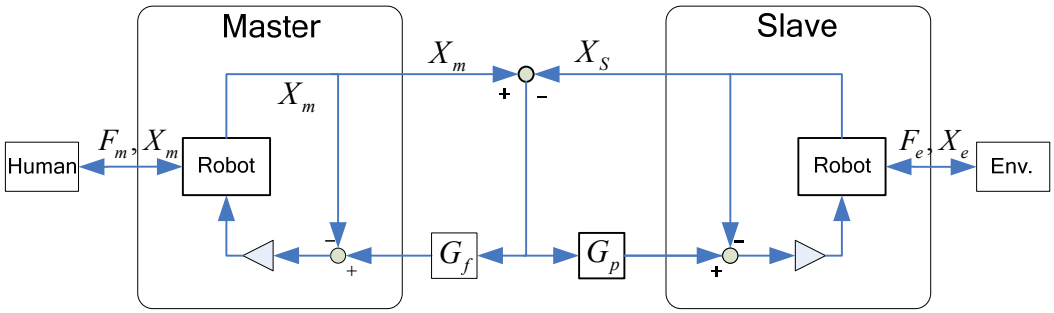

Figure 4-8 Position – Position Architecture for bilateral control

General	C_1	C_2	C_3	C_4	C_5	C_6	C_s	C_m
Position - Position	G_pC_s	0	0	G_fC_m	0	0	$C_s(1+G_p)$	$C_m(1-G_f)$

Table 4-3 Variable map for Position- Position scheme

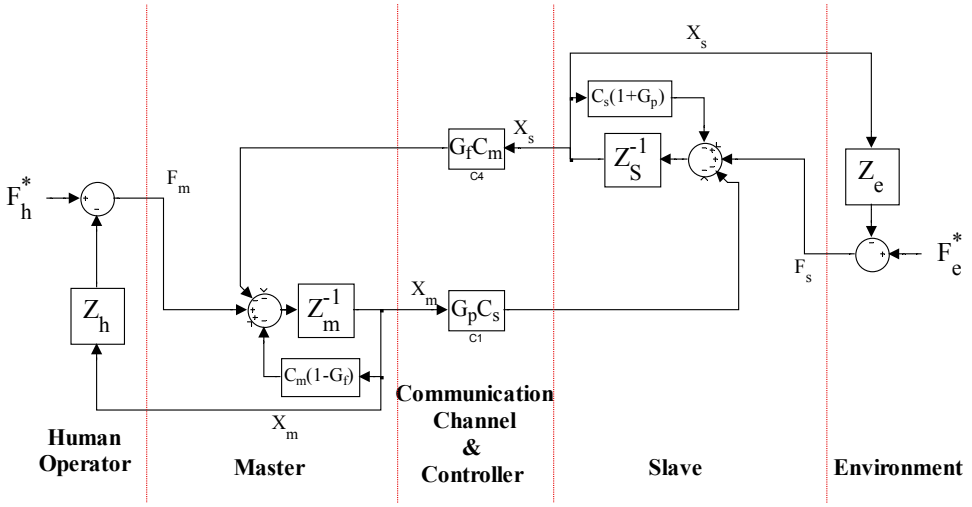

Figure 4-9 Position – Position scheme on general Architecture

4.5.2.3 Position Error Based Position Force Architecture

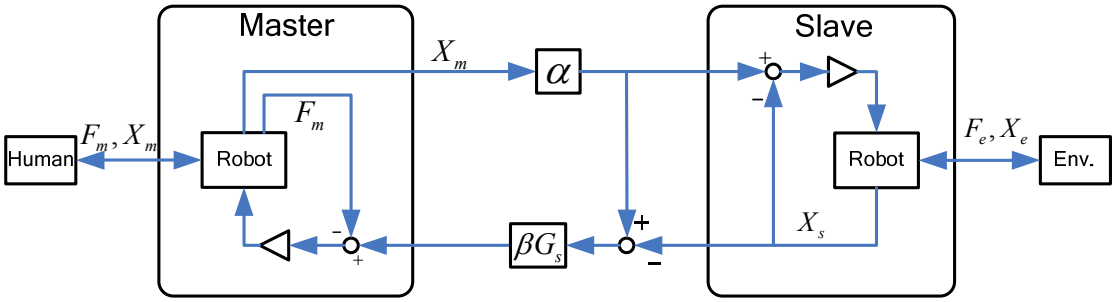

Figure 4-10 Position error based Position force architecture

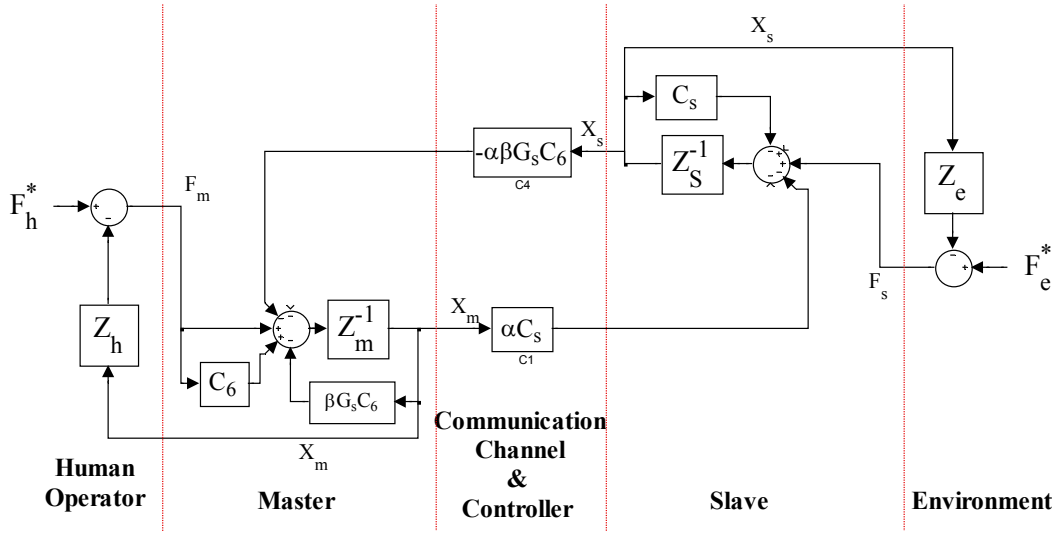

This scheme is another version of position-position architecture. The force acting on the slave system is estimated from the position error of slave side as discussed in section 3.3. This force is than fed back to the master. This scheme is useful as it decouples motion tracking of slave from the force feedback of master side [40].

H matrix for the Position Error bases Force feedback architecture becomes:

$$H = \begin{bmatrix} \dfrac{(Z_m + C_m)(Z_s + C_s) + C_1 C_4}{(1 + C_6)(Z_s + C_s)} & -\dfrac{C_2}{(1 + C_6)(Z_s + C_s)} \\ \dfrac{C_1}{Z_s + C_s} & \dfrac{1}{Z_s + C_s} \end{bmatrix} \tag{4.18}$$

4.5.2.4 Force-Force Architecture

In Force-Force architecture force information from two sides are exchanged bi-directional, since just force information is sent to the other side position drifts do occur (result of an open force-position, integrator in the structure). This architecture was implemented by [51], They reported positional drift between master and slave sides and offered a periodic position initialization between two sides. Because of this drift force-force architecture doesn't have too many followers [40].

4.5.2.5 Force Position Architecture

Force position architecture is the inverse of the position-force architecture. Force applied on the master robot is sent to the slave robot as a force reference, resulting position of the slave robot is than fed back to the master side position controller. In [52] this control structure is analyzed in details however application example is hard to find in literature [40].

4.5.3 Four Channel Bilateral Control Architectures

In four channel bilateral control scheme, force and position (or velocity) information are exchanged bidirectional. As all four channels are used general bilateral architecture applies to this scheme directly without simplification. Many researchers used four channel controllers with different approaches in literature. Lawrance [53] designed a theoretically transparent (according to his definition) four-channel bilateral control scheme and applied on his general teleoperation architecture. Zhu and Salcudean [54] applied the rate control to four channel architecture for transparent operation in rate control method. Sumiyoshi and Ohnishi also used a 4 channel architecture modified from General architecture based on compliance control. [3][18][40][55]

4.5.4 Four-Channel parallel Type Bilateral Controller Based on Natural Law

Katsura [76] introduced in idea of a four-channel parallel type bilateral controller based natural motion control. This controller can be used in situations where master and slave side robots are identical and impedance characteristics of the environment are compatible with the impedance of the human limb. Application to the systems that have different dynamics is very complicated.

In order to test the performance of the bilateral control system in this work we implemented full four channel bilateral control as shown below. Formulation of the parallel controller follows [76] closely for the system that have the same parameters. At the end of the chapter the implementation of the four channel bilateral control for systems that have different parameters is formulated.

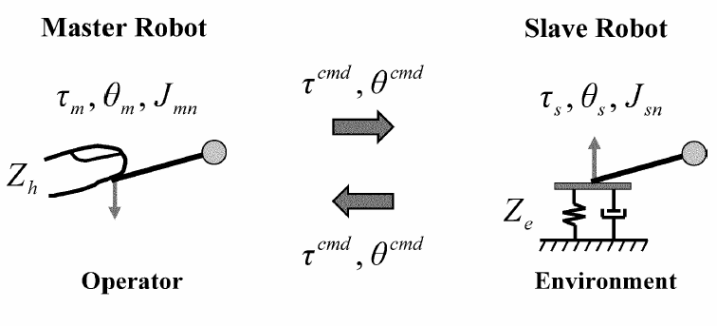

Figure 4-11 Model of a 4 channel bilateral control system

Ideal response of a bilateral system should have the same positions and the same amplitude but opposite sign torques developed at slave and master side. For bilateral system without contact with environment on the slave side tehis formulation gives

$$
\begin{aligned}
&\theta_m^{res} - \theta_s^{res} = 0 \\
&\tau_m^{res} + \tau_s^{res} = \frac{1}{2}(M_c + M_{hum})(\ddot{\theta}_m^{res} + \ddot{\theta}_s^{res}) \\
&+\frac{1}{2}(D_c + D_{hum})(\dot{\theta}_m^{res} + \dot{\theta}_s^{res}) \\
&+\frac{1}{2}(K_c + K_{hum})(\theta_m^{res} + \theta_s^{res}) \\
&\tau_m^{res} + \tau_s^{res} = \frac{1}{2}(M_c s^2 + D_c s + K_c + Z_{hum})(\theta_m^{res} + \theta_s^{res})
\end{aligned}
\tag{4.19}
$$

$$
Z_{hum} = (M_h s^2 + D_h s + K_h) \tag{4.20}
$$

When in contact with the environment having impedance Z_e the system becomes

$$
\begin{aligned}
&\theta_m^{res} - \theta_s^{res} = 0 \\
&\tau_m^{res} + \tau_s^{res} = \frac{1}{2}(M_c + M_h + M_{env})(\ddot{\theta}_m^{res} + \ddot{\theta}_s^{res}) \\
&+\frac{1}{2}(D_c + D_h + D_{env})(\dot{\theta}_m^{res} + \dot{\theta}_s^{res}) \\
&+\frac{1}{2}(K_c + K_h + K_{env})(\theta_m^{res} + \theta_s^{res}) \\
&\tau_m^{res} + \tau_s^{res} = \frac{1}{2}(M_c s^2 + D_c s + K_c + Z_h)(\theta_m^{res} + \theta_s^{res})
\end{aligned}
\tag{4.21}
$$

$$
Z_e = (M_{env} s^2 + D_{env} s + K_{env}) \tag{4.22}
$$

A force controller C_F and a position controller C_P are combined together in Figure 4-12 and form a force-position controller in acceleration dimension. To have an ideal response with a parallel structure torque and position commands to the systems are as follows.

$$
\begin{aligned}
&\theta_m^{cmd} = \theta_s^{cmd} = \frac{1}{2}(\theta_m^{res} + \theta_s^{res}) \\
&\tau_m^{cmd} = \tau_s^{cmd} = \tau_m^{res} + \tau_s^{res}
\end{aligned}
\tag{4.23}
$$

τ_m^{res} and τ_s^{res} are the observed external torques acting on the master and the slave sides with the reaction force observer.

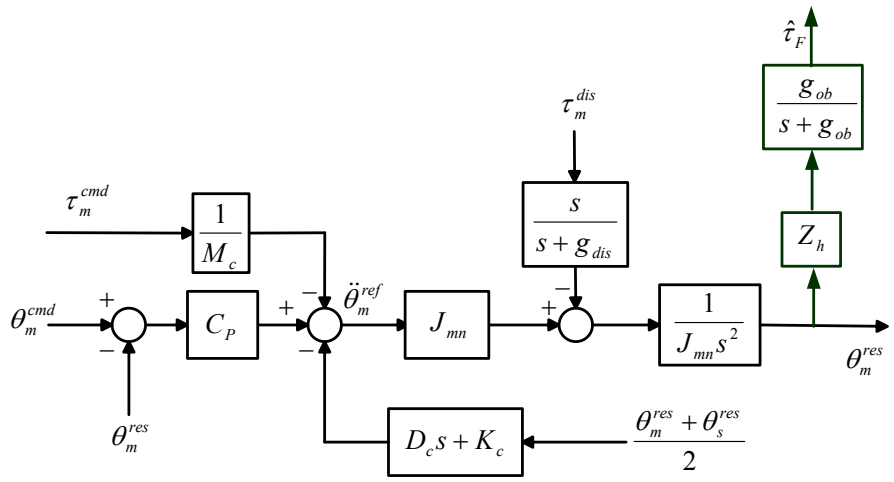

Figure 4-12 Force – Position control of master system in acceleration dimension

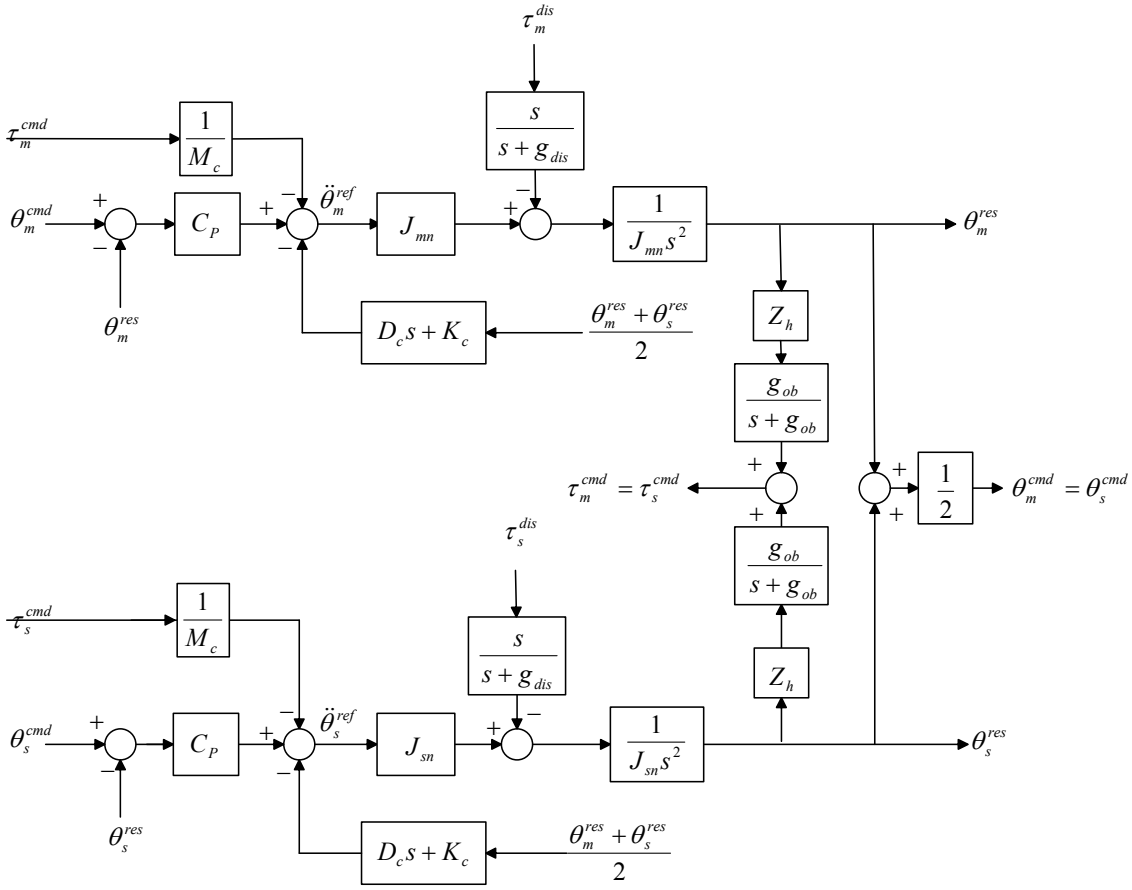

Figure 4-13 Four channel parallel type Force-position bilateral controller

Above solution and analysis is applicable for a bilateral system with identical dynamics on both slave and master side. That situation is unlikely in real applications. Because of this it is important to formalize the bilateral control system framework acting on two dynamically different systems. Desired ideal response of a bilateral system is described as

$$\begin{aligned} \theta_m &= \theta_s \\ \tau_m &= -\tau_s \end{aligned} \tag{4.24}$$

Dynamic models of the systems can be written as (4.25), τ^{dis} is the disturbance torque defined in chapter 2.

$$\begin{aligned} J_m\ddot{\theta}_m &= \tau_m - \tau_m^{dis} \\ J_s\ddot{\theta}_s &= \tau_s - \tau_s^{dis} - \tau_s^{ext} \end{aligned} \tag{4.25}$$

By adding disturbance observer output having first order LPF to the input of the system, dynamic equations (4.25) of the system turn into (4.26).

$$\begin{aligned} J_{mn}\ddot{\theta}_m &= \tau_m - \left(1 - \frac{g_{dis}}{s + g_{dis}}\right)\tau_m^{dis} \\ J_{sn}\ddot{\theta}_s &= \tau_s - \left(1 - \frac{g_{dis}}{s + g_{dis}}\right)\tau_s^{dis} - \tau_s^{ext} \end{aligned} \tag{4.26}$$

The term multiplying disturbance is a real differentiator which have very small gain for low frequencies thus making second term in both equations small if the disturbance torque is low frequency signal. In ideal conditions cutoff frequency of the disturbance observer is infinite and system's dynamic equation can be rewritten as (4.27).

$$\begin{aligned} J_{mn}\ddot{\theta}_m &= \tau_m \\ J_{sn}\ddot{\theta}_s &= \tau_s - \tau_s^{ext} = \tau_s' \end{aligned} \tag{4.27}$$

A bilateral control should be designed in such a way that the conditions (4.24) are satisfied. A design procedure that takes into consideration the stability of the bilateral system is outlined below. By defining ε_+ and ε_- as

$$\theta_m - \theta_s = \varepsilon_- \tag{4.28}$$

$$\theta_m + \theta_s = \varepsilon_+ \tag{4.29}$$

One can find the description of the bilateral system motion using new variables ε_+ and ε_-. Here we will first look at the problem for bilateral system with identical dynamics on the master and the slave sides. Assuming $J_m = J_s = J_n$ and assuming that disturbance observer loop is adjusted properly, by subtracting equations in (4.27) form each other gives (4.30).

$$J_n \ddot{\varepsilon}_- = \tau_m - \tau_s + \tau_s^{ext} = \tau_m - \overbrace{(\tau_s - \tau_s^{ext})}^{\tau_s'} = \tau_m - \tau_s' = \tau_- \tag{4.30}$$

Adding two equations in (4.27) together gives (4.31).

$$J_n \ddot{\theta}_m + J_n \ddot{\theta}_s = J \ddot{\varepsilon}_+ = \tau_m + \tau_s' = \tau_+ \tag{4.31}$$

τ_-, τ_+ are defined as the difference and the sum of the torques of the master and slave robots. Equations (4.30) and (4.31) represent virtual plants with control inputs τ_-, τ_+ which should be selected in such a way that ε_+ and ε_- are forced to be zero. If ε_+ and ε_- are forced to be zero than conditions for bilateral control (4.32) are fulfilled. The design could be easily done due to the fact that we are having two double integrator systems and making selection that the zero solution is stable should not represent any problem. Any controller that makes zero value of ε_+ and ε_- stable can be used. PD controller seems the simplest and it had been selected to be used in our experiments. Having designed controller for virtual plants (4.30) and (4.31) torque commands for master and slave systems can be calculated in terms of τ_- and τ_+ as given in the equations (4.32) and (4.33) thus completing the bilateral control design..

$$\begin{aligned}
\tau_m + \tau_s' &= \tau_+ \\
\tau_m - \tau_s' &= \tau_- \\
2\tau_m &= \tau_+ + \tau_- \\
\tau_m &= \frac{\tau_+ + \tau_-}{2}
\end{aligned} \tag{4.32}$$

$$\begin{aligned}
\tau_m + \tau_s' &= \tau_+ \\
\tau_m - \tau_s' &= \tau_- \\
2\tau_s &= \tau_+ - \tau_- \\
\tau_s &= \frac{\tau_+ - \tau_-}{2}
\end{aligned} \tag{4.33}$$

If dynamics of master and slave sides are not the same, assumption done in (4.30) becomes invalid. In this situation there are two possible solutions:

- first one can use the fact that by applying disturbance observer the moment of inertia of master and slave systems can be changed. According to results reached in section 2.3 too large difference between real and nominal moment of inertia would influence the behavior of the system with disturbance observer. Because of this a solution is not recommended for systems where master and slave are very different.

- Another solution to the four channel architecture for master and slave system with different inertias is given below. For the position error ε_- the motion is defined as in (4.34).

$$\ddot{\varepsilon}_- = \ddot{\theta}_m - \ddot{\theta}_s = \frac{\tau_m}{J_{mn}} - \frac{\tau_s'}{J_{sn}} = \ddot{\theta}_- \tag{4.34}$$

For the ε_+ equation can be written as in (4.35).

$$\tau_m + \tau_s' = J_{mn}\ddot{\varepsilon}_+ - \left(\frac{\Delta J_n}{J_{sn}}\right)\tau_s'$$

$$\ddot{\varepsilon}_+ = \frac{1}{J_{mn}}\tau_m + \frac{1}{J_{sn}}\tau_s' = \ddot{\theta}_+ \tag{4.35}$$

$$\Delta J_n = J_{mn} - J_{sn}$$

One can take $\ddot{\theta}_-$ and $\ddot{\theta}_+$ as the control input in (4.34) and (4.35) (the same idea is used in acceleration controller). Now the procedure is the same as in the previous case. By designing the control inputs $\ddot{\theta}_-$ and $\ddot{\theta}_+$ of the virtual plants (4.34) and (4.35) in such a way the zero values for ε_+ and ε_- are stable torque commands for master and slave systems can be calculated in terms of $\ddot{\theta}_-$ and $\ddot{\theta}_+$ as given in the equations (4.36).

$$\begin{aligned}
&\frac{\tau_m}{J_{mn}} - \frac{\tau_s'}{J_{sn}} = \ddot{\theta}_- \\
&\frac{\tau_m}{J_{mn}} + \frac{\tau_s'}{J_{sn}} = \ddot{\theta}_+ \\
&\ddot{\theta}_+ + \ddot{\theta}_- = 2\frac{\tau_m}{J_{mn}} \rightarrow \tau_m = \frac{\ddot{\theta}_+ + \ddot{\theta}_-}{2} J_{mn} \\
&\ddot{\theta}_+ - \ddot{\theta}_- = 2\frac{\tau_s'}{J_{sn}} \rightarrow \tau_s' = \frac{\ddot{\theta}_+ - \ddot{\theta}_-}{2} J_{sn}
\end{aligned} \tag{4.36}$$

Solution given in (4.36) is representing a generalized solution of the control system design for bilateral systems with different dynamics of the master and slave side. . It can be easily shown that Katsura *et.al.* [76] solution is a special case of this.

The design of the controller is not specifically treated here since that is a straight forward for double integrator systems. In the case that disturbance observer is not used, thus the original dynamics of the system is not reduced to the double integrators the design of the controller may be more complicated. That may explain the large number of different approaches to this problem present in the literature.

4.6 Performance Improvements for Bilateral Control

Due to the stringent requirements and complex structure the selection of controllers in bilateral control system is a challenge that has been attacked using many different control system design paradigms like compliance control [79] to deal with instability caused by delayed force reflections in system, local force feedback [4][45] and loop shaping tools [56][80] to increase stability, H_∞ control [81], model predictive control [78] and robust acceleration control [25] for canceling non-idealities , rate control [8][54] to overcome workspace limitations, adaptive control [67[82][83] to estimate parameters and environmental properties, Modal decomposition and functional control for decentralizing control structure [84]. There may be also other methods to increase the operational performance of the bilateral control system.

In this work the four channel bilateral control scheme is implemented and based on the acceleration controller discussed in chapter 2 with improvements in the system position and velocity measurement as discussed in chapter 3 and the disturbance observer as discussed in chapter 2.

4.7 Experimental Results

In appendix 1 experiment setup is described in details. Briefly, xperimental system is composed of two set of 400 watts 3-phase Maxon brushless DC motor working in current regulation mode with its own driver, a 10000 ppr encoder is connected to the motor shaft for high resolution position and velocity measurement. Whole system is connected to a dSPACE® 1103 real-time controller with a 100 usec measurement rate and a 1 msec control output rate as discussed in section 2.4. S method is used as the velocity measurement method as discussed in section 3.2.

In the following subsections the experimental results are presented in order to demonstrate the flexibility of the system and the basic functionality of different bilateral control schemes. The following structural components are applied; S method velocity measurement for precise velocity measurement as discussed chapter 3, Disturbance observer with variable and fixed step time on each axis as in chapter 2, Reaction force observer as discussed in chapter 3.

For each component application code is given in appendix C. The structure is developed in such a way that allows easy modification of controllers and measurement algorithms so to allow experimental verification of different bilateral control schemes.

4.7.1 Position Tracking

Position tracking is the main goal of a bilateral control system. Slave side tracks the position of the master with a low positional error at rate of 10^{-3} radians as depicted in Figures 4-14 and 4-15.

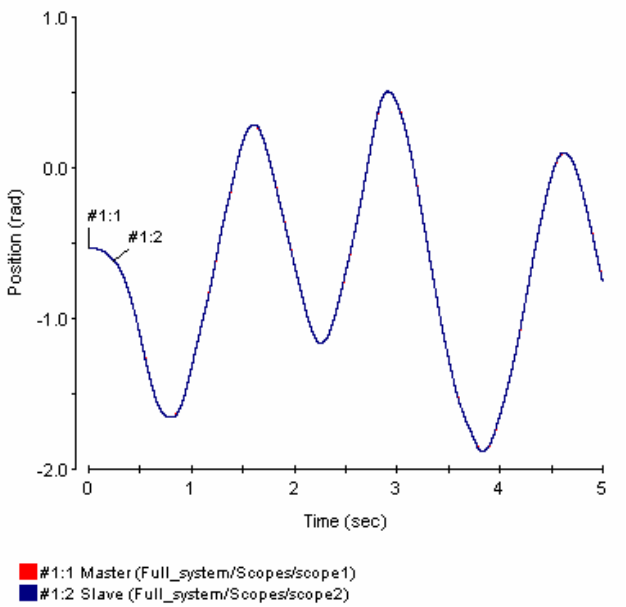

Figure 4-14 Position tracking of master and slave sides

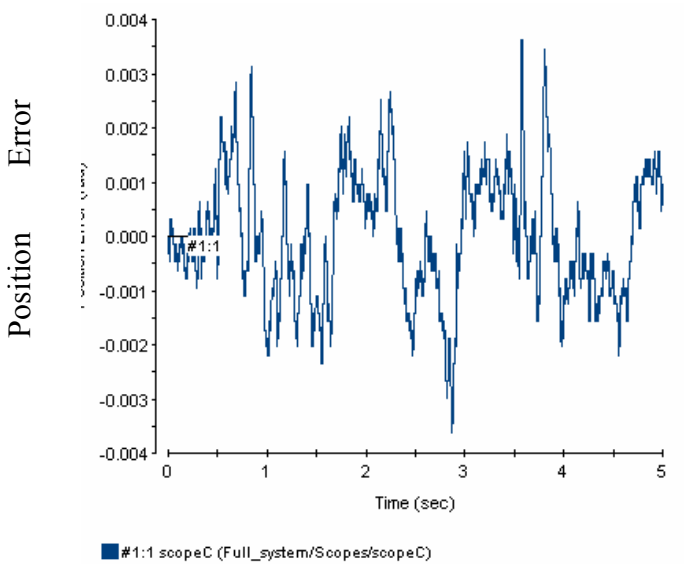

Figure 4-15 position error between master and slave without contact with the environment

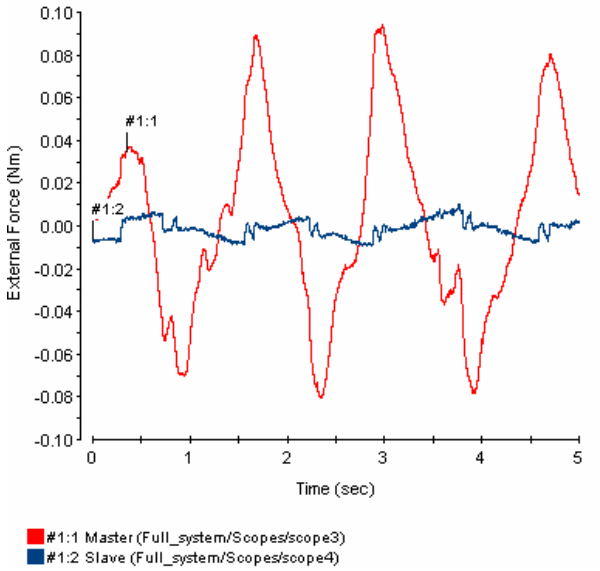

Figure 4-16 External torques acting on the master and slave sides

As we are applying force (torque) to the master side to move it external force is observed at master side. On the other hand as slave side is not in contact with any object there is no external force acting on it.

In order to demonstrate the behavior of the system the experiments are performed when slave side is in contact with soft environment (sponge) and hard environment (aluminum bar) as presented in the following 4.7.2 and 4.7.3.

4.7.2 Contact with the soft environment

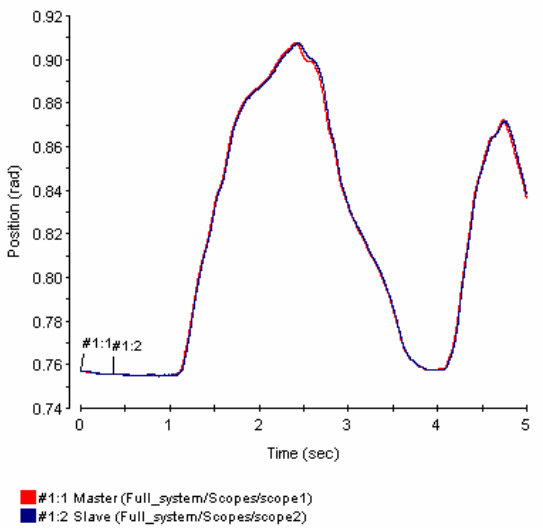

(a) position response of master and slave sides

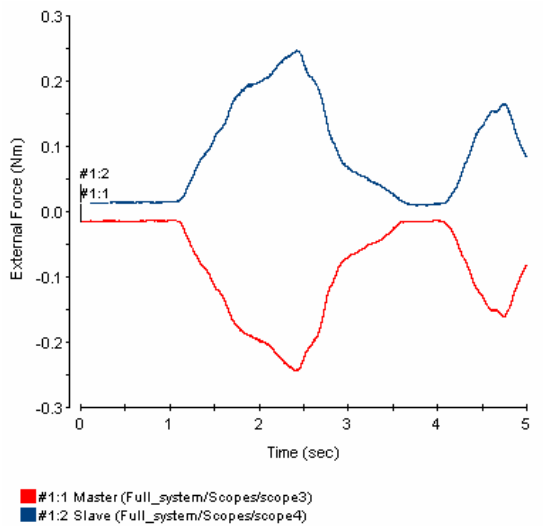

(b) External forces measured by Force observer

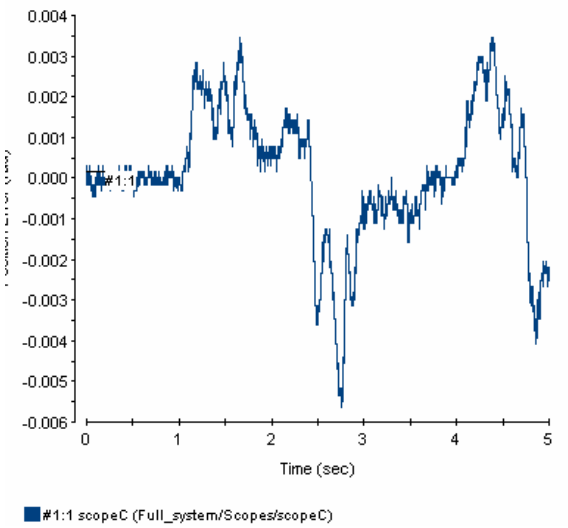

(c) Position error between master and slave sides

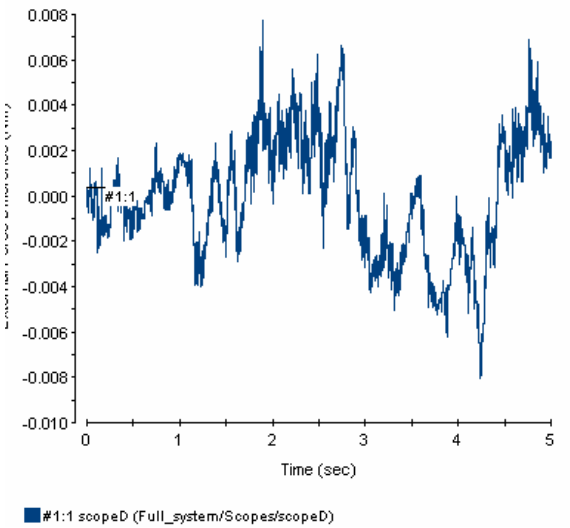

(d) Sum of torques at master and slave sides

Figure 4-17 Response of the bilateral system in contact with a soft environment

Due to the contact with soft environment slave side can still track the master position reference (Figure 4-17 (a)) while force reflected back to the master side is increasing (Figure 4-17 (b)). The controllers are capable of keeping the control error well.

4.7.3 Contact with a Hard Environment

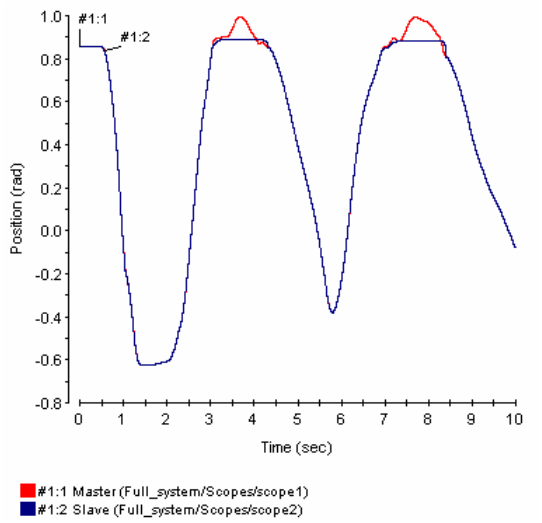

(e) position response of master and slave sides

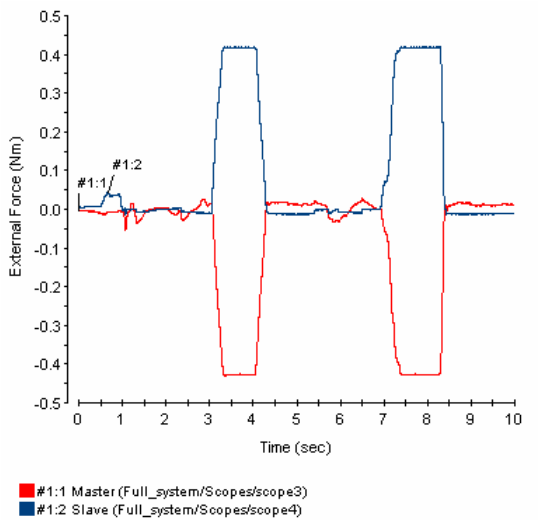

(f) External forces measured by Force observer

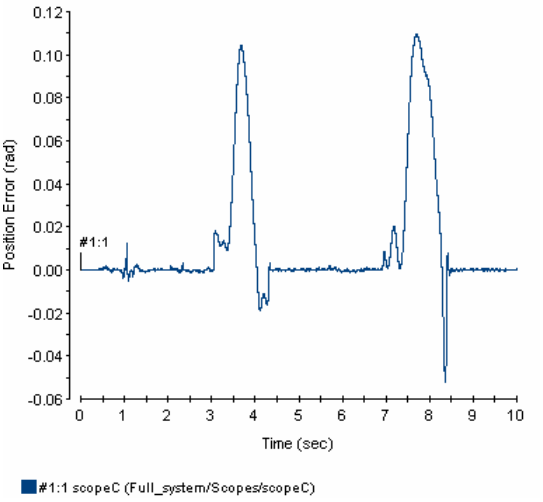

(g) Position error between master and slave sides

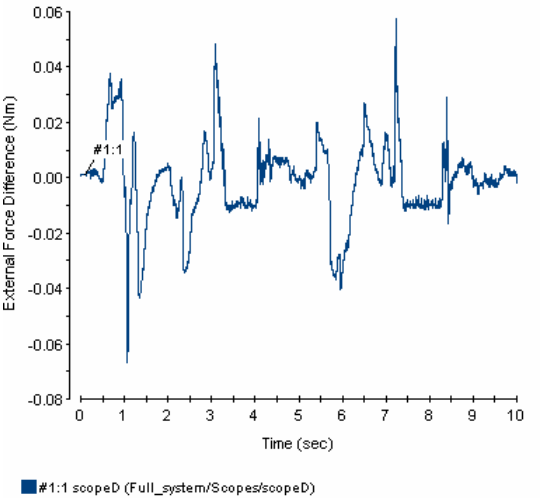

(h) Sum of torques at master and slave sides

Figure 4-18 Response of the bilateral system in contact with a hard environment

Due to the contact with hard environment slave side motion is limited and cannot track the master position reference (Figure 4-18 (a)) while force reflected back to the master side is controlled (Figure 4-18 (b)) and saturated to its maximum value. The

controllers are capable of keeping the position control error while not in contact with environment on the slave side. The force controller work well.

4.7.4 Contact with both Soft and Hard Environments at both sides

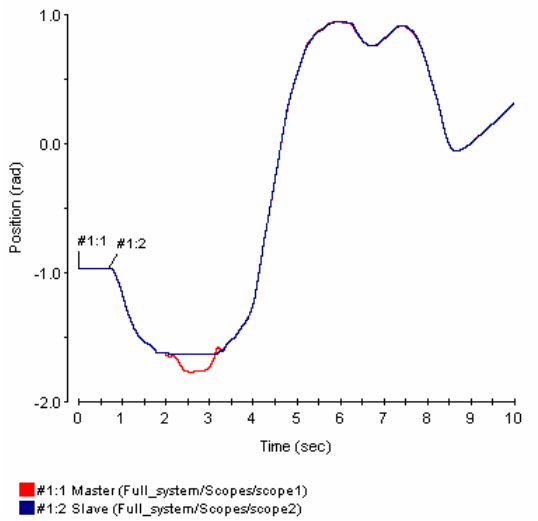

(i) position response of master and slave sides

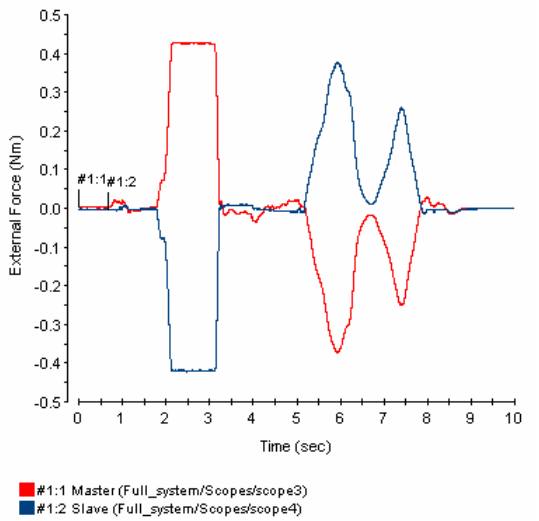

(j) External forces measured by Force observer

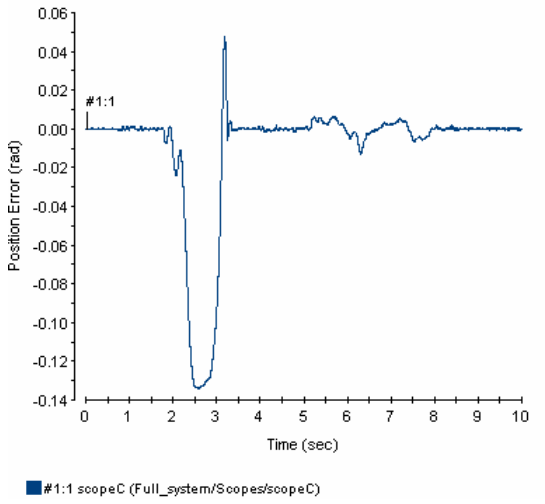

(k) Position error between master and slave sides

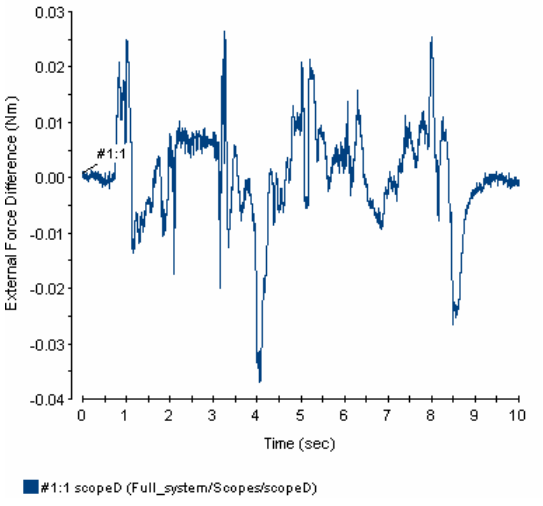

(l) Sum of torques at master and slave sides

Figure 4-19 Response of the bilateral system in contact with both soft and hard environments

The combination of the soft and hard environments is depicted in Figure 4-19. While moving to one side slave is hitting the hard environment and while moving on other side it is hitting soft environment. The transients are as expected and it shows that system controllers are capable of handling both, contact with soft and contact with hard environments on the slave side.

Chapter 5

Conclusion

In this work a variety different aspects for enhancing operation performance of a bilateral control system has been discussed. In chapter 2 acceleration controller based on disturbance observer has been introduced. Various works that has been done on disturbance observer has been discussed. Performance of disturbance rejection and effects of disturbance observer's bandwidth has been discussed. A multi-rate digital implementation of disturbance observer with stability criteria in mind has been built and validated by experiments.

Acquisition of position, velocity, and force information by using various techniques has been discussed in chapter 3. Velocity calculation techniques based on incremental encoders including a novel technique named S method has been discussed and experimentally tested. Due to known problems in force sensors application, which are result of varying and small bandwidth of traditional strain gauge based force sensors, reaction force observer has been introduced and used in our experimental system for force sensation. Reaction force observer gives a much wider force sensation bandwidth in comparison with a real force sensor. These bandwidth improvements directly affected the bandwidth of the whole bilateral control system and thus contribute to the fidelity of the overall system.

In chapter 4 various bilateral control systems had been discussed, ideal characteristics, performance criteria, issues of transparency, telepresence, stability, time delay, scaling and impedance shaping had been discussed. Models and operational limits for a human hand have also given to be able to get a feeling of requirements for a bilateral teleoperation system. Modified general teleoperation architecture has been introduced and performance of various bilateral control schemes discussed on general architecture. A four channel parallel type bilateral controller has been implemented on experimental system. A generalized version of that controller that can work with

different dynamics on master and slave sides has also been proposed. As a result a four channel bilateral system with robust digital multirate acceleration controller on master and slave sides with wide force sensation bandwidth has been designed and implemented.

In order to verify all of the proposed ideas a versatile bilateral system is designed and built and experimental verification is carried out on this system as described in appendixes A and B.

Further Work

Work done in the framework of this thesis and the experimental setup prepared can be a starting point for further work in the motion control systems like:

- Different architecture of disturbance observer and robust control
- Different architectures of bilateral control systems;
- Estimation of the interaction force

Due to the fact that bilateral system represent a architecture controlling interaction of the dynamical systems it will be very interesting to extend the formulation of the discussed in chapter 4 on the multilateral system with different dynamics.

Another interesting extension could be possibility to look at the extension of the virtual object definition (chapter 4) in order to include so called “function control” into the framework of bilateral control and possibly to control of dynamical systems (robots, mobile robots, parallel mechanism …) in interaction in general.

REFERENCES

[1] Merriam Webster Online Dictionary: http://www.m-w.com/dictionary/bilateral

[2] Y. Yokokohji and T. Yoshikawa, "Bilateral control of master-slave manipulators for ideal kinesthetic coupling," IEEE Trans. Robot. Automat., vol. 10, pp. 605-620, Oct. 1994.

[3] D. A. Lawrence, "Stability and transparency in bilateral telemanipulation," IEEE Trans. Robot. Automat., vol. 9, pp. 624-637, Oct. 1993.

[4] K. Hashtrudi-Zaad and S. E. Salcudean, "Transparency in time-delayed systems and the effect of local force feedback for transparent teleoperation," IEEE Trans. Robot. Autom., vol. 18, no. 1, pp. 108-114, Feb. 2002.

[5] K. Pool, "High resolution optical encoders" Computer optical products inc. web site: www.opticalencoder.com

[6] R. C. Kavanagh, "Shaft encoder characterization via theoretical model of differentiator with both differential and integral nonlinearities," IEEE Trans. Instrum. Meas., vol. 49, pp. 795-801, Aug. 2000.

[7] C. F. Lepple, "Implementation of a high-speed sinusoidal encoder interpolation system" Master thesis, Virginia Polytechnic Institute, Chap 4, Jan. 2004.

[8] S. E. Salcudean, M. Zhu, W.-H. Zhu, and K. Hashtrudi-Zaad, "Transparent bilateral teleoperation under position and rate control," Int. J. Robot. Res., vol. 19, pp. 1185-1202, Dec. 2000.

[9] C. Melchiorri and A. Eusebi, "Telemanipulation: System aspects and control issues," Proc. Int. Summer School Modeling \& Control of Mechanisms and Robots, C. Melchiorri and A. Tornambe, Ed. Singapore: World Scientific, 1996, pp. 149-183.

[10] Whitney, D., "Historical perspective and state of the art in robot force control," Robotics and Automation. Proceedings. 1985 IEEE International Conference on , vol.2, no.pp. 262- 268, Mar 1985

[11] Raneda, A., “2601050 Robotics and Teleoperation Lecture notes: Teleoperation,” Tampere University of Technology. Nov 2004 http://www.iha.tut.fi/education/IHA-3500/contents.shtml

[12] Katsura, S.; Matsumoto, Y.; Ohnishi, K., "Realization of "Law of action and reaction" by multilateral control," Industrial Electronics, IEEE Transactions on , vol.52, no.5pp. 1196- 1205, Oct. 2005

[13] Hogan, N., "Controlling impedance at the man/machine interface," Robotics and Automation, 1989. Proceedings., 1989 IEEE International Conference on , vol., no.pp.1626-1631 vol.3, 14-19 May 1989

[14] Katherine J. Kuchenbecker, June Gyu Park, and Günter Niemeyer. “Characterizing the human wrist for improved haptic interaction”. In Proc. ASME Int. Mechanical Engineering Congress and Exposition, volume 2, 42017, November 2003

[15] A. Z. Hajian and R. D. Howe, "Identification of the mechanical impedance at the human finger tip," ASME Journal of Biomechanical Engineering 119(1):109-114, Feb. 1997 [Feb. 1997]. Also presented at the International Mechanical Engineering Congress, American Society of Mechanical Engineers, Chicago, IL, November 1994, Proceedings ed. C. J. Radcliffe, DSC-vol. 55-1, p. 319-327.

[16] A. Z. Hajian, D. S. Sanchez, and R. D. Howe, "Drum roll: Increasing bandwidth through passive impedance modulation," Proceedings of the IEEE International Conference on Robotics and Automation, Albuquerque, New Mexico, April 20 - 25, 1997, pp. 2294-9.

[17] Y. Matsuoka and R. D. Howe, "Hand Impedance Change During Learning of a Novel Contact Task," 2000 World Congress on Medical Physics and Biomedical Engineering, Chicago, July 23-28, 2000.

[18] Tsuji, T. , “Motion Control For Adaptation To Human Environment” Ph.D. Dissertation, Keio University, Japan, 2005

[19] Kavanagh, R.C., "Improved digital tachometer with reduced sensitivity to sensor nonideality," Industrial Electronics, IEEE Transactions on , vol.47, no.4pp.890-897, Aug 2000

[20] Kavanagh, R.C., "Performance analysis and compensation of M/T-type digital tachometers," Instrumentation and Measurement, IEEE Transactions on , vol.50, no.4pp.965-970, Aug 2001

[21] Galvan, E.; Torralba, A.; Franquelo, L.G., "A simple digital tachometer with high precision in a wide speed range," Industrial Electronics, Control and Instrumentation, 1994. IECON '94., 20th International Conference on , vol.2, no.pp.920-923 vol.2, 5-9 Sep 1994

[22] Saito, K.; Kamiyama, K.; Ohmae, T.; Matsuda, T., "A microprocessor-controlled speed regulator with instantaneous speed estimation for motor drives," Industrial Electronics, IEEE Transactions on , vol.35, no.1pp.95-99, Feb 1988

[23] Se-Han Lee; Lasky, T.A.; Velinsky, S.A., "Improved velocity estimation for low-speed and transient regimes using low-resolution encoders," Mechatronics, IEEE/ASME Transactions on , vol.9, no.3pp. 553- 560, Sept. 2004

[24] Tsuji, T.; Mizuochi, M.; Nishi, H.; Ohnishi, K., "A velocity measurement method for acceleration control," Industrial Electronics Society, 2005. IECON 2005. 32nd Annual Conference of IEEE , vol., no.pp. 6 pp.-, 6-10 Nov. 2005

[25] Ohnishi, K.; Shibata, M.; Murakami, T., "Motion control for advanced mechatronics," Mechatronics, IEEE/ASME Transactions on , vol.1, no.1pp.56-67, Mar 1996

[26] Murakami, T.; Ohnishi, K., "Observer-based motion control-application to robust control and parameter identification," Motion Control Proceedings, 1993., Asia-Pacific Workshop on Advances in , vol., no.pp.1-6, 15-16 Jul 1993

[27] Shimono, T.; Katsura, S.; Ohnishi, K., "Abstraction and Reproduction of Force Sensation from Real Environment by Bilateral Control," Industrial Electronics, 2005. ISIE 2005. Proceedings of the IEEE International Symposium on , vol.4, no.pp. 1521- 1526, June 20-23, 2005

[28] Ohnishi, K.; Matsui, N.; Hori, Y., "Estimation, identification, and sensorless control in motion control system," Proceedings of the IEEE , vol.82, no.8pp.1253-1265, Aug 1994

[29] Bertoluzzo, M.; Buja, G.S.; Stampacchia, E., "Performance analysis of a high-bandwidth torque disturbance compensator," Mechatronics, IEEE/ASME Transactions on , vol.9, no.4pp. 653- 660, Dec. 2004

[30] Kobayashi, H.; Katsura, S.; Ohnishi, K., "An analysis of parameter variations of disturbance observer for haptic motion control," Industrial Electronics Society, 2005. IECON 2005. 32nd Annual Conference of IEEE , vol., no.pp. 6 pp.-, 6-10 Nov. 2005

[31] Shimono, T.; Katsura, S.; Ohnishi, K., "Improvement of operationality for bilateral control based on nominal mass design in disturbance observer," Industrial Electronics Society, 2005. IECON 2005. 32nd Annual Conference of IEEE , vol., no.pp. 6 pp.-, 6-10 Nov. 2005

[32] Godler, I.; Honda, H.; Ohnishi, K., "Design guidelines for disturbance observer's filter in discrete time," Advanced Motion Control, 2002. 7th International Workshop on , vol., no.pp. 390- 395, 2002

[33] D. S. Necsulescu, J. De Carufel, C. Canudas De Wit, Investigation on The Efficiency of Acceleration Feedback in Servomechanism With Friction, Dynamics and Control, Volume 7, Issue 4, Oct 1997, Pages 377 - 397,

[34] Glasson, D., "Development and applications of multirate digital control,"*Control Systems Magazine, IEEE* , vol.3, no.4pp. 2- 8, Nov 1983

[35] Fujimoto H., "*Sampling Control and Applications to Motion Control Systems*", Dissertation,University of Tokyo, 2000

[36] Fujimoto, H.; Hori, Y.; Yamaguchi, T.; Nakagawa, S., "Proposal of perfect tracking and perfect disturbance rejection control by multirate sampling and applications to hard disk drive control," *Decision and Control, 1999. Proceedings of the 38th IEEE Conference on* , vol.5, no.pp.5277-5282 vol.5, 1999

[37] Phillips, A.M.; Tomizuka, M., "Multirate estimation and control under time-varying data sampling with applications to information storage devices," *American Control Conference, 1995. Proceedings of the* , vol.6, no.pp.4151-4155 vol.6, 21-23 Jun 1995

[38] Mizuochi, M.; Tsuji, T.; Ohnishi, K., "Multirate Sampling Method for Acceleration Control System," *Industrial Electronics, 2005. ISIE 2005. Proceedings of the IEEE International Symposium on* , vol.4, no.pp. 1629- 1634, June 20-23, 2005

[39] Li, Y.F.; Chen, X.B., "On the dynamic behavior of a force/torque sensor for robots," *Instrumentation and Measurement, IEEE Transactions on* , vol.47, no.1pp.304-308, Feb 1998

[40] Gersem, D. G., "*Kinaesthetic feedback and enhanced sensitivity in robotic endoscopic telesurgery"*Ph.D. Dissertation, Katholieke Universiteit Leuven, Belgium, Feb 2005

[41] Hannaford, B., "A design framework for teleoperators with kinesthetic feedback," *Robotics and Automation, IEEE Transactions on* , vol.5, no.4pp.426-434, Aug 1989

[42] Raju, G. J., "*Operator adjustable impedance in bilateral remote manipulation*" Ph.D. dissertation, Massachusetts Institute of Technology, 1989

[43] Strassberg, Y.; Goldenberg, A.A.; Mills, J.K., "A New Control Scheme For Bilateral Teleoperating Systems: Performance Evaluation And Comparison," *Intelligent Robots and Systems, 1992., Proceedings of the 1992 lEEE/RSJ International Conference on* , vol.2, no.pp.865-872, 7-10 Jul 1992

[44] Colgate, J.E.; Brown, J.M., "Factors affecting the Z-Width of a haptic display," *Robotics and Automation, 1994. Proceedings., 1994 IEEE International Conference on* , vol., no.pp.3205-3210 vol.4, 8-13 May 1994

[45] Hashtrudi-Zaad, K. and S. Salcudean (1999, May). “On the use of local force feedback for transparent teleoperation”. *In Proceedings of the IEEE International Conference on Robotics and Automation*, Detroit, MI, pp. 1863–1869.

[46] Çavuşoğluglu, M. C., A. Sherman, and F. Tendick (2001, May). “Bilateral control design for telemanipulation of soft objects in a stiffness discrimination task.” *In Proceedings of the IEEE International Conference on Robotics and Automation (ICRA 2001)*, Seoul, Korea, pp. 1045–1052.

[47] Shimoga, K.B., "A survey of perceptual feedback issues in dexterous telemanipulation. I. Finger force feedback," *Virtual Reality Annual International Symposium, 1993., 1993 IEEE* , vol., no.pp.263-270, 18-22 Sep 1993

[48] Penin, L.F.; Caballero, A.; Aracil, R.; Barrientos, A., "Human behavior modeling in master-slave teleoperation with kinesthetic feedback," *Robotics and Automation, 1998. Proceedings. 1998 IEEE International Conference on* , vol.3, no.pp.2244-2249 vol.3, 16-20 May 1998

[49] Lee, S.; Lee, H.S., "Teleoperator control system design with human in control loop and telemonitoring force feedback," *Decision and Control, 1992., Proceedings of the 31st IEEE Conference on* , vol., no.pp.2674-2679 vol.3, 1992

[50] Brooks, T.L., "Telerobotic response requirements," *Systems, Man and Cybernetics, 1990. Conference Proceedings., IEEE International Conference on* , vol., no.pp.113-120, 4-7 Nov 1990

[51] Kazerooni, H.; Tsay, T.-I.; Hollerbach, K., "A controller design framework for telerobotic systems," *Control Systems Technology, IEEE Transactions on* , vol.1, no.1pp.50-62, Mar 1993

[52] Kobayashi, H.; Nakamura, H., "A scaled teleoperation," *Robot and Human Communication, 1992. Proceedings., IEEE International Workshop on* , vol., no.pp.269-274, 1-3 Sep 1992

[53] Lawrence, D.A., "Designing teleoperator architectures for transparency," *Robotics and Automation, 1992. Proceedings., 1992 IEEE International Conference on* , vol., no.pp.1406-1411 vol.2, 12-14 May 1992

[54] Zhu, M.; Salcudean, S.E., "Achieving transparency for teleoperator systems under position and rate control," *Intelligent Robots and Systems 95. 'Human Robot Interaction and Cooperative Robots', Proceedings. 1995 IEEE/RSJ International Conference on* , vol.2, no.pp.7-12 vol.2, 5-9 Aug 1995

[55] Flemmer, H.; Wikander, J., "Transparency and stability analysis of a surgical teleoperator system," *Haptic Interfaces for Virtual Environment and Teleoperator Systems, 2003. HAPTICS 2003. Proceedings. 11th Symposium on* , vol., no.pp. 382- 389, 22-23 March 2003

[56] Caiti, A.; Cannata, G.; Casalino, G.; Reto, S., "The local force control loop approach in bilateral control of master-slave systems," *Decision and Control, 1996., Proceedings of the 35th IEEE* , vol.1, no.pp.747-752 vol.1, 11-13 Dec 1996

[57] Sumiyoshi, Y.; Ohnishi, K., "The transformation of modified 4-channel architecture," *Advanced Motion Control, 2004. AMC '04. The 8th IEEE International Workshop on* , vol., no.pp. 211- 216, 25-28 March 2004

[58] Kim, W.S.; Hannaford, B.; Fejczy, A.K., "Force-reflection and shared compliant control in operating telemanipulators with time delay," *Robotics and Automation, IEEE Transactions on* , vol.8, no.2pp.176-185, Apr 1992

[59] Eppinger, S.; Seering, W., "On dynamic models of robot force control," *Robotics and Automation. Proceedings. 1986 IEEE International Conference on* , vol.3, no.pp. 29- 34, Apr 1986

[60] Eppinger, S.; Seering, W., "Understanding bandwidth limitations in robot force control," *Robotics and Automation. Proceedings. 1987 IEEE International Conference on* , vol.4, no.pp. 904- 909, Mar 1987

[61] Iida, W.; Ohnishi, K., "Sensorless force control with force error observer," *Industrial Technology, 2003 IEEE International Conference on* , vol.1, no.pp. 157- 162 Vol.1, 10-12 Dec. 2003

[62] Katsura, S.; Matsumoto, Y.; Ohnishi, K., "Modeling of force sensing and validation of disturbance observer for force control," *Industrial Electronics Society, 2003. IECON '03. The 29th Annual Conference of the IEEE* , vol.1, no.pp. 291- 296 vol.1, 2-6 Nov. 2003

[63] Katsura, S.; Matsumoto, Y.; Ohnishi, K., "Analysis and experimental validation of force bandwidth for force control," *Industrial Technology, 2003 IEEE International Conference on* , vol.2, no.pp. 796- 801 Vol.2, 10-12 Dec. 2003

[64] Hayashida, N.; Yakoh, T.; Murakami, T.; Ohnishi, K., "A friction compensation in twin drive system," *Advanced Motion Control, 2000. Proceedings. 6th International Workshop on* , vol., no.pp.187-192, 2000

[65] Ferrell, W. R., "Remote manipulation with transmission delay", Ph.D dissertation, Massachusetts Institute of Technology, 1965

[66] Anderson, R.J.; Spong, M.W., "Bilateral control of teleoperators with time delay," *Decision and Control, 1988., Proceedings of the 27th IEEE Conference on* , vol., no.pp.167-173 vol.1, 7-9 Dec 1988

[67] Niemeyer, G.; Slotline, J.-J.E., "Stable adaptive teleoperation," *Oceanic Engineering, IEEE Journal of* , vol.16, no.1pp.152-162, Jan 1991

[68] Chopra, N.; Spong, M.W.; Hirche, S.; Buss, M., "Bilateral teleoperation over the internet: the time varying delay problem," *American Control Conference, 2003. Proceedings of the 2003* , vol.1, no.pp. 155- 160, 4-6 June 2003

[69] Secchi, C.; Stramigioli, S.; Fantuzzi, C., "Digital passive geometric telemanipulation," *Robotics and Automation, 2003. Proceedings. ICRA '03. IEEE International Conference on* , vol.3, no.pp. 3290- 3295 vol.3, 14-19 Sept. 2003

[70] Hannaford, B., "Stability and performance tradeoffs in bi-lateral telemanipulation ," *Robotics and Automation, 1989. Proceedings., 1989 IEEE International Conference on* , vol., no.pp.1764-1767 vol.3, 14-19 May 1989.

[71] Itoh, T.; Kosuge, K.; Fukuda, T., "Human-machine cooperative telemanipulation with motion and force scaling using task-oriented virtual tool dynamics," *Robotics and Automation, IEEE Transactions on* , vol.16, no.5pp.505-516, Oct 2000

[72] Colgate, J.E., "Robust impedance shaping telemanipulation," *Robotics and Automation, IEEE Transactions on* , vol.9, no.4pp.374-384, Aug 1993

[73] Sheridan, T.B., "Telerobotics" *Automatica*, vol. 9, no.4.pp.487-507,1989

[74] Hokayem, P.F., Spong, M.W., "Bilateral Teleoperation:An Historical Survey" *paper submitted to Automatica,* 15 Feb. 2005 *url:http://decision.csl.uiuc.edu /~spong/Articles/teleoperation/survey.pdf*

[75] Ohmae, T., Matsuda T., Kamiyama K., Tachikawa M., "A microprocessor-controlled high-accuracy wide-range speed regulator for motor drives"- IEEE Trans. Industrial Electronics, Vol. 29, No. 3, pp. 207-211, 1982.

[76] Katsura S., "Advanced Motion Control Based on Quarry of Environmental Information" Ph.D. Dissertation, Keio University, Japan, 2004

[77] G. J. Raju, G.C. Verghese, and T. B. Sheridan. "Design issues in 2-port network models of bilateral remote manipulation." *In Proceedings of the IEEE International Conference on Robotics and Automation*, volume 3, pages 1316–1321, May 1989.

[78] Önal, C. D., "Bilateral Control – A Sliding Mode Control Approach" Ms. C. Thesis, Sabanci University, Spring 2005.

[79] Bejczy, A.K.; Won S. Kim, "Predictive displays and shared compliance control for time-delayed telemanipulation," *Intelligent Robots and Systems '90. 'Towards a New Frontier of Applications', Proceedings. IROS '90. IEEE International Workshop on* , vol., no.pp.407-412 vol.1, 3-6 Jul 1990

[80] Fite, K.B.; Liang Shao; Goldfarb, M., "Loop shaping for transparency and stability robustness in bilateral telemanipulation," *Robotics and Automation, IEEE Transactions on* , vol.20, no.3pp. 620- 624, June 2004

[81] Leung, G.M.H.; Francis, B.A., "Robust nonlinear control of bilateral teleoperators," *American Control Conference, 1994* , vol.2, no.pp. 2119- 2123 vol.2, 29 June-1 July 1994

[82] H.-K. Lee and M. J. Chung. “Adaptive controller of a master-slave system for transparent teleoperation.” *Journal of Robotic Systems*, 15(8):465–475, Aug. 1998.

[83] Linhui Li; Yuanchun Li; Guangjun Liu, "Nonlinear adaptive control of teleoperation systems with large time delay," *Control Applications, 2005. CCA 2005. Proceedings of 2005 IEEE Conference on* , vol., no.pp. 1522- 1527, 28-31 Aug.2005

[84] Tsuji, T.; Ohnishi, K., "Position/force scaling of function-based bilateral control system," *Industrial Technology, 2004. IEEE ICIT '04. 2004 IEEE International Conference on* , vol.1, no.pp. 96- 101 Vol. 1, 8-10 Dec. 2004

[85] Heui-Wook Kim; Seung-Ki Sul, "A new motor speed estimator using Kalman filter in low-speed range ," *Industrial Electronics, IEEE Transactions on* , vol.43, no.4pp.498-504, Aug 1996

[86] Fujita, K.; Sado, K., "Instantaneous speed detection with parameter identification for AC servo systems," *Industry Applications, IEEE Transactions on* , vol.28, no.4pp.864-872, Jul/Aug 1992

Appendix A

Experimental Setup

An bilateral experiment setup should have rapid and high resolution torque output, small moment of inertia, small friction, high resolution position and velocity measurement and a compliant control structure. As all of the components were selected from off the shelf materials from the laboratory, not every requirement for an optimal bilateral system was satisfied. However, experimental system was adequate to notice many application complications.

Due to the highest torque output of EC-40 among other motors available in our lab, EC-40 motor was selected for the setup. As gearbox slows the systems response and increase the friction on the system thus a direct drive scheme preferred. Due to the fact that EC-40 motor is equipped with a relatively low resolution (500 ppr) incremental encoder, highest possible resolution encoder available in our shelf was added to the output of the motor.

Due to the fact that metal part holding motor and encoder together was not able to machine properly axial misalignment between shafts of the motor and the encoder caused misreading of the encoder and increased frictions in the system. To overcome this problem motor and the encoder is coupled with a flexible coupling specifically designed to cope with misalignments.

In order to control the motor, Maxon DES 70/10 motor controller used in current regulation mode. A dSPACE 1103 real-time controller prototyping system is used to control the system. dSPACE system is equipped with quadrature encoder interface for encoders and 14 bit DAC outputs for motor drives. Even though dSPACE controller has 14 bits outputs DES current driver had only 10 bits resolution and a 1 kHz bandwidth. As a result of this constraint a multirate controller used with 1 kHz output frequency (see chapter 2). The bandwidth of the current controller also limited bandwidths of the

disturbance observer and force observers due to the stability limitations. The motor and the controller was designed to work in high speed servo applications, so at low speeds motor shaft has high frequency oscillation even when motor is still with no input to the current driver. This gives a bad feeling to the operator in operation, Even though this oscillation cause problem it also has a dithering effect to keep the static fiction effect at lower levels than expected.

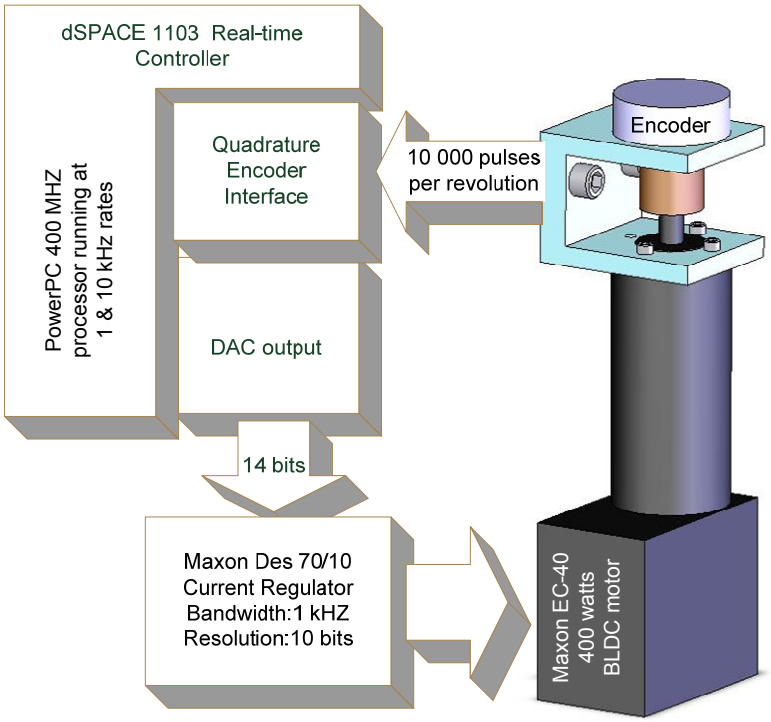

Figure A- 1 Control Structure of experimental setup

Figure A-1 shows the control structure of our setup. Velocity measurements, disturbance observer and force observer experiments have done on this one motor setup.

Two identical arms have been designed, arm's geometry designed in a way that rotational axis pass through the center of moment of inertia so minimum vibration occurs in the system. Additionally fully rotation of the arm has been disabled to prevent possible injuries during the experiments. Figure A-2 shows the experimental bilateral system. Table A-1 shows the parameters and some properties of the experiment system.

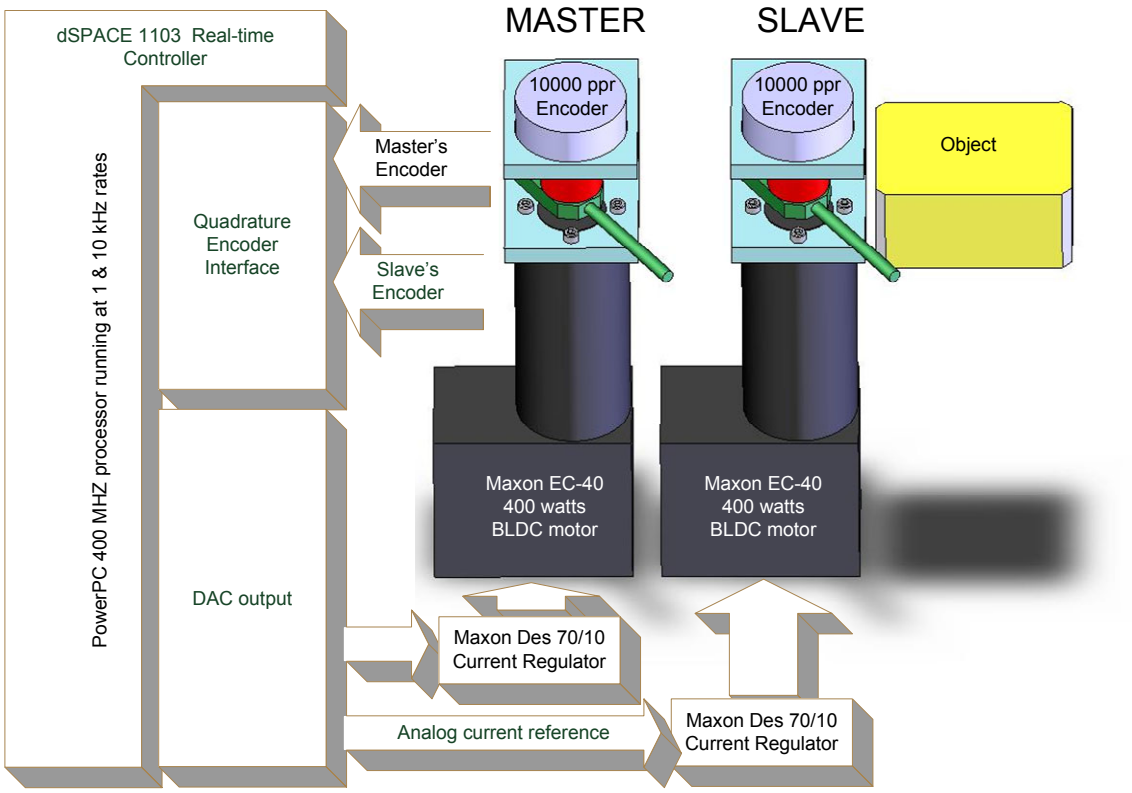

Figure A- 2 Structure of the bilateral experimental setup

Name	Value
Maxon motor model number	167132
Motor inertia	831 g/cm^2
Total system inertia	2016 g/cm^2
Motor Torque constant	85 mNm/A
DES controller model name	Maxon 4-Q-EC servo amplifier DES 70/10
Controller Current Limit	8 A
DES controller's input signal	±10 V analog
DES controller's input resolution	10 bits
Des controller's bandwidth	1 kHz
Encoder model and number	THALHEIM ITD 21B14 10000T NI KR1 S 6 IP65
Encoder resolution	10000 PPR, 40000 with quadrature interpolation
dSPACE controller model number	DS 1103 with 400 MHZ PPC controller
Encoder reading frequency	10 kHz.
Controller output frequency	1 kHz

Table A- 1

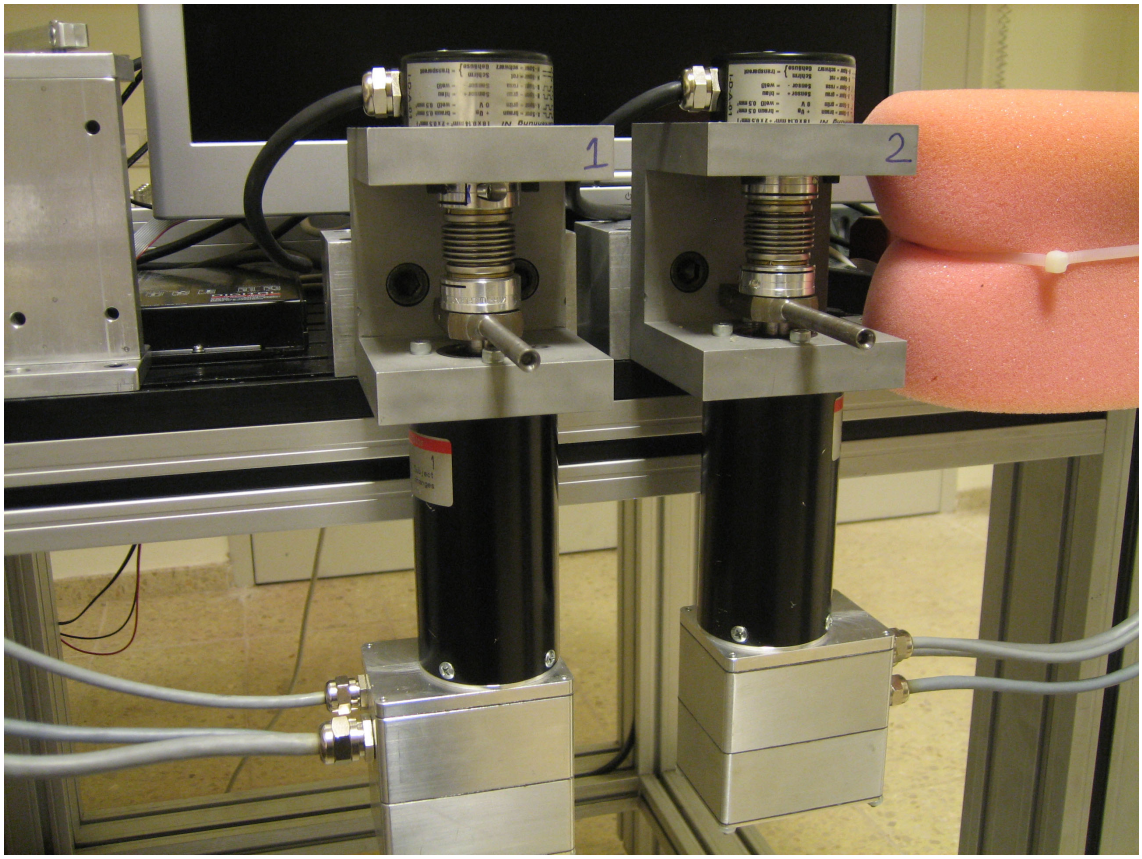

Figure A- 3 Image of experiment system

Appendix B

S Method Velocity Measurement Code

You can find the explanations of each variable of MOTOR class in appendix C. this function has been written with the simulation code supplied by Toshiaki Tsuji

```
int S_velocity(struct MOTOR *m)
{ //return true if a velocity update occurs in S Method, plus updates S_vel variable of the motor object
      m->S_term++; //number of sampling time for this measurement
//*** Alternate pulse alteration filtering
// Alternate pulse alteration occurs doue to the high frequency noise in the motor shaft
//these alterations occurs in a +1,-1 or -1,+1 manner to disable this or make alternate_PA_filter=FALSE
//comment this block to disable alternate pulse alteration property

 if (alternate_PA_filter == TRUE){

   if (m->S_Alteration == 2 && (m->S_state==-1 || m->S_state==-2)) //alternate pulse alteration occured
      {
         m->S_vel=m->S_base_Vel;
         m->S_term=0;
         m->S_state=2;
         return 1;
         }
   if (m->S_Alteration == -2 && (m->S_state==1 || m->S_state==2))
      {
          m->S_vel=m->S_base_Vel;
         m->S_term=0;
         m->S_state=-2;
         return 1;
         }
      //function should not live until here if alternate pulse occurs
   if (m->S_state==2 || m->S_state==-2)

      {// one cycle after alternate pulse should be managed
         m->S_Alteration=m->S_Alteration+ m->S_state/2;  //shift one up or down according to previous state
         m->S_state=0;

         }
```

```
    }
  // everything is normal as no alternate pulse occured in system. :)
  //*** Alternate pulse alteration filtering END


 //S_Alteration is the difference of the number of pulses read in this sampling time and
previous measurement, it is kind of a derivative of pulses read in one cycle
     // S_Alteration value is mostly -1,0,1 other values are mostly exceptions

     if(m->S_state == 0)
     {    //mode after no pulse alteration
          //this state runs after a velocity update is done or after zero pulse alteration.
          if (m->S_Alteration == 0) {

               // velocity calculation is done if no update occurs for a while
               if (m->S_vel <= m->S_base_Vel - m->S_Vunit/m->S_term)
                  { m->S_vel = m->S_base_Vel - m->S_Vunit/m->S_term; return 1;}
               if (m->S_vel >= m->S_base_Vel + m->S_Vunit/m->S_term)
                  { m->S_vel = m->S_base_Vel + m->S_Vunit/m->S_term; return 1;}

          } else if(m->S_Alteration == 1) {
            // if a pulse alteration occurs change the next state for measurement
               m->S_state=1;
          } else if(m->S_Alteration==-1) {
            // if a pulse alteration occurs change the next state for measurement
               m->S_state=-1;

          } else {
            //if pulse alteration mote than 1 calculate velocity directly
               m->S_base_Vel+= m->S_Alteration * m->S_Vunit;
               m->S_vel=m->S_base_Vel;
               m->S_term=0;
               m->S_state=0;
               return 1;
          }

     }// end off state 0
     else  if ( m->S_state == -1 )
     {
          //this state runs after a negative 1 pulse alteration.

          if (m->S_Alteration == 1) {
               //if an alteration of 1 occurs after -1 this means
           //there existed 1 alteration as an impulse so velocity update needs to be done
               m->S_vel=m->S_base_Vel - m->S_Vunit/m->S_term;
               m->S_term=0;
               m->S_state=0;
               return 1;
          } else {
        //if alteration is not +1 after a -1 alteration base velocity needs to be changed.
```

```
                m->S_base_Vel -= m->S_Vunit;
                m->S_term =1;
                if ( m->S_Alteration == 0 ) {
                    m->S_state=0;
                } else if ( m->S_Alteration == -1) {
                    m->S_state= -1;
                } else {
              //if pulse alteration mote than 1 calculate velocity and base velocity directly
                    m->S_base_Vel+= m->S_Alteration * m->S_Vunit;
                    m->S_vel=m->S_base_Vel;
                    m->S_term=0;
                    m->S_state=0;
                    return 1;
                }
            }
        }

        else if (m->S_state == 1)
        {       //this state runs after a positive 1 pulse alteration.

            if (m->S_Alteration == -1) {
                //if an alteration of -1 occurs after +1 this means
            //there existed 1 alteration as an impulse so velocity update needs to be done
                m->S_vel=m->S_base_Vel + m->S_Vunit/m->S_term;
                m->S_term=0;
                m->S_state=0;
                return 1;
            } else {
            //if alteration is not -1 after a +1 alteration base velocity needs to be changed.
                m->S_base_Vel += m->S_Vunit;
                m->S_term =1;
                if ( m->S_Alteration == 0 ) {
                    m->S_state=0;
                } else if ( m->S_Alteration == 1) {
                    m->S_state= 1;
                } else {
              //if pulse alteration mote than 1 calculate velocity and base velocity directly
                    m->S_base_Vel+= m->S_Alteration * m->S_Vunit;
                    m->S_vel=m->S_base_Vel;
                    m->S_term=0;
                    m->S_state=0;
                    return 1;
                }
            }
        }
        // return FALSE if no velocity update is done in function.
        return 0;

}
```

Appendix C

Motor Class & Experiment Code

Motor Class

Class definition

```
enum {Motor1,Motor2,Motor3};  /** this enumeration is for naming of
the motor in the system  */

//** this linear motor structure renamed to the motor structure to be
more general
struct MOTOR
{
        //~ system specification parameters
        char Name;    /**<enumerated Name of the specific motor to be
                          able to load motor specific parameters to
load.*/
        Float64 J;          /**< Motor Inertia */
        Float64 Kt;          /**<  Motors Torque Constant */
        Float64 B;             /**< Frictional constant */


        /* Trajectory parameters*/

        Float64 ref;      /**< reference displacement for motor*/

        //~ Position and velocity reading parameters and variables
        Float64 enc2pos;     /**< enc -> y conversion factor */
        Float64 pos2theta;     //< y -> theta conversion factor


        Float64 pos;         /**< Linear Position in Microns for
motor*/
        Float64 vel;    // motor velocity

        Float64 M_vel;       //Motor velocity with M method
        Float64 M_vel_filter; // M_vel with LPF applied

        //** S velocity Method parameters

        Float64 S_vel;           // output of S method
        Float64 S_vel_filter;    //low pass filtered output of S method

        Float64 S_term;          //time interval since last calculation
in DT
```

```
        Float64 S_base_Vel;     //base velocity
        int S_Alteration;   //number of pulse alterations
        Float64 S_Vunit;        //velocity value of 1 pulse unit
velocity
        Float64 S_Aunit;        //acceleration value of 1 pulse unit
acceleration
        int     S_state;        //state of the measurement
        Float64 S_Last_M;       //time of the last velocity
measurement for S velocity
        Float64 M;               //number of DT between two
measurement update
        Float64 M_filter;        //number of DT between two
measurement update for filter


         // Encoder positional variables
        Float64 enc_pos;    // variable to store encoder position for
motor
        Float64 enc_pos_1;  // previous value of enc_pos
        Float64 pos_abs;    //absolute position of shaft angle between
0-2*pi
        Float64 theta;      //motor position in angles
        Float64 enc_vel;    // encoder reading during 1 sampling time
in pulses
        Float64 enc_vel_1;  //previous value of enc_vel

        Float64 pos_1;     //previous actual position of motor shaft
(rad)
         Float64 vel_1;      //previous velocity of motor shaft
(rad/sec)

         //Velocity low pass filter variables

        Float64  VelFilterOut;   // output of LPF
        Float64 VelFilterOut_1;  // previous output of LPF
        Float64 VelFilterLastT; // timestamp of last update
        Float64 g_vel;           // cut off frequency of LPF
        Float64  VelFilterOutM;  // output of LPF for M type
measurement
        Float64 VelFilterOutM_1; // previous output of LPF for M type
measurement

        /*Disturbance Observer Parameters*/
        Float64 g;               //cut off frequency of LPF
        Float64 DistFilterIn;    //input of LPF in DOB
        Float64 DistFilterOut;   // output of LPF in DOB
        Float64 DistFilterOut_1; //previous output of LPF in DOB
        Float64 DistFilterTemp;  //a temporary value used in
calculation
        Float64 Disturbance; // calculated disturbance
        Float64 Dist_gain;       // gain at the output of DOB
        Float64 DistFilterLastT;// timestamp of last update

         // Reaction Force Observer Parameters */
        Float64 ForceFilterTemp; //a temporary value used in
calculation
        Float64 ForceFilterIn;//input of LPF in RFOB
        Float64 ForceFilterOut;// output of LPF in RFOB
        Float64 ForceFilterOut_1;//previous output of LPF in RFOB
        Float64 Force_gain;// gain at the output of RFOB
        Float64 Force;// calculated disturbance
```

```
        Float64 g_force;//cut off frequency of LPF
        Float64 Force_D;//calculated friction entering to the RFOB
        //friction calculation parameters
        Float64 Force_pos_gain; //gain of the sine wave
        Float64 Force_pos_offsett;//offsett of sine wave
        Float64 Force_pos_bias;   //bias of sine wave
        Float64 Force_pos;        //calculated friction changing with
the
                                        //   absolute position
        //Force Controller parameters
         Float64 FORCEcontrol; //output of force controller
        Float64 Ferr_1;     //error entering to the force controller
        Float64 ForceControl_K; // Gain of controller
        Float64 ForceControl_D; // derivative gain of

        //Additive ımpedance function variables
        Float64 Im;          //output
        Float64 Im_K;   //P gain
        Float64 Im_D;   //D gain
        Float64 Im_X_1; //previous output


        //~ PID Controller Parameters


         Float64 Kp;                        //Proportional Gain

        Float64 Ki;                         //Integral Gain
        Float64 Kd;                         //derivative gain
        Float64 PID_Uk;                 //Present  PID controller output
        Float64 PID_Uk_1;               //previous PID controller output
        Float64 Ek;                     //Present error signal(controller
input)
        Float64 Ek_1;                   //previous error signal
        Float64 Ek_2;                   //2 previous error signal
        Float64 Uk;                     //Plant Input (Total Controller
output)
        Float64 Uk_1;                   //Plant Input (Total Controller
output)
        Float64 Uk_p;                     //output of P term
        Float64 Uk_i;                     //output of I term
        Float64 Uk_d;                     //output of D term
        Float64 Uk_i_1;                   //previous output of I term


        //controller output variables and parameters
        Float64 v_out;  /**< Voltage sendto dSpace for motor*/

        Float64 offset_Vt;/**< Voltage offset for Motor Driver*/
        Float64 DAC_out;// output to the DAC between -1,1
        Float64 saturation_Vt_out_upper;/**< Upper Voltage saturation
for Driver after offset*/
        Float64 saturation_Vt_out_lower;/**< Lower Voltage saturation
for Driver after offset*/
        int dac_channel; /**< Channel number for the DAC */
        int enc_channel; /**< Int contains which channel number is
used for encoder*/
        int enc_index_ok; //true if encoder value is reset with the
index pulse at the begining
```

```
};
```

Class Initialization

```
void initMotor(struct MOTOR *m)
{
        /* COMMON VARIABLES AND PARAMETERS FOR ALL MOTORS*/

        //~ system specification parameters
        m->J = 2006.0e-7;   //946 without knob 2006 with knob
        m->Kt = 0.052556;    /**<  Motors Torque Constant */
        m->B= 0.0001;        /**< Frictional constant */
        /* Trajectory parameters*/
        m->ref = 0;      /**< reference displacement for motor*/
        /*Disturbance Observer Parameters*/
        m->DistFilterIn=0;
        m->DistFilterOut=0;
        m->DistFilterOut_1=0;
        m->DistFilterTemp=0;
        m->DistFilterLastT=0;
        m->Disturbance=0;
        m->Dist_gain=0;
        m->g=500;

        m->ForceFilterTemp=0;
        m->ForceFilterIn=0;
        m->ForceFilterOut=0;
        m->ForceFilterOut_1=0;
        m->Force_gain=1;
        m->Force=0;
        m->g_force=100;
        m->Force_D=0.0012;

        m->FORCEcontrol=0;
        m->Ferr_1=0;
        m->ForceControl_K=0;
        m->ForceControl_D=0;

        // Impedance 1

        m->Im=0;
        m->Im_K=0;
        m->Im_D=0;
        m->Im_X_1=0;

        m->pos=0;                                   /**< Linear Position in
Microns for motor*/
        m->vel=0;
        m->enc_pos = 0;               /**< variable to store encoder
position for motor */
        m->pos_abs = 0;
        m->enc_pos_1=0;
        m->enc_vel = 0;               /**< variable to store velocity
of the motor*/
        m->enc_vel_1 = 0;
        m->enc_index_ok = 0;
```

```
        m->M_vel=0;
        m->M_vel_filter=0;
        m->S_vel=0;
        m->S_vel_filter=0;
        m->S_term=0;        //time interval since last calculation in
DT
        m->S_base_Vel=0;     //base velocity
        m->S_Alteration=0;   //number of pulse alterations
        m->S_Vunit=(2.0*pi)/(40000*DT); //velocity value of 1
pulse: 2.0*pi/PULSE/DT
        m->S_Aunit=(2.0*pi)/(40000*DT*DT);//acceleration value of 1
pulse: 2.0*pi/PULSE/DT/DT
        m->S_state=0;        //state of the measurement
        m->S_Last_M=0;

        m->theta=0;
        m->enc_alter_sign=1;
        m->enc_alter_sign_1=1;
        m->pos_1=0;                          //older actual position of
motor shaft (rad)
        m->vel_1=0;                           //Older velocity of motor
shaft (rad/sec)
        m->M=0;
        m->M_filter=0;

        m->VelFilterOut=0;
        m->VelFilterOut_1=0;
        m->VelFilterOutM=0;
        m->VelFilterOutM_1=0;
        m->VelFilterLastT=0;
        m->g_vel=500;

        //~ PID Controller Parameters
        m->Kp=1;
        m->Ki=1;
        m->Kd=1;
        m->PID_Uk=0;                          //Present  PID controller
output
        m->PID_Uk_1=0;                        //Older PID controller
output
        m->Ek=0;                              //Present error
signal(controller input)
        m->Ek_1=0;                            //Older error signal
        m->Ek_2=0;                            //Older_older error signal
        m->Uk_1=0;                            //Plant Input (Total
Controller output)
        m->Uk_p=0;
        m->Uk_i=0;
        m->Uk_d=0;
        m->Uk_i_1=0;

        //~ controller output variables and parameters

        m->v_out=0;     /**< Volate fed to dSpace for motor*/
        m->fake_dist=0;


        /* init D/A converter in Transparent  mode */
        ds1103_dac_init(DS1103_DACMODE_TRANSPARENT);

        /* MOTOR SPECIFIC VARIABLES AND PARAMETERS*/
```

```
        if (m->Name == Motor1)
        {
               /*Controller parameters*/
                m->enc_channel=1;
                ds1103_inc_reset(m->enc_channel); // To reset the
specified encoder.
                ds1103_inc_init(m->enc_channel, DS1103_INC_CH1_TTL);
// To initialize an incremental encoder channel
                ds1103_inc_set_idxmode(m->enc_channel,
DS1103_INC_NO_RESETONIDX);
                m->enc2pos = -500/(500*29.64197530864198); /**< enc ->
X conversion factor */
                m->pos2theta  =
(2*3.14159265358979323846264338327795)/10000;  /**< y -> theta
conversion factor as 500 microns/rev */
                /*Input output parameters*/
                m->offset_Vt=-0.00335; /**< Volatge offset for Motor
Driver*/
                m->dac_channel = 1; /**< Channel number for the DAC */
                m->saturation_Vt_out_upper=8;/**< UPPER Volatage
saturation for the Motor Driver*/
                m->saturation_Vt_out_lower=-8;/**< LOWER Volatage
saturation for the Motor Driver*/

                m->Force_pos_gain=0.14;
                m->Force_pos_offsett=0.8;
                m->Force_pos_bias=0.165;
                m->Force_pos=0;

        } else if (m->Name == Motor2)
        {

                 m->enc_channel=2;
                ds1103_inc_reset(m->enc_channel); // To reset the
specified encoder.
                ds1103_inc_init(m->enc_channel, DS1103_INC_CH1_TTL);
// To initialize an incremental encoder channel
                ds1103_inc_set_idxmode(m->enc_channel,
DS1103_INC_NO_RESETONIDX);
                m->enc2pos = 500/(500*29.64197530864198); /**< enc ->
Y conversion factor */
                m->pos2theta  =
(2*3.14159265358979323846264338327795)/10000;  /**< y -> theta
conversion factor as 500 microns/rev */
                /*Input output parameters*/
                m->DAC_out=0;
                m->offset_Vt=-0.005359; /**< Volatge offset for Motor
Driver*/
                m->dac_channel = 2; /**< Channel number for the DAC */
                m->saturation_Vt_out_upper=8;/**< UPPER Volatage
saturation for the Motor Driver*/
                m->saturation_Vt_out_lower=-8;/**< LOWER Volatage
saturation for the Motor Driver*/

                m->Force_pos_gain=0.06;
                m->Force_pos_offsett=1.307;
                m->Force_pos_bias=0.168;
                m->Force_pos=0;

        }
        else if (m->Name == Motor3)
```

```
        {

                m->enc_channel=5;
                ds1103_inc_reset(m->enc_channel); // To reset the
specified encoder.
                ds1103_inc_init(m->enc_channel, DS1103_INC_CH1_TTL);
// To initialize an incremental encoder channel
                ds1103_inc_set_idxmode(m->enc_channel,
DS1103_INC_NO_RESETONIDX);
                m->enc2pos = 500/(500*29.64197530864198); /**< enc ->
Y conversion factor */
                m->pos2theta  =  -
(2*3.14159265358979323846264338327795)/500;  /**< y -> theta conversion
factor as 500 microns/rev */
                /*Input output parameters*/
                m->DAC_out=0;
                m->offset_Vt=-0.005359; /**< Volatge offset for Motor
Driver*/
                m->dac_channel = 3; /**< Channel number for the DAC */
                m->saturation_Vt_out_upper=8;/**< UPPER Volatage
saturation for the Motor Driver*/
                m->saturation_Vt_out_lower=-8;/**< LOWER Volatage
saturation for the Motor Driver*/

                m->Force_pos_gain=0.06;
                m->Force_pos_offsett=1.307;
                m->Force_pos_bias=0.168;
                m->Force_pos=0;

        }


    }
```

Input-Output functions

```
void MotorInput(struct MOTOR *m)
{
        m->enc_pos_1=m->enc_pos;
        m->enc_vel_1=m->enc_vel;
        m->enc_pos =4*ds1103_inc_position_read(m->enc_channel,
DS1103_INC_LINE_SUBDIV_4); // To get the current
        //position of an encoder channel for motor.
        m->pos=m->pos2theta*m->enc_pos/4;

        //~ Count the number of pulses in each period of time
        m->enc_vel = 4*ds1103_inc_delta_position_read(m->enc_channel,
DS1103_INC_LINE_SUBDIV_4);
        //M method velocity calculation

        m->M_vel = m->enc_vel * thetta/4;         //2*pi/10000/0.0001
=2*pi*m->enc_vel

        // Absolute shaft angle position calculation
        m->pos_abs=m->pos_abs + m->M_vel*DT;
        if ( m->pos_abs > thetta ) m->pos_abs = m->pos_abs - thetta;
        else if ( m->pos_abs < 0 ) m->pos_abs = m->pos_abs + thetta;
```

```
        //Smethod velocity calculation

        m->S_Alteration = (m->enc_vel - m->enc_vel_1);

}


void MotorOutput(struct MOTOR *m)
{
        if (m->v_out >= m->saturation_Vt_out_upper)
        {
                m->v_out= m->saturation_Vt_out_upper;
        } else if (m->v_out <=  m->saturation_Vt_out_lower)
        {
                m->v_out =  m->saturation_Vt_out_lower;
        }

        m->DAC_out=m->v_out/30 + m->offset_Vt;
        ds1103_dac_write(m->dac_channel,m->DAC_out);

}

void TorqueInput(struct MOTOR *m,Float64  Torque)
{
    m->v_out= Torque + m->Disturbance;
}
```

Disturbance Observer with fixed step time

```
Float64 MotorDistObs2(struct MOTOR *m)
{
        //standard disturbance observer with 10x multirare slow
        // simple analytical derivative
        m->DistFilterTemp=(m->vel *  ((m->J * m->g) / m->Kt));
        //~ Low pass filter for disturbance observer with time
constant g* M  ( M is the time between two reading)

        m->DistFilterIn= m->DistFilterTemp + m->v_out;
        m->DistFilterOut=(1-exp(-m->g*10*DT))*(m->DistFilterIn - m-
>DistFilterOut_1) +  m->DistFilterOut_1;
        m->DistFilterOut_1=m->DistFilterOut;
        m->Disturbance=m->Dist_gain*(m->DistFilterOut - m-
>DistFilterTemp);

        return m->Disturbance;

}
```

Disturbance Observer with varying step time

```
Float64 MotorDistObs3(struct MOTOR *m)
{
        // DOB modified with variable measurement time.

        m->DistFilterTemp=(m->vel *  ((m->J * m->g) / m->Kt));
        //~ Low pass filter for disturbance observer with time
constant g* M  ( M is the time between two reading)

        m->DistFilterIn= m->DistFilterTemp + m->v_out;
        m->DistFilterOut=(1-exp(-1.0*m->g*m->M))*(m->DistFilterIn - m-
>DistFilterOut_1) +  m->DistFilterOut_1;
        m->DistFilterOut_1=m->DistFilterOut;
        m->Disturbance=m->Dist_gain*(m->DistFilterOut - m-
>DistFilterTemp);

        return m->Disturbance;


    }
```

External Reaction Force Observer

```
Float64 MotorReactionForce(struct MOTOR *m)
{

        if (m->vel>1.0){
                m->Force_pos=m->Force_pos_gain*sin(m->pos_abs+m-
>Force_pos_offsett) + m->Force_pos_bias;
            }
       else if (m->vel<-1.0){
                m->Force_pos=m->Force_pos_gain*sin(m->pos_abs+m-
>Force_pos_offsett) - m->Force_pos_bias;
              }
        else {m->Force_pos=m->Force_pos_gain*sin(m->pos_abs+m-
>Force_pos_offsett);

            }

         //   m->Force_pos=0;
        m->ForceFilterTemp=(m->vel *  ((m->J * m->g) / m->Kt));
        //~ Low pass filter for disturbance observer with time
constant g* M  ( M is the time between two reading)
        m->ForceFilterIn= m->ForceFilterTemp + m->v_out - (m-
>Force_D*m->vel + m->Force_pos);
        m->ForceFilterOut=(1-exp(-1.0*m->g_force*m->M))*(m-
>ForceFilterIn - m->ForceFilterOut_1) +  m->ForceFilterOut_1;
        m->ForceFilterOut_1=m->ForceFilterOut;
        m->Force=m->Force_gain*(m->ForceFilterOut - m-
>ForceFilterTemp);

        return m->Force;

    }
```

Low-pass filters for velocity

```
Float64 VelocityLPFilter(struct MOTOR *m)
{
        //~ Low pass filter for disturbance observer with time
constant g* M  ( M is the time between two reading)

        m->VelFilterOut=((1-exp(-m->g_vel*m->M))*(m->vel - m-
>VelFilterOut_1)) +  m->VelFilterOut_1;

        m->VelFilterOut_1=m->VelFilterOut;
        m->VelFilterLastT=t;

        m->vel=m->VelFilterOut;
        return m->vel;


    }
Float64 VelocityLPFilterM(struct MOTOR *m)
{
        //~ Low pass filter for disturbance observer with time
constant g* M  ( M is the time between two reading)

        m->VelFilterOutM=((1-exp(-m->g_vel*DT))*(m->M_vel - m-
>VelFilterOutM_1)) +  m->VelFilterOutM_1;

        m->VelFilterOutM_1=m->VelFilterOutM;


        return m->VelFilterOutM;

}
```

PD PID position- force controllers

```
Float64 Impedance(struct MOTOR *m, Float64 X)
{
        m->Im = m->Im_K*X + m->Im_D*(X - m->Im_X_1)/(10*DT);
        m->Im_X_1=X;
        return m->Im;
}

Float64 PDposition(struct MOTOR *m, Float64 Ek)
{
        m->Ek=Ek;
        m->Uk_d=m->Kd*(m->Ek-m->Ek_1)/(10*DT);
        m->Uk_p=m->Ek * m->Kp;
        m->Ek_1=m->Ek;
        m->PID_Uk=m->Uk_p + m->Uk_d;
           return m->PID_Uk;
}


void TorqueInput(struct MOTOR *m,Float64  Torque)
{
    m->v_out= Torque + m->Disturbance;
}
```

```
void PIDpositionControl(struct MOTOR * m)
{ //PID Controller with disturbance observer for position control


        m->Ek = m->ref - m->pos ;
        m->Uk_p=m->Ek*m->Kp;
        m->Uk_d=(m->Ek - m->Ek_1)*(m->Kd/DT);

        m->Uk_i=m->Uk_i_1 + m->Ek*DT*m->Ki;

        // anti wind-up
        if (fabs(m->Uk_i) >= m->saturation_Vt_out_upper)
        {
                m->Uk_i=m->Uk_i_1;
        }

        m->PID_Uk= m->Uk_p + m->Uk_i + m->Uk_d;


        m->Uk_i_1=m->Uk_i;
        m->PID_Uk_1=m->PID_Uk;
        m->Ek_2=m->Ek_1;
        m->Ek_1=m->Ek;

}

Float64 PDForce(struct MOTOR * m,Float64 Ferr) {

        m->FORCEcontrol = m->ForceControl_K * Ferr + m->ForceControl_D
* (Ferr - m->Ferr_1)/(10*DT);
        m->Ferr_1=Ferr;
        return m->FORCEcontrol;
}
```

Miscellaneous Class Functions

```
void index_reset(struct MOTOR *m)
{
     if (ds1103_inc_index_read(m->enc_channel,0))
                {
                    ds1103_inc_reset(m->enc_channel);
                    m->pos_abs=0;
                    m->enc_index_ok=1;
                    }

}
```

Main Program Code

```
/*********************************************************************
********
* RELATED FILES:
*   Brtenv.h TraceFileGlobals.h bilateral.h Motor.h
*
* DESCRIPTION: Bilateral control experiments base system code for
multi axis
 Teoman Naskali & shahzad Khan's linear motor contol code v 0.9 has
been used for
general structure and layout of this code all the controllers and main
code rewrittten
S method measurement code supplied by Toshiaki Tsuji,his code has been
rewritten
for this environment.

by Ahmet Altınışık

$Coding started: 23.09.2005 $

*********************************************************************
********/
/** \file
        Contains the main c code of the system some header and source
files have been included for modular programming

 **/
#define DT     1.0e-4          /**< 100 us simulation step size */
#define pi      3.14159265358979323846264338327 95
#define thetta  6.28318530717958647692528676655 9
#include <stdio.h>
#include <Brtenv.h>
Float64 Dist_KK;
Float64 t = 0;                   /**< variable for RT clock */
int MultiRate=0;
int update=0;
#include <math.h>
#include <motor.h>
/* ---------------------------- STRUCTS ------------------------------
----------*/

struct MOTOR Master; /** Master side motor  (includes smc
parameters)*/
struct MOTOR Slave; /** Slave side motor  (includes smc parameters)*/
struct MOTOR Knob;

#include <TraceFileGlobals.h>  /**  This file is included to overcome
-you cannot use structures when comminicating with the host system
error */

Float64 exec_time;  /**< execution time of the system*/

Float64 Cp=1;
Float64 Mc=1;

Float64 V_Impedance=0;
Float64 ForceCmd=0;
Float64 ThetaCmd=0;
Float64 MasterT=0;
Float64 SlaveT=0;
```

```
/** \fn isr_timerA()
    \brief Function which for Interrupts Service Routine for Real Time
Process
    \def outputs to system detail*/

void isr_timerA(void)
{

         //standard DSPACE service routine begining
        RTLIB_SRT_ISR_BEGIN();                                          /*
overload check */
        host_service(1, 0);                                              /*
TRACE service */
        RTLIB_TIC_START();
         //update time
         t=t + DT;       /* start time measurement */
         //update variables from user interface
         DSpaceComputerInput();

         //resets the encoders position for once with index pulse
         if (!Master.enc_index_ok) {
                index_reset(&Master);
        }
        if (!Slave.enc_index_ok) {
                index_reset(&Slave);
        }
        if (!Knob.enc_index_ok) {
                index_reset(&Knob);
        }

         //read encoder values from motors
        MotorInput(&Master);
        MotorInput(&Slave);
        MotorInput(&Knob);

              //if velocity reading changes call disturbance observer
to calculate disturbance
              //reaction force observer also works with the velocity
update for master

        if(S_velocity(&Master)) {


                Master.M=t - Master.S_Last_M;
                Master.S_Last_M=t;
                Master.vel=Master.S_vel;
                VelocityLPFilter(&Master);
                MotorDistObs3(&Master);
                MotorReactionForce(&Master);
        }

              //if velocity reading changes call disturbance observer
to calculate disturbance
              //reaction force observer also works with the velocity
update for Slave
        if(S_velocity(&Slave)) {

                Slave.M=t - Slave.S_Last_M;
                Slave.S_Last_M=t;
                Slave.vel=Slave.S_vel;
                VelocityLPFilter(&Slave);
```

```
                MotorDistObs3(&Slave);
               MotorReactionForce(&Slave);
        }


        MultiRate++;

        if (MultiRate==10) { // this task runs at 1/10 rate of the
first if expression so 1 KHZ

            //comment out section required for your experiment

            V_Impedance =  Impedance(&Slave,((Master.pos-
Slave.pos)/2));
            ForceCmd=(Slave.Force+Master.Force) ;
            ThetaCmd=(Slave.pos+Master.pos)/2;

            //~ //position position
            //~ //better response if master's DOB =0
            //~ MasterT=PDposition(&Master,ThetaCmd-Master.pos);
            //~ SlaveT= PDposition(&Slave,ThetaCmd-Slave.pos);

            //~ //position position with impedance
            //~ MasterT=(PDposition(&Master,ThetaCmd-Master.pos))-
V_Impedance;
            //~ SlaveT= (PDposition(&Slave,ThetaCmd-Slave.pos))-
V_Impedance;

             // 4 channell with impedance

            MasterT=(PDposition(&Master,ThetaCmd-Master.pos))-
V_Impedance - (ForceCmd/Mc) ;
            SlaveT= (PDposition(&Slave,ThetaCmd-Slave.pos))-
V_Impedance - (ForceCmd/Mc) ;

            //~ //Force observer tuning
            //~ MasterT=0;
            //~ SlaveT =0;

            //Master position Slave Force mode

            //~ MasterT=PDposition(&Master,Knob.pos-Master.pos);-
V_Impedance - (ForceCmd * Mc) ;
            //~ SlaveT= ForceCmd * Mc ;

              // send calculated torques/currents to the acceleration
controller
           TorqueInput(&Master,MasterT);
           TorqueInput(&Slave,SlaveT);
           MotorOutput(&Master);
           MotorOutput(&Slave);
           MultiRate=0;
        }

        // send data to the user interface
        DSpaceComputerOutput();

        exec_time = RTLIB_TIC_READ();
        RTLIB_SRT_ISR_END();                          /* overload check
*/
         //end of ınterrupt service routine
```

```
}

/*-----------------------------------------------------------------------
-------*/

/** \fn main()
    \brief Main function of the program
    \def outputs to system detail*/

void main(void)
{
        init();                                 /* DS1103 and RTLib1103
initialization */

        Master.Name = Motor1;   /* MOTOR 1 Names the motor to be able
to fetch their specific paramters*/
        Slave.Name = Motor2;
        Knob.Name = Motor3;


        initMotor(&Master); /*Initialization of Motor Master*/
        initMotor(&Slave); /*Initialization of Motor Slave*/
        initMotor(&Knob); /*Initialization of Motor Slave*/

         // gains are here for ease of changing while development for
initial values.

          Dist_KK=1;
        gain1=250;      //g vel
        gain2=100;      // g
        gain3=100;    //g_force
      //  gain4=1;
        gain5=0.5;    //IM_K
        gain6=1;
        gain7=0.002;  //IM_D
        gain8=1; //Cp
        gain9=20; //Mc
        gainA=Slave.Force_pos_gain;
        gainB=Slave.Force_pos_offsett;
        gainC=Slave.Force_pos_bias;
        gainD=0.1; //Force command
        gainF=0;
        Dist_gain=1;
         // To generate an information message.
        msg_info_set(MSG_SM_RTLIB, 0, "Bilateral Control Experiment
system started.");
        RTLIB_SRT_START(DT, isr_timerA);        /* start sample rate
timer */
        /* Background tasks */
        while(1) {

                RTLIB_BACKGROUND_SERVICE();                         /*
background service */

        }

}
```

Include File – Trace file globas

```
/** \file Holds the Global variables that will be in direct relation
with the trace file*/
/*Must be added before most `.h` files*/

/** The naming convetion for these files is the removal of the `.`
between
the structre instances name and its variable and replaceing it with
`_` */

/*---------------------------GLOBALS FOR TRACEFILE*/


       int     ref_start = 0; /**< Input Reference start for all
drives*/

        Float64 Dist_gain=0;
        Float64 Slave_ref=0;
        Float64 Slave_Kp=50;
        Float64 Slave_Ki=2;
        Float64 Slave_Kd=0.2;
        Float64 Slave_vout=0;

        Float64 gain1=0;
        Float64 gain2=0;
        Float64 gain3=0;
        Float64 gain4=0;
        Float64 gain5=0;
        Float64 gain6=0;
        Float64 gain7=0;
        Float64 gain8=0;
        Float64 gain9=0;
        Float64 gainA=0;
        Float64 gainB=0;
        Float64 gainC=0;
        Float64 gainD=0;
        Float64 gainE=0;
        Float64 gainF=0;

        Float64 scope1;
        Float64 scope2;
        Float64 scope3;
        Float64 scope4;
        Float64 scope5;
        Float64 scope6;
        Float64 scope7;
        Float64 scope8;
        Float64 scope9;
        Float64 scopeA;
        Float64 scopeB;
        Float64 scopeC;
        Float64 scopeD;
        Float64 scopeE;
        Float64 scopeF;
/*-------------------------------------------------------------------
-----*/
```

```
void DSpaceComputerInput(void){
/** \fn Gives values to the global trace file varialbles*/

   Slave.g=gain2;
        Slave.Dist_gain=Dist_gain;
       // Slave.ref=gain5+gain3*sin(gain4*t);
        Slave.Kp=Slave_Kp;
        Slave.Ki=Slave_Ki;
        Slave.Kd=Slave_Kd;
        Slave.g_vel=gain1;
        Slave.g_force=gain3;
        Slave.Force_pos_gain=gainA;
        Slave.Force_pos_offsett=gainB;
        Slave.Force_pos_bias=gainC;
        //~ use same parameters for master side also
        Master.g=gain2;
        Master.Dist_gain=Dist_gain;
       // Master.ref=Slave.ref;
        Master.Kp=Slave_Kp;
        Master.Ki=Slave_Ki;
        Master.Kd=Slave_Kd;
        Master.g_vel=gain1;
        Master.g_force=gain3;

        Cp=gain8;
        Mc=gain9;
        Slave.Im_K=gain5;
        Slave.Im_D=gain7;

}
void DSpaceComputerOutput(void){
       /*X axis*/
       //~ Master_pos         = Master.pos;
  scope1 = Master.pos;
        scope2 = Slave.pos;
        scope3 =Master.Force*Master.Kt;
        scope4 =Slave.Force*Slave.Kt;
        scope5 = Slave.v_out;
        scope6 = Master.v_out;
        //scope6 =Slave.PID_Uk;
        //~ scope7 =Slave.Uk_p;
        //~ scope8= Slave.S_Alteration;
        // scope8 = Slave.Disturbance;
        scope8 = Knob.pos;
        scope9 = Master.enc_pos;
        scope7 = Slave.pos;
        scopeA = ForceCmd;
        scopeB = ForceCmd/Mc;
        scopeC = Master.pos-Slave.pos;
        scopeD = scope4+ scope3;
         //~ //For force sensor tuning
        //~ scopeA =Slave.Disturbance;
        //~ scopeB =Slave.Force;
        //~ scopeC =Slave.Force_pos;
        //~ scopeD =Slave.vel;
        //~ scopeE =Slave.pos_abs;
        // scope9 =1000*Slave.v_out;

    }
```

D-space variable trace file

```
sampling_period = 1.0E-4
_floating_point_type(64,IEEE)
_integer_type(32)
-- signals available for TRACE
--
-- signal name         type  address
group "Full_system"
    group "SLave"
    Slave_ref                        flt
    Slave_Kp                         flt
    Slave_Ki                         flt
    Slave_Kd                         flt
    Slave_vout                       flt
    Dist_gain                        flt
    endgroup
group "Gains"
        gain1                       flt
        gain2                       flt
        gain3                       flt
        gain4                       flt
        gain5                       flt
        gain6                       flt
        gain7                       flt
        gain8                       flt
        gain9                       flt
        gainA                       flt
        gainB                       flt
        gainC                       flt
        gainD                       flt
        gainE                       flt
        gainF                       flt
    endgroup
    group "Scopes"
        scope1                      flt
        scope2                      flt
        scope3                      flt
        scope4                      flt
        scope5                      flt
        scope6                      flt
        scope7                      flt
        scope8                      flt
        scope9                      flt
        scopeA                      flt
        scopeB                      flt
        scopeC                      flt
        scopeD                      flt
        scopeE                      flt
        scopeF                      flt
   endgroup
endgroup
```